.

University of Alberta

The use of modern metabolomics and proteomics to address the health challenges facing the Canadian cattle industry

by

Fozia Saleem

A thesis submitted to the Faculty of Graduate Studies and Research
in partial fulfillment of the requirements for the degree of

Doctor of Philosophy

in

Microbiology and Biotechnology

Department of Biological Sciences

©Fozia Saleem
Fall 2013
Edmonton, Alberta

Permission is hereby granted to the University of Alberta Libraries to reproduce single copies of this thesis and to lend or sell such copies for private, scholarly or scientific research purposes only. Where the thesis is converted to, or otherwise made available in digital form, the University of Alberta will advise potential users of the thesis of these terms.

The author reserves all other publication and other rights in association with the copyright in the thesis and, except as herein before provided, neither the thesis nor any substantial portion thereof may be printed or otherwise reproduced in any material form whatsoever without the author's prior written permission.

Abstract

Naturally cattle only consumed grass, hay and other forage crops but modern cattle industry has started shifting them from a natural grazing diet to a more balanced grain-rich diet. However, feeding dairy cows grain rich diet is associated with a rapid release of large amounts of SCFA that have been linked to acute and sub-acute rumen acidosis and related metabolic diseases. However, one disease in particular had more profound impact than all of other disaeses-- bovine spongiform encephalopathy (BSE). When BSE was discovered in Alberta in 2003 it nearly wiped out Canada's beef export industry.

The central objective of my thesis is to address: 1) Ruminal acidosis and acidosis-related metabolic disorders, 2) BSE, commonly known as mad mcow disease. More specifically, I tested the hypothesis that modern cattle feeding practices (i.e. grain rich diets) significantly changed the rumen environment, its chemical composition and is responsible for all of these conditions. Metabolomics is such a powerful approach for studying the chemical changes in biological systems. To test these hypotheses, I chose to use modern metabolomics techniques including NMR, GC-MS and DFI-MS to characterize the ruminal fluid of dairy cattle fed with different diets. From these experiments I determined that grain-rich diets led to ruminal acidosis along with unusually high levels of ruminal LPS. Based on the association of high-grain diets with various metabolic diseases, this suggests that feeding practices lower the ruminal pH and alter the chemical content of the ruminal fluid, thereby leading to elevated levels of LPS which, in turn, lead to greater risk for developing these diseases. LPS induces the conversion of helical

native prion proteins into protease-resistant, beta-sheet rich proteins similar to that of infectious prions. This suggests that elevated levels of LPS in the rumen from grain-rich diets may also play a role in the induction of BSE.

Acknowledgement

First of all, Ultimate thanks to **Allah,** who gives me strength to complete this work.I owe my gratitude to all those people who contributed in some way to the research described in this thesis and because of whom my graduate experience has been one that I will cherish forever.

First and foremost, I would like to thank Dr. David S. Wishart, for accepting me into his research group and being an excellent supervisor for me. I have been amazingly fortunate to have a supervisor who contributed to a rewarding graduate school experience by giving me intellectual freedom in my work, supporting my attendance at various conferences, engaging me in new ideas, and demanding a high quality of work in all my endeavors and constant encouragement during the course of my research program. He has inspired me to become an independent researcher and helped me realize the power of critical reasoning. Without his guidance and support, I would not have been able to succeed in my graduate studies.

Besides my advisor, I would like to thank my other supervisor, Dr. Burim Ametaj, who introduced me to cattle physiology. He has been always there to listen and give me advices. I would also like to thank him for introducing me to new ideas, and for encouraging and helping me to shape my research interest and hypotheses. My sincere thanks must also go to Dr. Lisa Stein, members of my thesis committee for her encouragement and wonderful advices throughout this project.

I would also like to extend my appreciation to Drs. Carol Ladner and Trent Bjorndahl for their wise suggestion, helping in designing and running some of the

experiments, for guiding me how to write scientific papers and for many valuable discussions that helped me understand my research area better. I am indebted to Dr. Rupa Mandal, the lab's metabolomics manager, who has been a great source of help and wonderful suggestions during my entire project. My thanks go to her for questioning me about my ideas, helping me think rationally and even for hearing my research problems. I would like to specially thank An Chi Guo for her hard work in constructing Rumen Metabolome Database.

My greatest appreciation and friendship goes to my closest friend, Souhaila Bouhatra, who was always a great support in all my struggles and frustrations in my new life and studies in this country. Thanks to Souhaila for being a great reliable person to whom I could always talk about my problems and excitements.

Most importantly, none of this work would have been possible without the love and patience of my family, my husband Muhammad Kshif Usman and my lovely sons Mahd and Muhammad who were born during my PhD studies here in Canada. They have given me real insight into what is most important in life. Thanks for all their love and support, for putting up with my moods and grumpiness at times, and for allowing me time away from family matters to get the dissertation completed, and to you this thesis is dedicated.

I am also forever indebted to my mother Azra Bibi and father Ch.Muhammad Saleem for all their sacrifices for us. To whom I cannot thank enough for the opportunities they have given me, the constant encouragement they provide and for always being there for me. Though you were so far from me but I am so fortunate to have parents like you, who are supportive and motivating in equal

measures. Much thanks also to my lovely brothers Imran and Faizan and sister Nazia who are so supportive in whatever I do in life.

.
Finally, I would like to thank my generous funding sources including Higher Education Commission of Pakistan, Alberta Prion Research Institute (APRI), and Alberta Livestock and Meat Agency (ALMA) for the financial support.

Table of Contents

List of Figures

List of Tables

List of Terms and Abbreviations

3-PP	3-phenylpropionate
AFO	Animal feeding operation
AMDIS	Automated Mass Spectral Deconvolution and Identification System
ARA	Acute rumen acidosis
BRDB	Bovine Rumen Database
BSE	Bovine spongiform encephalopathy
CD	Circular dichroism
CFIA	Canadian Food Inspection Agency
CMC	Critical micelle concentration
CSF	The human cerebrospinal
CVL	Central Veterinary Laboratory
DFI-MS/MS	Direct flow injection tandem mass spectrometry
DOPE	Dioleoyl-phosphatidyl-ethanolamine or
FFI	Fatal Familial Insomnia
FTE	Feline transmissible encephalopathies
FTIR	Fourier Transform Infrared Spectroscopy
GC-MS	Gas chromatography - mass spectrometry
GNB	Gram-negative bacteria
GPI	Glycosylphosphatidyl inositol
GSS	Strausler-Scheinker Disease
HCA	Hierarchical clustering analysis
ICP-MS	Inductively coupled plasma mass spectrometry
LPS	Lipopolysaccharides

MA	Methylamine
MBM	Meat and bone meal
MCA	Metabolic control analysis
MS	Mass spectrometry
NIST	National Institute of Standards and Technology
NMR	Nuclear magnetic resonance
PC	Phosphatidylcholine
PC	Principal components
PCA	Principal components analysis
PE	Phosphatidylethanolamine
PK	Proteinase-K
PLS-DA	Partial least squares discriminant analysis
PMCA	Protein misfolding cyclic amplification
PMSF	Phenylmethanesulfonyl fluoride
POPG	1-palmitoyl-2-oleoyl-phosphatidylglycerol
PrP^{C}	Cellular PrP conformation
PrP^{Sc}	Pathogenic PrP isoform
RF	Radio frequency
SARA	Sub-acute rumen acidosis
SCFA	Short-chain fatty acids
SDS	Sodium dodecyl sulfate
SM	Sphingomylein
TEM	Transmission electron microscope

TME	Transmissible mink encephalopathy
TSEs	Ttransmissible spongiform encephalopathies
vCJD	Variant Creutzfeldt Jakob Disease
VFA	Volatile fatty acids
VIP	Variable importance in the projection

Chapter 1

General Introduction

Introduction

Cattle industry is an important driver of both agriculture and the agri-food economy in Canada. It is estimated that there are more than 86,500 cattle farms across Canada, of which 15% (~12,500) are dairy farms and the remaining are beef cattle farms or ranches (*1*). Canadian beef and dairy products are world-renowned for their excellence and are as diverse as the country's land and people. Cattle industry products include not only high quality foods such as meat, milk, cheese, butter and yogurt but also essential household items such as textiles (leather), soaps, glue, waxes, gelatin and a wide assortment of pharmaceuticals and cosmetics. In addition to being a major source of many key household products, the Canadian beef and dairy industry is known for its strict enforcement of quality control standards both on farms and in processing plants as well as its strong commitment to modern animal welfare practices and proactive environmental sustainability (*2*). The beef and dairy industries contribute more than $40 billion in total to the Canadian economy each year, with the gross revenue from beef cattle activities being >$27 billion and the gross revenue from all dairy farms being $13.1 billion (*3*). The province of Alberta has the largest share of cattle production in Canada, contributing about 52.9% of Canada's total cash revenue from this industry (*4*). Due to the superior quality of the Canadian cattle herd, there is a growing demand for Canadian cattle and their associated products from around the world. Therefore, a healthy beef and dairy industry is an important factor and a significant contributor to the well-being of all Canadians.

In order to keep the Canadian beef and dairy economy active and growing it is important that its cattle are healthy. This requires providing them with a healthy, balanced and nutritious diet. Historically beef and dairy cattle only consumed grass, hay and other forage crops. More recently the cattle industry has started shifting from a natural grazing diet to a grain-rich diet, which is thought to be one of the most important factors for improving milk and meat production. However, feeding dairy cows diets rich in starch is associated with a rapid release of large amounts of short-chain fatty acids (**SCFA**) that have been linked to acute and sub-acute rumen acidosis (**SARA**) (*5*) as well as other diseases such as laminitis (*5*), fatty liver disease (*6*), bovine endotoxicosis (*7*), systemic inflammation (*7*) and milk fever (*8, 9*). Dairy cows are particularly susceptible to these conditions with one in every two dairy cows in Canadian herds has been shown to be affected by one or more of these metabolic diseases (*6*). All of these metabolic conditions are associated with significant economic losses totaling $650 million a year.

In addition to these common metabolic diseases, there are also other kinds of bovine diseases that can have a significant impact on not only cattle health but the profitability of the beef and dairy farms. These include listeriosis, black leg, bloat, metritis, shipping fever, foot-and-mouth disease as well as a variety of parasitic conditions. However, one disease in particular has had a far more profound impact than all of these conditions combined -- bovine spongiform encephalopathy (**BSE**). When BSE was discovered in Alberta in May 2003 it nearly wiped out Canada's beef export industry. BSE, which is specific to dairy and beef cattle, is a transmissible neurodegenerative disease that causes lethal

degenerative changes to the brain and other nervous tissue (*10*). It is also transmissible to humans in the form of variant Creutzfeldt Jakob Disease (**vCJD**). The detection of BSE in Alberta on May 20, 2003 led to more than 34 countries, including the U.S. and Mexico, to immediately ban imports of live cattle and their products from Canada (*10*). Before the U.S. border was closed to cattle exports in May 2003, more than one million live cows were being exported to the U.S. for slaughter each year (*11*). At the time of the ban, two-thirds of Canada's cattle farms were located in Alberta, and of those farms, 37% percent were beef cattle ranches. That single case of BSE in Alberta caused an estimated loss of more than $10 billion to the beef industry. In other words, BSE had a profound, negative impact not only on the Alberta economy but also on farming operations and families involved in the cattle industry across Canada.

These data clearly show that the economic costs of beef and dairy cattle diseases is highly significant with losses averaging more than $1 billion/year in Canada, alone. Likewise the costs associated with veterinary care, medications, BSE monitoring and other activities to ensure the health of Canada's dairy and beef herds probably exceeds $100 million/year. Clearly if these diseases could be mitigated and the economic losses reduced, not only would the health of the Canadian cattle herd improve, but the Canadian cattle industry could become much more profitable.

Based on data presented in this chapter, it is hypothesized that many of the most significant and costly diseases in beef and dairy cattle are brought on by what we

feed or how we feed them. To test this hypothesis I will first investigate how dietary modifications fundamentally alter the chemical content of the bovine ruminal fluid. Using modern metabolomic techniques, I will evaluate whether the feeding of grain-rich diets to cows leads to ruminal acidosis and of ruminal and serum LPS (lipopolysaccharide) that likely contribute to inflammatory conditions. I will further show that LPS, which may be generated from a high-grain diet as well as meat and bone meal from slaughtered cows or bacterially contaminated feed, may also play a role in the induction of BSE (bovine spongiform encephalopathy). In particular, using a variety of advanced biophysical techniques (circular dichroism, electron microscopy, gel electrophoresis) I will demonstrate how LPS induces the conversion of helical native prion proteins into protease-resistant, beta-sheet rich proteins that exhibit the hallmarks of infectious prions. In other words, by exploring the metabolites that may be involved in metabolic diseases in dairy cows, I intend to show a possible link between grain-rich diets and the occurrence of BSE.

In this introductory chapter (Chapter 1), I will provide the background information and motivation for my PhD research program. This chapter is organized as follows: after a brief summary of the history and importance of the cattle industry in Canada, a review regarding the occurrence of metabolic disorders in cows associated with high grain diets will be provided. This will offer the foundation to two later chapters in this thesis (Chapters 2 and 3) that describe my research work on the metabolomic characterization of ruminal fluid in dairy cows that were fed grain-rich diets. In the second part of this introduction, a brief

history of BSE and its discovery in Canada, and the mechanism underlying BSE and other related diseases (prion diseases) will be summarized. This will provide the background material to Chapter 4 which describes a possible connection between high-grain diets (which lead to high levels of LPS) and the generation of infectious prions.

1.1 The Cattle Industry in Canada: A Brief Review

1.1.1 Historical Development of the Cattle Industry

The cattle industry in Canada began in the early 16th century when French settlers arrived with cattle that were native to France. Between 1660 and 1670, New France (present-day Quebec) imported significant numbers of French cattle (such as Normande, Charolais and Limousin). As time passed, more cattle were brought to Port de Grave on the west side of Conception Bay, Newfoundland, to establish an agricultural colony for settlers from Britain (*12*). The rapid growth of settlements in Upper and Lower Canada led to an increased need for milk and meat, which in turn led to the spread of farming across the country. At the end of the eighteenth century large numbers of cows were brought to Upper Canada (Ontario) with the arrival of United Empire Loyalists (*13*), who then began to import cows from the nascent U.S. The Hudson's Bay Company distributed cows from south of the border to its forts along the Saskatchewan river, down the Mackenzie River, up to Fort Simpson, and as far west as British Columbia (*14*).

Cattle were used for two main purposes until 1750: to produce meat and milk, and to pull farm equipment. Even in the early 19th century, cattle played a relatively

limited role in the Canadian economy, since they were not considered a significant source of profit. The initial boom in the Canadian cattle industry occurred during the American Civil War, when the Union Army needed large quantities of meat and Canada was able to meet the demand. This demand boosted cattle and pork prices and led to the creation of a rail-based continental-scale beef industry in 1865.

The Alberta cattle industry began in the late 1860s when a small group of cattle from Fort Garry (Manitoba) was brought to Morleyville, Alberta. These were the first domestic cattle in the province of Alberta, and were followed by large numbers of cattle brought from B.C. in 1875. Alberta's cattle ranching industry grew rapidly during the 1880s and 1890s (*15*). Even though Canada exported some cattle to the U.S. in the 1860s, the U.K. was actually the first major cattle exporter. The U.K.'s cattle import market facilitated the growth of the cattle industry in Ontario and in Western Canada from the late 19th century to the first decade of the 20th century (*16*). By the turn of the 20th century, live cattle ranked third among Canada's exports to the U.K, accounting for 20% of the total value of exports to that country. Though some cattle were exported from Manitoba to the U.S. in the late 1830s, the major export period started in 1910. Around that time, Canadian cattle exports to the U.K. began to decline and the U.S. became the major importer of Canadian beef (*17*). However, the major driving force in the growth of the Canadian cattle industry was the end of World War II. This is when the industry's importance in Canadian agriculture and its economy increased

dramatically due to a worldwide increase in the demand for beef (*17*). Today, Canada is ranked among the top 20 beef producing countries in the world, a role that is significant for both the provincial and national economies.

1.1.2 Canadian Cattle Production's Contribution to the Canadian Economy

Cattle production is a major industry in Canada and plays an important role in the agricultural sector. The cattle industry not only contributes to a safe and nutritious food supply but also has significant impact on the national and provincial economies (*18*), in part by creating employment in related sectors such as meat processing, retail, food services and exports. The transport of cattle alone contributes more than $20 billion to the Canadian economy each year (*18*). Canadian dairy products are world famous, and dairy is the third-most-profitable product in the country's agriculture sector, behind grains, oil seeds, and red meats. The dairy sector has a well-managed supply system that depends on domestic production, pricing and demands for exports. International trade is an important component of the Canadian dairy industry. In 2011, Canada's dairy industry contributed total net farm receipts of $5.8 billion and sales of $13.7 billion, representing 16.4% of the Canadian food and beverage sector (*19*).

The Canadian beef industry is also an important driver of Canada's economy. Canadians consume only about 50% of the country's total beef production. The remaining half is sold to the international market (*19*). In 2002, Canada ranked fourth among the world's largest beef exporters (after Australia, the U.S. and

Brazil). In 1999, estimated cash receipts from the export of cattle and calves were $6.2 billion, or 18.5% of all farm cash receipts in Canada. Canada's beef production is a major part of farm cash receipts and because of the abundance of highly productive beef cattle breeds in Canada, there is a growing demand for Canadian cattle across the border, especially for slaughter cattle. Canada's beef industry was worth $6.16 billion in 2010, and it contributed $24.6 billion to the country's economy (*20*). This represents 15% of the value of agriculture in Canada. During the past decade, the meat industry generated an average of 15.4% of a total Canadian farm cash income.

Although the oil and gas sector receives most of the credit for Alberta's economic growth, the agriculture sector -- particularly the cattle industry -- plays a very important role in the province's economy (*21*). Alberta leads Canada in cattle production, with slightly more than half the farm cash income from sales of cattle and calves. Alberta contributed to 68% of Canada's fed-cattle production, followed by Ontario (21%), Saskatchewan, Manitoba, and British Columbia (combined at 9%). Statistics from 2010 showed that Alberta produced 5.5 million head of cattle, or nearly 40% of the country's total head count of 14 million (*22*). In 2009, it was estimated that 53% of Alberta farms raised cattle that earned almost 34% of the Canada's total agricultural revenue receipts in 2010 (*21*). Alberta's annual beef and cattle exports are valued at approximately $1.4 billion. The regions in the U.S. that consume the most beef are closer to Alberta than they are to the parts of the U.S. that produce large amounts of beef. This unusual cultural-geographical anomaly has greatly helped Alberta's cattle

export market (*23*). According to 2009 estimates, 16% of Alberta's beef is sold within the province, 45% to the rest of Canada, 31% to the U.S. and 8% to other countries. In 2009, Alberta exported 31% of its beef to the U.S., for a total value of $708 million. Clearly Alberta's beef industry is important not only to Alberta's agricultural sector but also to its overall economy.

1.2 Modern Cattle Feeding Practices

A feedlot is a type of animal feeding operation **(AFO)** to efficiently feed cattle (particularly beef cattle) so they will be heavy enough to be sold on the market. Cattle feedlots vary in size, from less than a hundred animals to very modern operations feeding more than 40,000 animals. In Canada during past two decades, cattle feedlots have developed into a very competitive, high throughput industry. To help reduce operating costs and take advantage of "economies of scale," feedlot sizes have increased dramatically. To be highly competitive and remain active in the industry, feedlot owners do everything possible to minimize production costs. The most effective way for cow/calf producers to reduce feeding costs is to use limit-feeding programs. These programs, which have been used successfully throughout North America, reduce the quantity of a cow's feed intake, but because the food stock is so efficient, the cows gain the same amount of weight that they would if they were fed more. Cattle fed these feed-limit diets have been observed to maintain an average daily weight gain with 5 to 10% lower feed intake (*24*).

There are several reasons why high energy grain-rich diets are fed to dairy and beef cows:

1) In winter, when the forage supply is scarce, cereal grains might be a more attractive food source, as they are less expensive with high energy density and easier to transport than forage or silage.
2) It lowers the feed cost and improves diet digestibility and efficiency, which will result in reduced manure production, less feed mixing and hauling, and a reduced need for forage or silage (*25, 26*).
3) It will fulfill a dairy cow's increased nutritional needs at the onset of lactation and in the last trimester of gestation when roughage-based diets (i.e. hay and grasses) are not enough to maintain proper growth.
4) A diet high in grain allows cattle to grow, fatten, and be butchered more quickly, which helps food producers meet the increased global demand for beef.

1.2.1 Feeding High Grain Diets to Cattle

Cows are herbivores born and raised in pastures. Their digestive system is well adapted to consuming and digesting grasses, legumes, and other forages composed of high fiber. Cows belong to a group of mammals known as ruminants. Ruminants have a complex digestive system, which is characterized by a four-chambered stomach, of which the rumen is the largest part. The rumen and the fluid within it (i.e.,ruminal fluid) contains billions of microbes that help the cattle to digest the feed. So the digestive system of cows has evolved through a

close symbiotic relationship with a vast ensemble of rumen microbes (i.e., the microbiota). These microbes give cattle important metabolic capabilities, including the ability to digest cellulose-rich foodstuffs and convert them into a wide range of compounds important for body maintenance and milk production. To be healthy, it is critical for cows to maintain a stable and healthy rumen microbiota (*5*, *7*). Although their stomachs are adapted to digest the fibrous materials (via a herbage-based diet), their rate of digestion is slow (*27*). For cattle, proper digestion relies on slow fermentation of feedstuffs in the rumen. Therefore plant matter consumed by cattle may be required to spend a long time in the digestive tract in order for all the digestible components to be extracted (*27*). Normally, during rumen fermentation, resident microbes slowly ferment components of the plant cell wall (i.e., cellulose, lignin hemicellulose) and the rumen pH mostly stays near 6-7. Many fiber-digesting fibrolytic bacteria are present in the rumen and grow optimally at this neutral pH (*28*). But today's intensive cattle industry encourages feedlot owners to use a grain-rich diet to enhance growth performance, milk and meat yield and cost efficiency. Transitioning from a diet of roughage to one of grains significantly changes the rumen environment of both dairy cows and beef cattle from the native state in which most rumen microbes and the host animal co-evolved. Consider the example of barley, a cereal widely used in Western Canada and elsewhere as one of the main energy components of dairy cattle feedlots (15–40% in diet dry matter) and beef cattle feedlots (40–85%) (*29*). In the rumen, the starch in barley

degrades rapidly and entirely changing its environment as compared to forages-based diets.

1.2.2 Harmful Changes Including the Release of Endotoxins in Ruminal Fluid

A cow fed a grain-rich diet often accumulates large amounts of SCFA in the rumen. This acidifies the ruminal fluid, pl] lowering the rumen pH to between 4.9 to 6.0 (*5, 30*). At this low pH, the only bacteria that can grow are those that are acid-tolerant, predominantly lactate-producing bacteria which include *Streptococcus bovis* and *Lactobacillus spp.* (*28, 31, 32*). The low ruminal pH also affects the growth of fibrolytic bacteria and protozoa (*33*). Furthermore, a low ruminal pH induced by grain-rich diets supports the growth of *Streptococcus bovis, Escherichia coli,* and *Megasphaera elsdenii* in the rumen fluid (*31*). These pathogenic microbiota tend to release a variety of bacterial proteins and other compounds, including endotoxins or lipopolysaccharides, which can contribute to the pathogenesis of inflammation and injury to the host (*34*).

Recent investigations have revealed an association between changes in the composition of the microbiota in the gastrointestinal tract and the release of large amounts of endotoxins in the ruminal fluid. In particular, several studies have reported a 14 to 20 fold increase in the concentration of endotoxins in the ruminal fluid following high-grain consumption (*7, 35-37*). With grain-based diets carbohydrate breakdown occurs quickly leading to large amounts of SCFAs. As a result there is an abundance of available energy in the form of SCFA in the

rumen. This accumulation can disrupt the normal microbial balance which is accompanied by significant changes to the rumen's metabolic pathways (*38, 39*). If a high grain diet is not regulated properly, it can lead to many problems for cattle health**.**

1.2.2.1 Structural Features of Lipopolysaccharides (Endotoxins)

Lipopolysaccharides (**LPS**), also known as endotoxins or lipoglycans, are part of the outer membrane of the cell wall of most Gram-negative bacteria (*40-46*). LPS consists of sugars, phosphates, and fatty acids, which is why it was originally named as "lipopolysaccharide"(*47*). The total estimated number of LPS molecules in a single bacterium (e.g., *E. coli*) is about 2 million (*48*). As a component of the outer cell membrane, LPS is essential for the survival of Gram-negative bacteria (**GNB**). It acts as a permeability barrier, allowing only hydrophilic nutrients or waste products to pass through it. This prevents the penetration of bile salts and other toxic molecules from the host's GI tract into the bacterium. Overall, LPS acts as a shield, protecting bacteria from cellular host defense strategies, bile acids, lysozymes and hydrophobic antibiotics. It also plays a major role as a bacterial adhesin used in colonization and growth in the host. However, the LPS that is shed during bacterial growth or cell lysis, plays a major role in severe Gram-negative bacterial infections, sepsis, and septic shock (*49, 50*). LPS also acts as one of the strongest natural activators of the host's innate immune system.

Lipopolysaccharide has three major components: 1) O-specific chain; 2) the core oligosaccharide and 3) Lipid A (hydrophobic lipid section). Usually the O-

specific chain is a hetero-polysaccharide, and is comprised of repeated subunits of oligosaccharides that extend out from the bacterial cell membrane. These oligosaccharides vary in number (1 to 25 oligosaccharide units), in sequence, type, ring form, substitution, and type of linkage in different bacterial strains. These variations contribute to the oligosaccharides' antigenic specificity and structural diversity. These oligosaccharides, in turn, are composed of repeated subunits of monosaccharides that vary between 1 and 8 units (*51*). During infections, O-chains, which are antigenic in nature, usually come into contact with the host organism. The structural variability of these O-specific chain saccharides also serves as the basis for serotype classification of bacterial genera; hence the term O-antigen. The O-chain part of LPS not only provides protection against the lytic action of the host defenses but also neutralize the effects of antibiotics.

There are two distinctive phenotypes of LPS: the smooth type (S-LPS) and the rough type (R-LPS). The smooth type, with a fully expressed O-specific chain, is considered to be more virulent; whereas the rough form (R-LPS) has a substantially reduced or entirely missing outer core section and therefore is known to be less virulent (*52, 53*). However, O-antigens do not show endotoxin activity against the host if they are separated from the lipid A component of the LPS. The core polysaccharide, which is more uniform than the O-chain in many Gram-negative bacteria, can be subdivided into an inner and outer core region. The outer core region, which is proximal to the O-specific chain, is composed of mainly heptose (ketoheptose) monosaccharides (the most common of which is L-glycero-α-D-manno-heptopyranose configuration). The inner core region is

composed mainly of one to three molecules of 3-deoxy-D-manno-octulosonic (or 2-keto-3-deoxyoctonic) acid (Kdo) and two L-glycero-D-manno-heptose residues. The Kdo linked to the glucosamine of the lipid A moiety via a glycoside bond is essential for the biological activity of LPS as it is present at the reducing end of the oligosaccharide chain. The inner core glycan residue units are typically substituted by charged phosphate groups, e.g., pyrophosphate or amino-ethyl phosphate, resulting in an overall increase in the negative charge of LPS. It is this negative charge in the inner region that helps to stabilize the LPS structure. The outer core of the lipopolysaccharide is structurally more diverse than the inner core due to variations in hexose composition (galactose, glucose, and N-acetylglucosamine).

The lipid A part of LPS, which is a highly conserved structure among diverse Gram-negative bacteria, is composed of a phosphorylated glucosamine disaccharide (β-glucosamine-(1→6)-glucosamine-1‑phosphate) base bound to O- and N-linked saturated long-chain fatty acids ester or hydroxyl fatty acids ester and accounts for about half the lipids in the outer bilayer. The number and length of these acyl chains may vary among different strains but are highly conserved within a bacterial species. The lipid A domain is known to be responsible for much of the toxic effects of infections caused by Gram-negative bacteria. Furthermore, many studies have suggested that only a small structural diversity among both natural and synthetic variants of lipid A determines the endotoxic activity of LPS (*54*, *55*).

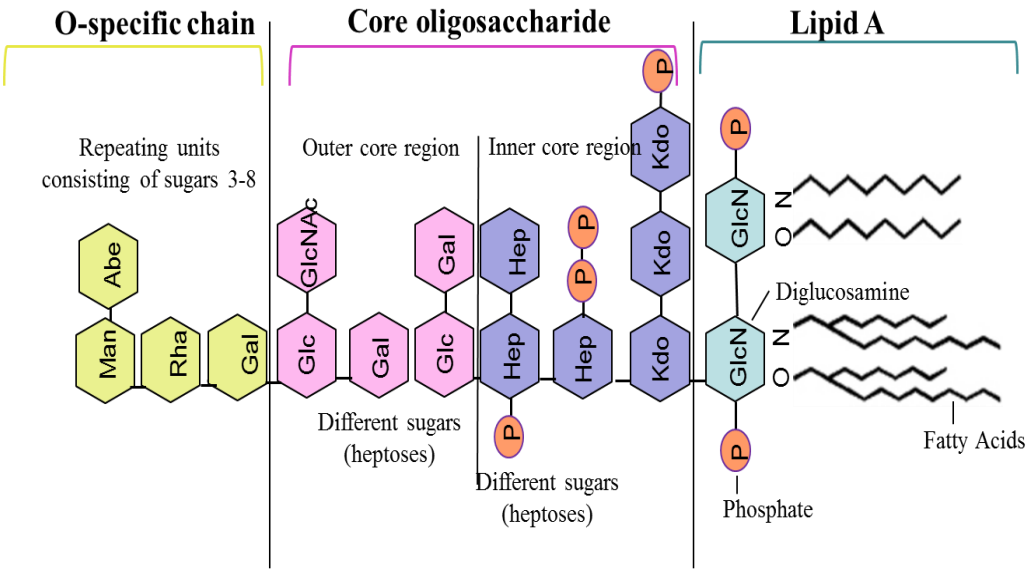

Figure 1.1 The composition of a Gram-negative bacterial membrane lipopolysaccharide.
Lipopolysaccharide composed of three distinct components: lipid A, the oligosaccharide core, and the O-antigen.

1.2.3 Potential Metabolic Diseases Associated With Grain-rich Diet

The ruminal acidic conditions associated with grain-rich diets often lead to a pathological condition referred to as acute or sub-acute rumen acidosis (**ARA** or **SARA**) (*5*) or to other acidosis-related metabolic diseases (i.e., liver abscesses, laminitis, milk fever and bloat) in dairy cows. Such conditions diminish a cow's health status and reduce its performance, yield and production efficiency. Interestingly, it is well known that most of these diseases appear to be related to feeding grain-rich diets to cattle and to events that occur in the rumen. Only a few metabolic diseases (rumen acidosis, laminitis and liver abscess) will be described

in detail, but there are many other diseases that appear to be related to grain-rich diets. These include mastitis, metritis, ketosis, fatty liver disease, displaced abomasum, milk fever, retained placenta, udder edema, sudden death syndrome, milk fat depression syndrome, and infertility (*56*). Space constraints make it difficult to provide details of all these diseases here. For more information, please refer to the comprehensive review article by Ametaj et al. (*35*).

1.2.3.1 Rumen Acidosis

Once established after calf's birth, the microbial population is fairly stable in the rumen. Even though the microbiota generally adapt and re-stabilize to every new rumen environment (*57*), the microbiota can become disturbed and unbalanced if their diet changes abruptly. If ruminants are fed excess amounts of grain or other readily degradable carbohydrates, rumen disruption or micribiota disruption can occur very quickly. This is associated with the release of a large amount of volatile fatty acids (**VFA**) and lactate, which will accumulate in the rumen and lower its pH (*58*). This acidic pH favors the growth of lactate-producing bacteria in the rumen, which makes the environment even more acidic, causing ARA and SARA (*59*). Symptoms of cows with ARA and SARA include loss of appetite, diarrhea, dehydration, and mucus in the feces (*60*). Acidic ruminal fluid has also been shown to increase the concentration of free LPS in ruminal fluid. This occurs because the low pH in the rumen increases the growth of Gram-negative bacteria (*61*). Recent studies have shown that SARA caused by a grain-rich diet stimulates an inflammatory response because free LPS is released into the ruminal fluid (*62*). This differs from what happens to cows that are fed alfalfa, and, thus excludes the

possibility that all LPS molecules are equally toxic. It was observed that SARA induced by a grain-rich diet causes *Streptococcus bovis* and *Escherichia coli* to grow in the rumen (*38, 63*). Although SARA and the corresponding inflammatory responses are more severe due to the unique structure (three-dimensional conformations) of LPS released by *E. coli* during grain-rich feeding (*38, 62*). *Fibrobacter succinogenes* are the predominant Gram-negative bacteria in the rumen which release the majority of LPS when animals are fed on high forage diet (*62*).

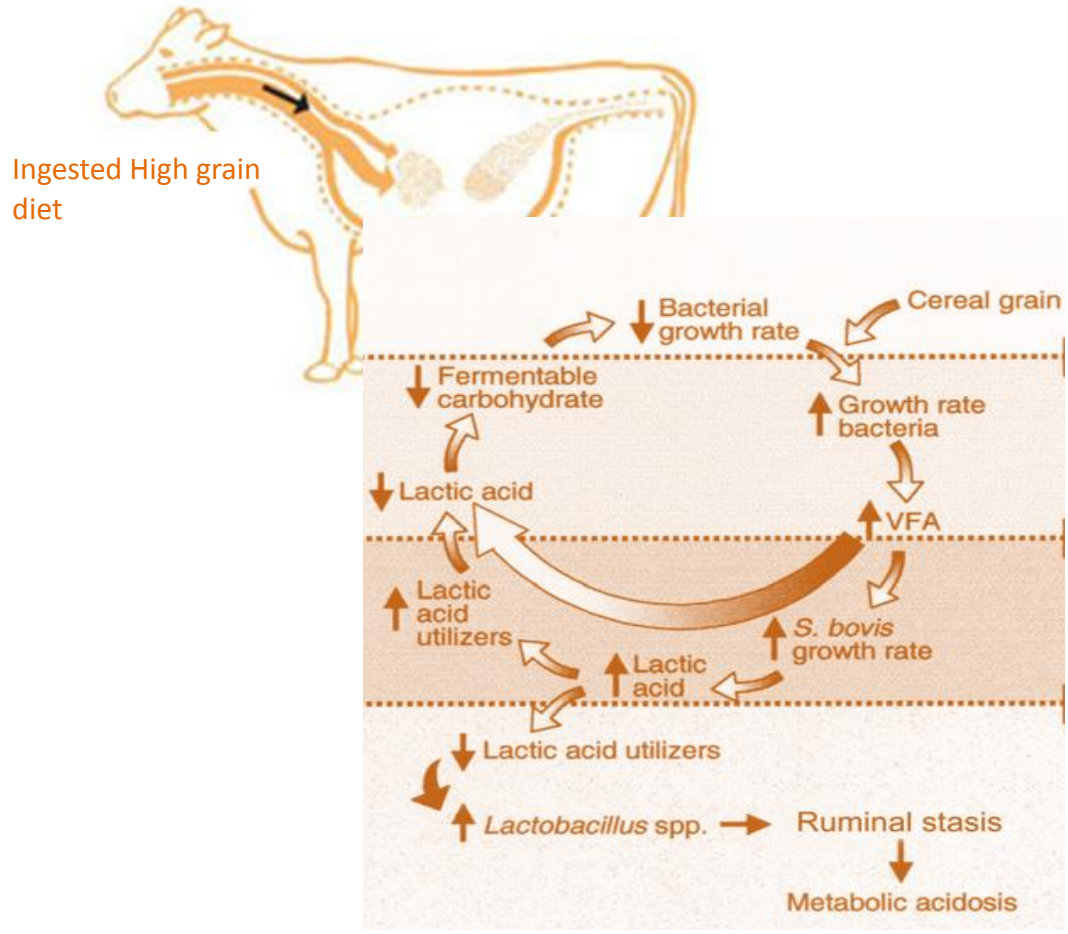

Figure 1.1 Metabolic consequences to the ruminal pH and microbial populations that occur when cows are fed a grain-rich diet.
In the majority of animals, ruminal pH decreases below 6.0 without a significant increase in ruminal lactic acid concentration or in numbers of *Streptococcus bovis* in the rumen. (Modified from Schwartzkopf-Genswein et al. 2003).

1.2.3.2 Laminitis

Laminitis is a metabolic disorder of the lamina of the foot (*47*) in cattle and is known to have a connection with rumen acidosis. Feeding practices that cause the ruminal pH to drop below 5.5 are partially responsible for this disorder (*64*). Laminitis usually occurs when animals are fed a diet of concentrated grain

without a proper adaptation period. During rumen acidosis, many metabolites are released either by digestion or ruminal bacteria. This disturbs the blood circulation in the cow's feet, which results in laminitis. However, rumen acidosis is not the only reason for this metabolic disorder, which affects more than 80% of dairy cows. Several studies have shown that endotoxins and subsequent inflammatory events play a major role in the pathophysiology of acute laminitis. Although laminitis may be present in cattle without showing any symptoms, it is estimated that the incidence of laminitis can range from 60 to 90% in both dairy and beef cattle (*65, 66*). Economic losses due to laminitis mainly depend on its severity and time-span. According to one study, the occurrence of laminitis in dairy cows resulted in a decreased milk yield of up to 2761 kg per month and gross income losses of up to $791.40 per month (*67*).

1.2.3.3 Liver Abscesses

Liver abscess in cattle are also associated with ruminal acidosis caused by excessive consumption of grain. That is why this condition is most common in beef cattle in the United States, Canada, Europe, Japan, and South Africa (*68*). Ruminal lesions resulting from acidosis allow two of the most common pyrogenic bacteria to enter into the systemic circulation and infect the liver, eventually causing liver abscesses (*69, 70*). Two types of bacteria: *Fusobacterium necrophorum* and *Actinomyces pyogenes* release a protein known as leucotoxin, which hinders the animal's immune response to infection by killing white blood cells (*57*). Although some cattle are genetically more prone to this disease, a number of dietary and other management factors are involved, most important

among them is a diet rich in grain. Cows with liver abscesses usually start eating less and losing weight, thereby decreasing feed efficiency(*70*). The prevalence of liver abscesses varies by feedlot, its general incidence can average from 12 to 32% in slaughtered beef cattle (*71*) and specifically in cows fed grain-rich diet, its prevalence is significantly higher ranging from 1% to as high as 95% (*70*). Livers affected with severe abscesses are condemned. The consumption of affected livers by humans is prohibited which causes an economic loss of $5-6 per cow(*72*).

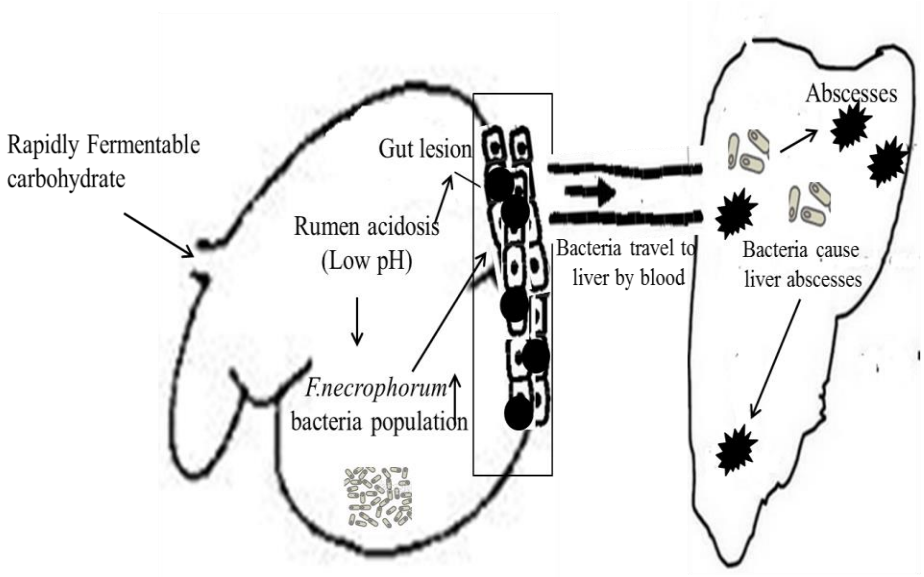

Figure 1.2 Pathogenesis of liver abscesses in cattle fed a grain-rich diet. Liver with abscesses is characterizes with pus-filled capsules that vary in thickness, and range in size from less than 1 mm to over 15 cm in diameter (Modified from Nagaraja et al., 1998) (*70*).

1.3 Metabolomics: An Emerging Field of Omics Science

Metabolomics, also known as metabolic profiling, is a relatively new member of the "omics" family. It is mainly concerned with characterizing the physiological

status of an organism by determining the concentration of all metabolites (small-molecule compounds) within an organism (*66*). Like other 'omics' sciences, metabolomics takes a global or system-wide view attempting to understand the physiological status of a sample or an organism in light of its full physiological potential. In particular, metabolomics allows one to explore problems in which physiology is altered due to disease, nutritional imbalances, stress, or during chemical, viral, or bacterial insults. This fact may explain why the field of metabolomics has grown so dramatically over the last few years. Advances in analytical techniques such as high-resolution nuclear magnetic resonance (**NMR**), high-performance liquid chromatography (**HPLC**),and gas chromatography - mass spectrometry (**GC-MS**) are also contributing to its rapid growth. These advanced analytical methods are now being used to create complete inventories of small molecule metabolites (< 2000 DA) for a range of organisms, cell types and biofluids (*73-77*). Recent studies conducted on human subjects indicates that metabolomics holds considerable promise as clinically useful technology for disease diagnosis and detection. This is because metabolomics enables facile monitoring of normal biological processes as well as rapid detection of perturbations in the concentrations and fluxes of endogenous metabolites involved in key disease pathways (*78, 79*). Over the past decade, metabolomics has been applied to wide range of life science disciplines, including clinical chemistry, drug toxicity screening, nutritional research, environmental monitoring, and disease biomarker discovery. Overall metabolomics provides mechanistic insights

by allowing researchers to explore the correlation of biochemical changes in metabolites with an organism's phenotype (*76, 80-82*).

1.3.1 Defining the Metabolome

The metabolome can be defined as the complete set of low-molecular-weight compounds (i.e. metabolites) produced by cells. These compounds include peptides, organic acids, carbohydrates, amino acids, lipids, nucleotides, vitamins, toxins, minerals, cofactors and any compound with a molecular weight < 2000 Da that is chemically produced or transformed during metabolism (*77*). Originally, the metabolome was described in the context of metabolic control analysis (**MCA**) as the complete set of low molecular weight endogenous molecules synthesized by an organism (*83*). Eventually the definition of the metabolome was modified and redefined to mean the collection of all small molecules that can be measured within a biological system (*84*). This includes not only endogenous but also exogenous metabolites such as drugs, toxins, and pollutants. Using modern metabolomics techniques many attempts have been made to estimate the total numbers of metabolites in a variety of organisms and to construct comprehensive metabolome databases. However this has proved challenging as the size of the metabolome varies with the organism's diet and depends on the organism being studied. For instance, the *E. coli* metabolome is composed of > 2,600 metabolites with links to ~1500 different genes and proteins (*73*), the yeast metabolome is estimated to be > 2,000 metabolites (*75*), and the complete set of metabolites within humans is thought to include over $40,000$ endogenous and exogenous

metabolites (*77*). The human metabolome is particularly complex because of the variety of foods that humans eat. Plants tend to have somewhat more complex metabolomes than single cell animals, with rice having at least 5,000 identified metabolites (*85*). The estimated number of metabolites in the plant kingdom is almost ~200,000 (*85*). While the characterization of organism-specific metabolomes is challenging because of the multi-compartmental and multi-tissue nature of complex eukaryotes, more success has been achieved by looking at biofluid-specific metabolomes. For example, the human cerebrospinal fluid (**CSF**) metabolome is composed of ~1005 metabolites, the size of the human serum/plasma metabolome is ~4600 compounds, and human urine metabolome contains ~3000 metabolites (*77, 86, 87*). However even within a given compartment or a given biological fluid, the number of metabolites in each metabolome still varies significantly depending on the physiological, developmental, or pathological state of the organism (including age, gender or disease condition) (*88, 89*). Thus, the metabolome is often defined as a "state function" of an individual at a particular time point (*76*).

1.4 Analytical Platforms for Metabolomics

Unlike the genome and proteome, the metabolome is very dynamic and changes constantly. Its complexity and heterogeneity make it impossible to analyze the entire range of compounds using a single analytical method. Currently, GC/LC-MS and 1H NMR spectroscopy are the most commonly used platforms to detect, identify, and quantify small molecule compounds from biological samples. Every

analytical platform has its own specific advantages and disadvantages, but to provide the broadest possible coverage of the metabolome MS and NMR-based platforms were selected to conduct this research project. The basic principles of these two techniques and their individual application for metabolomics will be described. Of course there are many other analytical platforms being used in metabolomics, including infrared spectroscopy, immunodetection, and capillary electrophoresis. For a more comprehensive introduction to these other kinds of metabolomics technologies, please refer to two recent and very excellent review articles (*74*, *90*).

1.4.1 NMR Spectroscopy

The theory of NMR was initially proposed in 1924 by Wolfgang Pauli, who discovered that certain atomic nuclei had the properties similar to magnetic moments and spin. In 1946, Bloch & Packard and Purcell used these observations by Pauli to independently measure the NMR phenomena (*91*, *92*). They were awarded the Nobel Prize in physics in 1952. Since then, NMR spectroscopy has evolved to become the primary tool used by chemists to characterize the structure of both small and large molecules. For these reasons, NMR has also become an important and popular tool for metabolomics studies. The basic principle behind NMR measurement is that certain nuclei (such as ^{1}H and ^{13}C) have a spin that generates a small, local magnetic field. When a chemical compound (which consists of atoms and nuclei that are chemically bonded together) is put into an external magnetic field, it is possible to transfer energy to the chemical's nuclei

(or cause their nuclear spins to flip) from a low to a high-energy level by exposing the nuclei to a weak, oscillating magnetic field at a "resonance" frequency that matches each of the nuclei's spinning frequency. The oscillating magnetic field use in NMR is generated through a radio frequency **(RF)** pulse. The resonance frequency that causes a given nucleus in a chemical compound to spin flip or jump in energy is determined by its chemical/nuclear composition, its chemical structure, the chemical environment and the strength of the external magnetic field. As the nucleus (or nuclei if one is referring to a molecule) returns to equilibrium (a low level state) energy is released at a frequency that corresponds to the characteristic resonance frequency of the nucleus (or nuclei) in the biological sample. This energy can be detected via a radio frequency receiver and the oscillating signal can be Fourier transformed to produce an NMR spectrum. This spectrum is characterized by multiple lines (or signals or peaks) at different positions that correspond to chemical shifts. Chemical shifts represent the characteristic resonant frequencies that different nuclei have in different parts of a molecule. The relative height of each peak in an NMR spectrum corresponds to the percentage abundance of each nucleus (usually ^{1}H) type. Information collected from an NMR spectrum can be used to determine the chemical structure of pure substances. It can also be used to determine the chemical composition of liquid mixtures. The most sensitive NMR-active nucleus is the hydrogen nucleus, which has a half-integer spin (i.e. 1/2, 3/2, 5/2). As hydrogen is naturally abundant and found in nearly every organic molecule, NMR spectroscopy is an ideal method to use to characterize organic molecules. Currently, one-dimensional

(1D) and two-dimensional (2D) NMR methods are most frequently used to determine the structure of known metabolites. However, 1D proton spectra are the quickest and easiest to collect (>100 samples/day is attainable), which is why it is the main approach used in NMR-based metabolomics. Other features that have made NMR a platform of choice for many large-scale metabolomics projects are that it is a nondestructive and noninvasive technique that does not require derivatization or chromatographic separation. NMR spectra are also highly reproducible, meaning that the results of NMR-analyzed samples are consistent from one spectrometer to another (*93*). NMR is also capable of simultaneously quantifying multiple classes of metabolites. The major disadvantages to NMR are cost and quality. NMR spectrometers are expensive, and have low resolution and relatively poor sensitivity. The current detection limits for ^{1}H-NMR are 1-5 μM in biological fluid samples.

1.4.2 MS-based Platforms

Mass spectrometry (**MS**) represents a universal, highly sensitive analytical technology that is widely used for the comprehensive profiling of small molecules (metabolites) in metabolomic studies (*84, 94*). Mass spectrometry is a powerful analytical technique used to provide both qualitative (structure) and quantitative (molecular mass or concentration) information about molecules within a sample, after their conversion to ions. Mass spectrometry works by ionizing chemical compounds (using an ionization source) to generate charged molecules. The ions then travel through a mass analyzer where they come in contact with an ion

detector. The detector of mass spectrometer separates the ions according to their mass/charge (**m/z)** ratio and measures detected ions in proportion to their relative abundance. The MS detector generates useable signals in the form of mass spectrum that shows the relative abundance of the ions versus their mass-to-charge ratio. MS-based techniques are gaining popularity in metabolomics research because MS is much more sensitive than NMR. Usually MS-based techniques detect metabolites that are present in concentrations two to three orders of magnitude below the detection limit of ^{1}H-NMR (*76*). In metabolic studies, other chemical separation techniques such as gas chromatography (**GC**) or liquid chromatography (**LC**)) are usually integrated with MS detection to form hyphenated GC-MS or LC-MS analysis platforms. Using these combined separation and detection techniques, thousands of metabolites can be identified and semi-quantified according to their unique mass-to-charge ratio (m/z), their intensity and retention time.

In metabolomics, GC-MS is often considered the gold standard for analytical techniques (*95*). It offers a high degree of reproducibility and chromatographic resolution. With GC-MS, compounds that have a low-molecular weight (< 500 Da), and are volatile and thermally stable (such as sugars, fatty acids, and amino acids), are first separated in the gas (GC) phase and then ionized and detected in electron-impact mass spectrometers. Current detection limits for MS-based approaches are 10 nM, allowing the detection of ~1,000 metabolites, with typical acquisition times of ~30 minutes per sample (*90*). However, MS-based methods tend to be somewhat more time-consuming than NMR. The major disadvantages

of MS-based techniques (particularly LC-MS) lies in the high number of false positives or noise peaks, the lack of spectral reproducibility or consistency, and the requirement for metabolite-specific calibration curves (or isotopic standards) for any kind of absolute quantification.

1.5 Metabolomics for the Study of Rumen-Related Diseases Biomarkers

Although the relationship between rumen metabolism and host health status is widely accepted, relatively little work has been done on characterizing the rumen metabolome. Consequently it is not yet clear which of the compounds that originate from the activity of rumen microbiota under conditions of diet-induced stress (i.e., a grain-rich diet) are significant indicators of a cow's health status. Moreover, little is known about microbial-mediated changes in rumen metabolism when cows are fed different proportions of cereal grain. So far, most conventional metabolic (as opposed to metabolomic) studies addressing rumen metabolism have focused on the dietary effects of a single class of compounds, such as SCFA, and have not attempted a comprehensive metabolomic characterization of all compounds in the rumen. While metabolomics has opened new areas in the field of nutrition research for humans (*96*), the use of modern metabolomics techniques to address nutritional issues in ruminant animals has been very limited. In the dairy industry, epidemiological data indicate that 50% of dairy cows can be affected by one or more metabolic-related disorders within the first month after calving (*72*). These disorders include rumen acidosis, laminitis, mastitis, metritis,

ketosis, fatty liver disease, displaced abomasum, milk fever, retained placenta, udder edema, sudden death syndrome, milk fat depression syndrome, and infertility (*56*). Interestingly, most of these diseases appear to be related to the feeding of rapidly fermentable carbohydrates (in the form of cereal grains) and to events that occur in the bovine gastrointestinal tract. Despite much progress in understanding the probable nutritional causes of these diseases, it is not clear why or how so many different disorders are connected. As metabolites play key roles in a number of metabolic pathways or cellular processes any changes in their concentrations can serve as very good indicators of those metabolic processes that are being disturbed. Consequently, in this study metabolomics technology was chosen to characterize the rumen metabolome in dairy cattle under a variety of graded, grain-rich diets. By associating changes in the rumen metabolome with other toxins (endotoxins and other small molecule uremic toxins) and various disease conditions I hope to provide some further rationale into the causes and connections between these common metabolic disorders. Chapters 2 and 3 of this thesis describe these studies in detail. In chapter 4 of this thesis I turn to address another (non-metabolic) disorder that is found in cattle, namely BSE. However, as mentioned in the introduction to this chapter, there may well be a connection between the metabolic perturbations we see in cattle that are fed high grain diets and the development of BSE. Chapter 4 will explore these connections and provide compelling evidence that LPS can trigger prion conversion to a potentially pathogenic and infectious form.

1.6 Bovine Spongiform Encephalopathy

Bovine Spongiform Encephalopathy **(BSE)** or "Mad Cow Disease" is one of a group of fatal neurodegenerative diseases known as "prion" or transmissible spongiform encephalopathies **(TSEs)** that occur in cattle. This condition is characterized by the unusual appearance of spongy degeneration in the brain, which leads to severe symptoms of severe neurological deterioration, but no inflammatory or immune response (*97, 98*). To date, several theories have been put forward to explain the origin of BSE. One is that it was spread to cattle through the high-protein feed supplements, another hypothesis is that was/is spread through the consumption of meat and bone meal **(MBM)**, which contained TSE-infected products from sheep and goats infected with scrapie (*99*). But various other factors, including commercial feeding practices (i.e., antibiotics, hormones, grain-rich diet and protein to increase productivity in modern cattle farming) cannot be dismissed. Regardless of how the disease was initiated, there is near universal consensus that a self-propagating protein known as a prion acts as the final transmissible disease agent, not only for BSE but for all prion diseases (*99*).

1.6.1 BSE in Britain

The first confirmed case of BSE in the U.K. was reported in November 1986 by scientists at the Central Veterinary Laboratory **(CVL)** following the referral of the brain of two cows with severe but unusual progressive neurological signs and symptoms. The disease was considered a type of spongiform encephalopathy

because of the neurological degenerative signs and symptoms, which were similar to those of scrapie disease seen in the sheep. As the pathology of this disease had never before been described in cattle, it was classified as a new disease and named BSE or "mad cow disease." In the following year (1987), after the first case was confirmed, more cases were diagnosed, and BSE was considered an epidemic of a new emerging disease in cattle. The disease peaked in 1993, with almost 1,000 cows being diagnosed every week. By the end of 1994 (97), 137,000 confirmed cases of BSE had been reported, six times more than the U.K. government had predicted in its "worst case scenario".

Because of the similarities in the neuropathological symptoms of BSE in cows and scrapie in sheep, the scientific community started to think about (*100*) who ate BSE-infected beef or had come into contact with other products (brain tissues) of infected cows as the disease jumped from sheep to cows through MBM. The human version of this the disease is known as variant Creutzfeldt-Jakob disease (**vCJD**). Although all the evidence supported the hypothesis that BSE could potentially cross the species barrier, the British government initially insisted that British beef was safe and posed no threat to human health (*1, 101*). The British government only began to believe the possible threat to human health in March 1996, when scientists confirmed vCJD, which they had hypothesized, was linked to BSE. The British government subsequently banned the consumption of beef but it was too late: British citizens had lost trust in the government and scientific authorities.

Since 1986, 200,000 cases of BSE have been confirmed in the U.K, but, mathematical modelling of the epidemic suggests that between one million and three million cows might have been infected (*102, 103*). Most of these infected cattle were used for human consumption before signs of the disease appeared. Also since 1986, there have been 101 confirmed and 36 probable deaths due to vCJD (*98*). BSE had a huge impact on cattle and cattle products from the U.K.: the U.S. stopped importing British beef in 1989, and Canada followed suit in 1990 (*104*). In all, the U.K. lost almost £4 billion during the epidemic. After being identified in Britain, BSE quickly spread not only to other European countries, but also to Japan, Israel, the US and Canada.

1.6.2 BSE in Canada

Canada's first BSE-infected cow was identified in Alberta on December 8, 1993. It had been imported from the U.K. in 1987 (*95*). On May 20, 2003, the Canadian Food Inspection Agency (**CFIA**) identified Canada's first non-imported domestic case of BSE, in Wanham, Alberta. This marked the beginning of Canada's BSE crisis. In August 2003, shortly after BSE was confirmed in Canada, more than 40 countries, including Canada's largest customers (the U.S., Mexico and Japan) imposed import restrictions on Canadian beef and live cattle (*104*), although low-risk Canadian beef products were still traded on the worldwide market (*98*).

The Canadian cattle and beef industry depends largely on exports. Prior to 2003, almost 50% of the cattle sold in Canada was exported either alive or as beef products. In 2002, the year before the ban, the industry had a market value of

about $4.1 billion, exporting almost 521,500 tons of beef in 2002 with 70% of it going to the United States, 15% to Mexico, 5% to Japan and 3% percent to South Korea. Within three months after the first BSE case was identified and the subsequent ban on beef exports, the value of the exports had dropped to almost zero (*105*). The ban on Canadian beef exports led to an oversupply of beef on the domestic market. Canada did not have the capacity to process these extra animals, and as a result, the price of cattle plummeted (prior to May 20th $108/cwt to as low as $35/cwt in July 2003). Though the BSE crisis hurt the entire country, the hardest-hit province was Alberta, which was (and still is) the largest cattle and the beef-producing province in Canada. Alberta lost almost $160 million each month for the next two years after the first reported case of BSE in May 2003 (*106*). Next hardest-hit were Ontario, where export losses averaged $62 million each month; Saskatchewan ($23 million); and Quebec ($11 million) (*105*).

One cow tested positive for BSE in Washington State in December 2003; however it was concluded that cow had come from Canada. Meanwhile, in Alberta, a ten-year old cow tested positive for BSE on December 30th, 2004 and a six-year-old cow tested positive shortly after, on January 11th, 2005 (*10*). By May 2009, a total of 17 confirmed cases of BSE had been identified in Canada (Source: www.cdc.gov). In April 2006, some countries partially lifted the export ban for some Canadian beef products and live cattle under the age of 30 months, but borders remained closed for the export of live cows and beef products. The BSE crisis in Canada also affected employment in several beef-related sectors, including food processing, meat packing and transportation.

1.6.3 A Brief History of TSEs or Prion Diseases

Transmissible spongiform encephalopathies (**TSEs**) diseases or prion diseases represent an emerging group of rare, fatal neurodegenerative diseases in both humans and animals. Some prion diseases, such as Kuru (in humans) and scrapie (in sheep and goats) have existed for hundreds, if not thousands of years. Others, such as vCJD and BSE, have either recently emerged in humans and animals or may have existed for a long time but are only now being described and officially recognized. Although they are rare, (CJD affects an estimated one person per million annually) they have gained the attention of the scientific community worldwide because of the unique biology of the transmissible agent (i.e. prions). Currently, these rare neurodegenerative diseases are not treatable and are uniformly fatal. In this section, we will discuss where and when they began.

Scrapie was first recognised in Great Britain, France and Germany in the early 18th century (*107*). It was characterized by vacuolar or spongiform changes in the central nervous system (**CNS**) of sheep. But sheep breeders knew that scrapie-free flocks developed this disease only after exposure to infected sheep. This led to the conclusion that scrapie is transmissible (*108*). The human version of this disease was first described in Germany, Switzerland and Austria in the early 1920's. Various forms of the disease took different names, among them Gerstmann-Strausler-Scheinker Disease (GSS), Creutzfeldt-Jakob disease (CJD), and Fatal Familial Insomnia (FFI). In 1957, Zigas & Gajdusek discovered a scrapie-like disease in the Fore tribe in Papua, New Guinea, where it was known as Kuru

(*109*). Later the cause of Kuru was identified as the ritualistic cannibalism of brain tissue of dead tribe members. In particular for the people of the Fore tribe, it was common for relatives to eat the brain tissue of those who had died from the disease. It was Hadlow, a veterinary neuropathologist, who noted the similarity of kuru brain pathology to that of scrapie in sheep, and suggested that if animals were inoculated with Kuru material, they have to be kept a long time to develop this disease. Armed with this information, Gibbs and Gajdusek showed that inoculating monkeys with brain material infected with Kuru, CJD and GSS (*110, 111*) caused the monkeys to develop those conditions. Although kuru has been almost completely eliminated since cannibalism was banned in New Guinea but the nature of the causative agent has been the focus of further intense research.

Although TSE diseases are rare, public awareness has increased dramatically in last two decades, largely due to BSE. The main cause for the establishment and spreading of BSE has been BSE-infected meat and bone meal (MBM), a widely used supplementary foodstuff rich in proteins that is produced by the rendering process (Prusiner, 1998). The consequences to human health became particularly profound after vCJD appeared in humans in the UK late 1995 (*112*). (*112*). vCJD, a rare and fatal human neurodegenerative condition, is one of the most recently identified transmissible TSEs. It is widely postulated that vCJD was transmitted to the human population via ingestion of cattle products affected by BSE (*113*). Until now, no direct link between BSE and vCJD has been demonstrated, although the possibility remains that vCJD may be transmitted (*114*) from BSE-infected cattle to humans. However, several cases of human-to-human

transmission of vCJD have been confirmed (*114*). The fear that there may be a large number of people with subclinical vCJD, due to contact with BSE-contaminated meat, has led to intensive research into prion diseases.

All prion diseases involve signs of brain damage, and for centuries scientists were confused about both the mechanism and cause of these diseases. At first, the causative agent was thought to be a slow virus, as the diseases appeared to have very long (years) incubation periods. But research done by Alper and colleagues (in 1967) demonstrated that the infectious agent responsible for scrapie in sheep was extremely resistant to high dosages of UV and ionizing radiation treatments that normally destroy the infectious material (nucleic acids) of viruses (*115*). In the same year, physicist J.S. Griffith introduced the possibility that the main causative agent for transmitting these diseases might simply be a protein that could replicate in the body. Researchers in Stanley B. Pruisner's lab developed evidence to prove that a protein could be the infectious agent responsible for scrapie when they successfully transmitted scrapie into Syrian golden hamsters (*116, 117*). This effort led to the so-called "protein-only," hypothesis which states that a specific protein (which Prusiner called the "prion" protein or PrP^{Sc}) is itself the infectious agent for these diseases. In particular, the catalytic conversion of the normal cellular form of the prion protein (PrP^{C}) to PrP^{Sc} (the scrapie form of the prion) is the crucial pathogenic event (*118, 119*). It is now abundantly evident that the prion protein plays a critical role in all prion disease processes and that a viral theory of pathogenesis is not a sufficient explanation for the available data. However, the molecular details of the process by which normal

PrP^{C} converts into infectious PrP^{Sc} molecules are currently unknown. Furthermore, attempts to use highly purified recombinant PrP to confirm the "protein only" hypothesis have largely failed. Only impure prions prepared from brain homogenate appear to be infectious (*120*). This suggests that prion proteins may need some help from endogenous cofactors to aid or catalyze the conversion process.

1.6.3.1 Human Prion Diseases

Human prion diseases are a group of progressive and invariably fatal neurodegenerative conditions caused by prions and usually characterized by rapidly progressive dementia; myoclonus; visual impairment; cerebellar dysfunction including lack of muscle coordination; pyramidal/extrapyramidal dysfunction (reflexes, tremors, spasticity and rigidity); and a kinetic mutism. CJD is the most common human prion disease and it has three subtypes: infectious, sporadic, and familial. The recognized human diseases caused by prions are listed under Table 1. For more details of these conditions please refer to (*121*).

Table 1.1 The Human Prion Diseases

Disease	Abbreviation	Mechanism of Pathogenesis
Kuru	Kuru	Infection through ritualistic cannibalism
Creutzfeldt-Jakob disease	CJD	Unknown mechanism
Sporadic CJD	sCJD	Unknown mechanism; possibly somatic mutation or spontaneous conversion of PrPc to PrPSc
Variant CJD	vCJD	Infection presumably from consumption of BSE-contaminated cattle products and secondary blood borne transmission
Familial CJD	fCJD	Germline mutations in PrP gene
Latrogenic CJD	lCJD	Infection from contaminated corneal and dural grafts, pituitary hormone, or neurosurgical equipment
Gerstmann-Sträussler-Scheinker syndrome	GSS	Germline mutations in PrP gene
Fatal familial insomnia	FFI	Germline mutations in PrP gene

1.6.3.2 Animal Prion Diseases

Scrapie was first described or discovered in the 18th century in Europe. At that time it was thought that only sheep could be infected, but after 200 years scrapie was shown to be transmissible to other animals. In addition to scrapie in sheep and goats, and BSE in cattle, other animal prion diseases were identified including chronic wasting disease (CWD) in deer and elk, transmissible mink encephalopathy (TME), and feline transmissible encephalopathies (FTE). These are listed in Table. 2. For more details, refer to Sigurdson (*122*).

Table 1.2 The Animal Prion Diseases

Disease (host)	Abbreviation	Mechanism of Pathogenesis
Scrapie (sheep, goats, mouflon)		Infection in genetically susceptible sheep
Bovine spongiform encephalopathy (cattle)	BSE	Infection with prion-contaminated feedstuffs
Chronic wasting disease (mule deer, white-tailed deer, Rocky Mountain elk)	CWD	Unknown mechanism; possibly from direct animal contact or indirectly from contaminated feed and water sources
Exotic ungulate encephalopathy (nyala, greater kudu and oryx)	EUE	Infection with BSE-contaminated feedstuffs
Feline spongiform encephalopathy (cats)	FSE	Infection with BSE-contaminated feedstuffs
Transmissible mink encephalopathy (mink)	TME	Infection with prion-contaminated foodstuffs

1.6.4 Prion Structure and Characteristics

The word "prion" is a combination of the words "protein" and "infectious," and was first coined by Prusiner in 1982 to distinguish the infectious agent responsible for prion disease as a pathogen different from parasites, fungi, bacteria and viruses (*116*). A prion is essentially an abnormally folded proteinase-resistant sialoglycoprotein which has a molecular size of 27-30 kDa designated PrP27-30 (*123*). The prion protein is the first protein known to consist of two different active isoforms, designated as PrP^{C} and PrP^{Sc}. Normal or cellular prion protein designated as PrP^{C} is a highly conserved, approximately 250 amino acid glycoprotein protein with a molecular weight of 33-35 kDa. Its function has not yet been revealed although studies suggest that the prion protein may have a possible role in cellular signalling or in regulation (*124-126*).

PrP^C is itself a harmless, protease-sensitive protein, which is naturally expressed abundantly in the neurons and glia of the central nervous system (CNS). It is also known to be found in several leukocytes and peripheral tissues (*127, 128*). The prion protein is highly conserved in mammals and is encoded by a single exon of the PRNP gene located on the short arm of chromosome 20 (20p) in humans. PrP^C is post-translationally processed by the loss of a 22-amino-acid, N-terminal signal peptide and a 23-amino-acid, C-terminal peptide followed by the addition of a glycosylphosphatidyl inositol **(GPI)** anchor that secures the protein to the cellular membrane. Further modification involves the formation of a disulphide bridge and asparagine-linked glycosylation at two glycosylation sites.

According to extensive comparative structural data compiled over the past two decades, the PrP^C structure may be divided into two main parts: the C-terminal half, which is globular and flexible; and the N-terminal half, which is disordered (*129*). NMR studies of several different types of recombinant prion proteins have revealed that PrP^C exists in a monomeric state and its C-terminal is folded and predominantly composed of α-helices (*130*). In particular, the C-terminus of PrP^C has three α-helices, and two small antiparallel β-sheets that are thought (by some) to form a small interface between the PrP^C and PrP^{Sc}. (*125, 131, 132*). Unlike the C-terminus, to date there is no high resolution structural information of N-terminal. The N-terminus, which is the most highly conserved PrP region, consists of a number of octarepeats (8 residue repeats) that have been shown to bind divalent metal ions (Cu^{2+}, Zn^{2+}) (*95*).

Although the two prion isoforms, PrP^{C} and PrP^{Sc}, have the same primary structures (i.e. identical amino acid sequence) they have very different physiochemical properties. The most important difference between the normal and the abnormal isoforms is in their tertiary structure. Due to the insolubility and aggregated state of PrP^{Sc}, it is very difficult to study its native conformation. Fourier Transform Infrared Spectroscopy (**FTIR**) and circular dichroism (**CD**) studies have indicated that, unlike the PrP^{C}, which is composed of mostly alpha-helical structures (42%) and fewer beta- sheets (about 3%), the PrP^{Sc} contains higher percentages of beta-sheet (30-43%) and a small percentage of alpha-helical structures (10%). Further, PrP^{Sc} tends to form large oligomers, insoluble aggregates and fibril-like structures. This suggests that the formation of PrP^{Sc} must involve the transformation of α-helices from PrP^{C} into β-sheets. Despite having the same primary structure, these divergent features of PrP^{C} and PrP^{Sc} allow the two isoforms to be easily differentiated biochemically. Normally, PrP^{C} is known to be soluble in mild detergent and readily digested by proteinase K, while PrP^{Sc} is partially protease-resistant with a proteolytically stable core (PrP 27-3). This core has been shown to spontaneously re-arrange into amyloid rods,

where these rods or amyloid fibrils accumulate in the brain and causes disease.

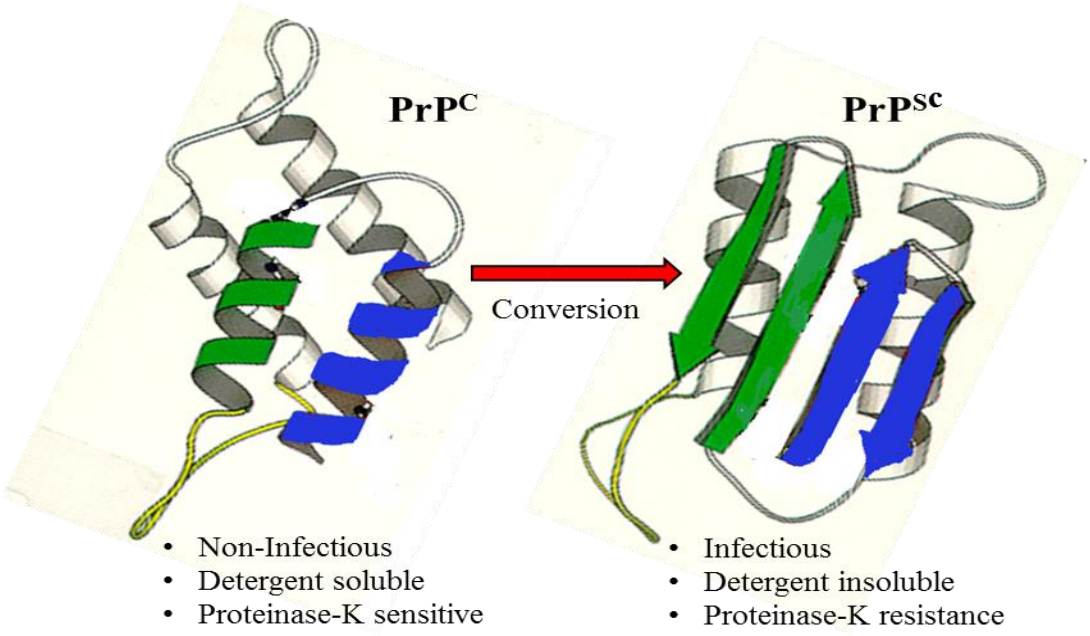

Figure 1.3 Structural and biochemical differences between normal (PrP^{C}) and pathogenic prion protein (PrP^{Sc}).

In conclusion, the prion protein may adopt two distinct active conformations. The normal or cellular PrP conformation (PrP^{C}) is predominantly monomeric and α-helical, while the pathogenic PrP isoform (PrP^{Sc}) is rich in β-sheets and prone to aggregation.

1.6.5 Models of PrP^{Sc} Replication

It has long been known that different protein isoforms can have different biochemical properties while still sharing the same amino acid sequence (*133*). Conformational changes or post translational modifications are often responsible for structural or functional differences between isoforms. However, the exact molecular mechanism involved in converting PrP^{C} to PrP^{Sc} remains unclear.

Currently two competing models have been proposed to explain the mechanism of infectious prion conformational transformation and its replication: the template assisted polymerization model and the nucleation model.

1.6.5.1 Template Assisted Polymerization Model

This conformational model for prion replication was originally proposed by Cohen et al. in 1994 (*134*). It postulates that all the conformational change during prion conversion is kinetically controlled, and that under normal conditions, a high energy barrier prevents a spontaneous conformational change of normal PrP^{C} to abnormally folded infectious PrP^{Sc}. However, a stochastic fluctuation in the structure of PrP^{C}, resulting in a reversible generation of a partially unfolded monomer designated as PrP*, acts as an intermediate in the transformation to PrP^{Sc} . The PrP* monomers that normally exist in low concentrations have the possibility to revert back to PrP^{C}, be degraded, or be converted to the infectious conformation of PrP^{Sc}. The resulting PrP^{Sc}, which is normally formed in minor quantities or exogenous infectious prion (PrP^{Sc}), not only acts as a template, it also lowers the energy barrier and promotes the conversion of PrP* to PrP^{Sc}. This leads to the formation of highly ordered oligomers followed by aggregation into long fibrils. This exponential propagation of prion aggregation causes prion diseases in animals and humans. In this model, all of these conformational changes are kinetically controlled. In addition to this kinetic control mechanism, it is also proposed that mutations within the prion protein gene and chaperone molecules play a role to facilitate this prion conversion process (*135*).

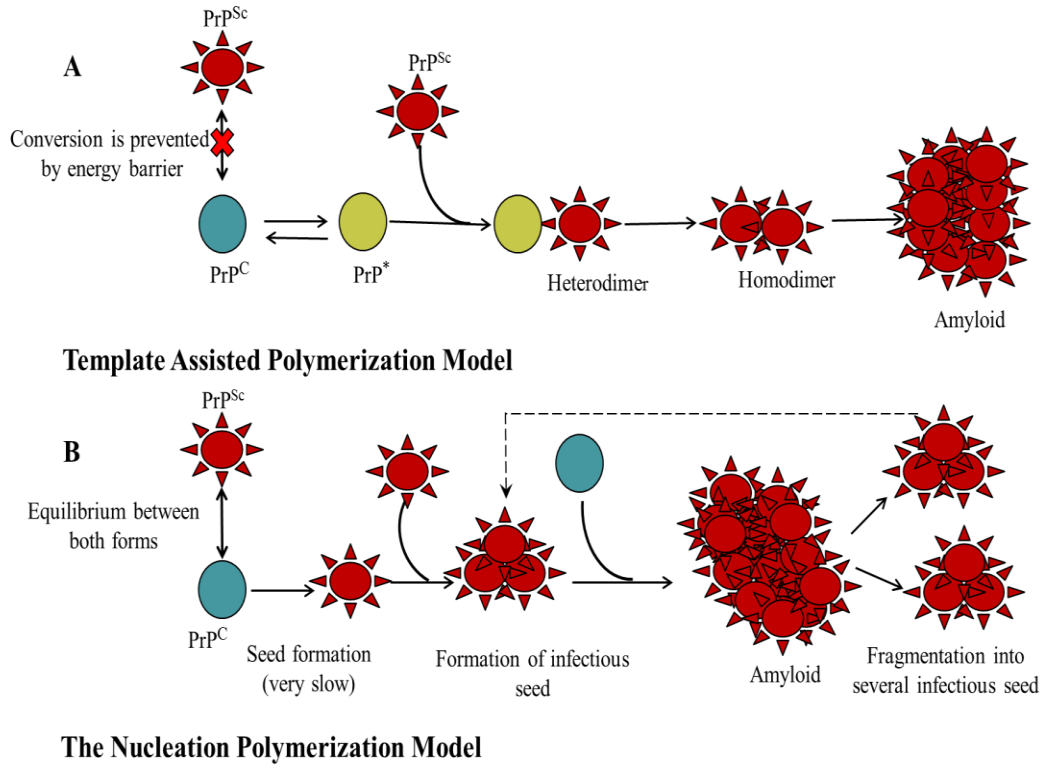

Figure 1.4 Models of PrP^{Sc} replication.

In the template-assisted polymerization model **(A),** the formation of an intermediate state (PrP^{*}) is the main step. This intermediate can interact with PrP^{Sc} (monomeric), which acts as a template for its conversion and further propagation into amyloid. In the nucleation/polymerization model **(B)**, the formation of small oligomeric infectious PrP^{Sc} is a very slow process but once formed, it acts as a seed for further recruiting, converting and stabilizing the misfolding of normal PrP^{C}.

1.6.5.2 The Nucleation Polymerization Model

This model was initially introduced by Oosawa and Asakura in 1975 to describe the polymerization of proteins, and it was not specifically meant for prion proteins. Later in 1997, Harper and Lansbury applied it to explain amyloid formation. The model proposes that in solution, PrP^{Sc} exists in a thermodynamic equilibrium with PrP^{C} that strongly favors the formation of a PrP^{C} / PrP^{Sc}

heterodimer complex, but only in minor amounts. This is because the equilibrium is shifted largely towards higher concentrations of PrP^{C} under non-disease conditions. Usually in non-disease conditions, monomeric PrP^{Sc} is harmless and highly unstable. However, it starts stabilizing when it adheres or binds to a crystal-like aggregate of PrP^{Sc}. Once this aggregate becomes stable, it acts as a seed in a nucleation-dependent polymerization process of amyloid formation (*136*). Further fragmentation of these amyloid aggregates results in the formation of more nuclei or seeds, which can recruit further PrP^{Sc} monomers that lead to the replication of the infectious agent. Consistent with the nucleation polymerization model, *in-vitro* conversion studies showed that PrP^{Sc} aggregates are able to convert normal recombinant PrP^{C} into a new PK-resistant PrP^{Sc} entity (*137-141*).

1.6.6. Cofactors Involved in Prion Conversion

There is a great deal of information in the literature supporting the "protein-only" hypothesis, which suggests that misfolded prion proteins act as the template(s) in the conversion and incorporation of the native, monomeric protein into the fibrilar complex. However, the exact triggers that initiate misfolding and produce an infectious protein template remain elusive. *In-vitro* conversion of prion proteins has been achieved using a variety of denaturing conditions (*120*). These denaturing conditions overcome the energy barriers associated with protein stabilization, thus allowing the protein to refold into a beta oligomeric or fibrilar form with physiochemical properties and morphologies similar to those observed in pathological tissues. Although in-vitro assays have demonstrated certain self-

propagating properties of in-vitro converted prions, the cell-free prion conversion assay that uses recombinant PrP^{Sc} as a template to convert PrP^{C} (purified from cultured cells) is not as infectious as compared to PrP^{Sc} isolated from brain homogenates (*142*). This difference in infectivity caused by these two assays suggests the presence of unknown factors in the brain homogenates that not only promote efficient self-prion propagation but also cause infectivity.

Although no specific cofactors have been identified to date, several studies using model systems suggest that other than PrP^{C}, host-encoded factors may be involved to propagate prions *in vitro* and *in vivo (119, 143-147).* Several non-proteinaceous molecules such as RNA fragments, proteoglycan molecules, and lipid molecules have been identified as one type of cofactor. These cofactors stimulate the prion-seeded conversion of PrP^{C} into PrP^{Sc} molecules and prion infectivity, possibly by forming physical complexes with PrP (*142, 143, 148, 149*). Recently, infectious "synthetic" prions were generated by mixing recombinant PrP with total liver RNA and synthetic 1-palmitoyl-2-oleoyl-phosphatidylglycerol (**POPG**) lipid molecules via a technique known as protein misfolding cyclic amplification (**PMCA**). This result suggests that a non-protein molecular component may exist, that is responsible for augmenting the prion conversion process (*150*). In this particular PMCA experiment, the buffer actually contains Triton X-100 and SDS detergents, both of which share the biophysical properties of lipids and might be playing a role of a lipid-like conversion cofactor. Furthermore, the restricted range of neuronal and non-neuronal cell types that are susceptible to infection by prions also supports the existence of cofactors for prion

propagation (*151-153*). Indeed, glycosaminoglycans, gangliosides and glycosylceramides have all been isolated with brain-derived prions (*154, 155*).

To date, only two kinds of cofactors, lipids and polyanions, are known to interact with normal PrP^{C} and change its conformation to a β-sheet-rich isoform -- a conformational change similar to PrP^{C}-to-PrP^{Sc} conversion (*148-150*). Though it is believed that cofactors might be involved in many steps of prion conversion, the exact mechanism and how these cofactors help the conversion are unclear. There are many possible explanations for this mechanism. First, the binding of a cofactor to PrP^{C} might make it either more susceptible to prion conversion or facilitate the process of converting PrP^{C} to PrP^{Sc}. Another possibility could be that the infectious PrP^{Sc} conformation is stabilized by the binding of a cofactor to it and in this way the cofactor becomes a part of this infectious seed. Several lines of evidence suggest that a poly-anionic cofactor seems to be important for prion conversion but is not critical for its infectivity. On the other hand, lipids are not only known to be important for prion conversion and replication, but also play a significant role in making it infectious. It has been observed that prion infectivity increased by ∼100-fold when the purified prion is re-incorporated into liposomes (*156*).

1.7 Unnatural Feeding Practices Relating to BSE

Although the exact origin of BSE in cattle is still undetermined, it is believed that BSE arose as a result of unnatural feeding practices used by the modern cattle industry, particularly feeding cows meat and bone meal (**MBM**). Therefore,

MBM containing the tissues of BSE-infected animals is suspected as the cause of bovine spongiform encephalopathy (BSE) when it first appeared in the 1980s. It was hypothesized that introducing cost-saving strategies such as lowering the temperature of sterilization used in the meat-and-bone-meal production process was responsible for spreading BSE, as lower temperatures increased the survival rate of the infectious agent (*157*). That hypothesis led the British Government, in 1988, to ban the practice of feeding blood-bone meal to ruminants. To minimize the risk of disease transmission among both animals and humans, the U.K. government also banned the human consumption of "high risk" materials, particularly the brain, spinal cord and intestines from cattle in 1989 and 1995. Although these control measures resulted in a consistent decline in the number of confirmed cases of BSE from a high of 36,682 in 1992 to 1044 cases in 2002, it became evident in 1991 that the MBM feed ban was possibly not totally effective, as cases of BSE have continued to occur in cows born after the feed ban (**BABs**) (*157*).It is estimated that almost 44,000 cases of confirmed BSE have been reported in cows born after these feed controls were introduced. This suggests that feeding MBM is not the only reason that BSE is spreading. Epidemiologists are trying to find clues about the origin of these BSE cases from cows born after the MBM ban, but to date no convincing explanation has been found.

It is assumed that BSE must occur in young calves, because it has a long incubation period. Therefore calf feeding practices are often of great interest and have had a major impact on the epidemic. It is evident that there is a higher

incidence of BSE in dairy cattle as compared to beef cattle and a likely reason is because dairy cattle are fed a grain-rich diet (*158*). One epidemiological study observed that 58% of BSE-infected cows had been fed a grain-rich diet from an early age (*159*). Interestingly, most outbreaks of chronic wasting diseas (CWD) in farmed deer and elk have been also associated with herds being fed or having access to grain-rich diets (*160, 161*), so it is possible to conclude that there is a common element to blood bone meal and a grain-rich diet that might be responsible for BSE. LPS is present in large amounts in meat and bone meal, blood meal, and tallow products from cattle carcasses ranging from 96 ng/g to 497 ng/g. Certainly past practices of using rendered cattle parts as cattle feed (which is thought to have started the BSE epidemic in the UK (*65*) would have exposed animals to high levels of both LPS and prions. We have also shown that LPS is increased by up to 14-fold in the rumen fluid of ruminant animals during feeding with grain-rich diets (at 45% of the diet dry matter) and that LPS is able to permeate through the rumen and colon layers into the bloodstream (*7, 29*).

Studies in the U.K. also demonstrated that cattle feed that was treated with solvents that destroy LPS was correlated with a lower incidence of BSE, whereas animal feed that was only treated via heat (which does not destroy LPS) was correlated with higher levels of BSE (*162*). Other research has demonstrated that LPS disrupts the blood-brain barriers and can bind to cells in the central nervous system (*163*). LPS is ubiquitously found in nature (in feces, the gut, and in the blood), and is present in all non-sterile environments (animal houses, labs).

Further, LPS exhibits amphipathic features similar to known prion conversion/co-purification co-factors such as POPG, RNA, polyanions, glycosaminoglycans and glycolipids. Given these facts, it seems possible that LPS may play a role in the conversion and propagation of infectious BSE and in the oral transmission of TSEs or prions. Based on this hypothesis, a series of experiments with LPS were conducted to explore the ability of this molecule to convert and propagate prion conversion. The results of this study are reported in Chapter 4

Chapter 2

A Metabolomics Approach to Uncover the Effects of Grain Diets on Rumen Health in Dairy Cows[1]

[1]A version of this chapter has been published previously: Saleem, F., Ametaj, B. N., Bouatra, S., Mandal, R., Zebeli, Q., Dunn, S. M., and Wishart, D. S. (2012) A metabolomics approach to uncover the effects of grain diets on rumen health in dairy cows, *Journal of Dairy Science 95*, 6606-6623**.**

Author Contributions

I conducted most of the experiments, analyzed the data and wrote the initial draft of the manuscript. The DFI-MS experiments were originally by R. Mandal. S. M. Dunn, and Q. Zebeli, provided me with the ruminal samples. D. S Wishart, (supervisor and Co-PI) and B. N Ametaj, (co-supervisor and PI) edited this paper. B. N. Ametaj oversaw and designed the experimental set up with the dairy cattle at the Dairy Research Centre.

Introduction

Early lactation is a very critical phase in the nutrition and management of dairy cows. During early lactation dairy cows are fed diets with a high proportion of cereal grains to meet the high energy and nutrient demands for milk production and alleviate any negative energy balance. Because cereal grains are rich in starch, and because starch is rapidly degraded in the rumen it releases large amounts of volatile fatty acids (VFA), including acetate, propionate, and butyrate, as well as other organic acids such as lactate (*164*). The rapid release of large amounts of these short-chain fatty acids (**SCFA**) causes rumen metabolic disorders such as SARA, which is associated with major changes in the rumen environment (*165*). Multiple lines of evidence support the idea that feeding large amounts of grain contributes to the high incidence of diseases in dairy cattle (*166*). Recent reports have demonstrated that feeding high proportions of grain causes major changes in the composition of rumen microbiota in favor of gram-negative bacteria (i.e., *Escherichia coli* and *Megasphaera elsdenii*;(*167, 168*) and the composition of rumen fluid metabolites (*169*).

Despite much progress made in the understanding and prevention of SARA in dairy cattle (*170*)), the etiopathogenesis of SARA and its consequences to the host health still remain unknown. Recent advances made using throughput, quantitative metabolomic methods (*171*) have opened new avenues to elucidate the associations of feeding starch-rich diets and rumen health. Preliminary data from our group suggests that in addition to endotoxin, several other metabolites

released into the ruminal fluid due to high-grain diets might also contribute to disease development or disease exacerbation.

In particular, a pilot nuclear magnetic resonance (NMR)-based metabolomic study conducted by our group in 2009 looked at the rumen fluid from dairy cows fed graded amounts of cereal grain (*169*). Results from this study showed significant elevations of several harmful or potentially harmful compounds in the rumen fluid including methylamine, nitrosodimethylamine, and ethanol with increasing amounts of dietary grain. We also pointed out how these compounds might play a role in the development of some periparturient diseases in dairy cows (*169*). In an effort to confirm and extend these studies, we have undertaken a much more comprehensive, quantitative metabolomic analysis of this same dairy cow cohort, applying much improved metabolite detection techniques, including proton ^{1}H NMR, GC-MS, and direct flow injection **(DFI)** tandem mass spectrometry (MS/MS). We have also performed significantly more assays on a larger number of samples covering many more time points to ascertain the temporal effects of diet adaptation (wash-in) and washout. By using a variety of sophisticated multivariate and metabolic pathway analyses we have been able to confirm several of our pilot study results, but have also identified several additional rumen fluid compounds and rumen metabolic perturbations that might be involved in periparturient disease etiology. This study also provides a more comprehensive view of the diet-induced symbiotic effects between dairy cows and their microbiota that may help unravel the effects of diet on periparturient diseases (*169*). We also show that the use of these modern metabolomic techniques could

also prove helpful in the development and validation of new disease biomarkers for a variety of dairy cattle diseases.

2.1 Materials and Methods

2.1.1. Animals and Diets

Eight ruminally cannulated (100-mm diameter; Bar Diamond Inc., Parma, ID) primiparous and clinically healthy Holstein cows were used in a replicated 4 × 4 Latin square design at the University of Alberta's Dairy Research and Technology Centre (Edmonton, AB, Canada). The total experimental period was 21 d, with the first 11 d serving as a diet adaptation period. Based on similar feeding experiments, an adaptation period of 11 d was considered sufficient to allow wash-in of the experimental diets before metabolomic measurements. The remaining 10 d were allocated for collection of rumen fluid samples. At the start of the experiment, the cows were at (mean ± SD) 60 ± 15 d postpartum. All cows were fed the same basic ration, which was supplemented with increasing proportions of barley grain at 0, 15, 30, or 45% in DM. The cows were housed in tie stalls with free access to water and were fed once daily at 0800 h and milked twice at 0500 and 1600 h, with milk yield recorded electronically. Daily rations were fed as TMR to meet or exceed the requirements of a 680-kg lactating cow as per NRC (2001) guidelines.

All experimental procedures were approved by the University of Alberta Animal Policy and Welfare Committee, and animals were cared for in accordance with the guidelines of the Canadian Council on Animal Care (*172*) (CCAC, 1993).

Data related to the endotoxin concentrations and pH of the rumen fluid, plasma acute-phase proteins, and milk production for this cohort of animals have been reported previously (*169, 173*).

Estimated protein and energy contents were designed to be similar across the different diets. Ingredients and nutrient composition of TMR containing increasing proportions of rolled barley grain are given in (*202*). Individual feed intake was recorded daily throughout the 10-d rumen collection period by determining the difference between the total daily feed given to each cow with the feed refusals the next morning. The daily feed intake of cows is also reported previously (*202*). All cows remained healthy during the entire experimental period and their health was monitored daily based on their daily feeding (i.e., DMI) and milking (i.e., milk yield) behavior as well as for clinical signs of disease by a veterinary technician.

2.1.2. Rumen Fluid Collection

For this study, a set of total 64 rumen fluid samples were collected from 8 cannulated cows for both d 1 and 10 of the measurement period (i.e., d 12 and 21), yielding a total of n = 16 for each of the 4 dietary treatments. All rumen fluid samples (100 mL each) were collected through a cannula using a tube fitted with a strainer and a syringe, which were connected to a 140-mL sterile plastic container. Rumen fluid samples were collected 15 to 30 min before the morning feeding from all cows. The pH of the rumen fluid was determined immediately after collection by a mobile pH meter (Accumet AP61; Fischer Scientific, Ottawa, ON,

Canada). Subsequently, rumen fluid samples were centrifuged at 6,000 × *g* for 15 min (Rotanta 460 R; Hettich Zentrifugan, Tuttlingen, Germany), and the supernatant was filtered through a disposable 0.22-μm sterile, pyrogen-free filter (Fischer Scientific, Fairlawn, NJ). All rumen fluid samples were frozen at −20°C within 2 h to minimize any possible metabolite degradation. All rumen fluid samples were thawed on ice for approximately 2 h before metabolomic analysis.

2.1.3. Endotoxin Analysis of Rumen Fluid

The concentration of cell-free endotoxin was determined by the Pyrochrome Limulus amebocyte lysate assay according to manufacturer instructions (Associates of Cape Cod Inc., East Falmouth, MA) as described previously (*202*). Samples were tested in duplicate, and the optical density values read on a microplate spectrophotometer (Spectramax 190; Molecular Devices Corp., Sunnyvale, CA) at a wavelength of 405 nm. The intra-assay coefficient of variation was <10% for all assays.

2.1.4. NMR Compound Identification and Quantification

All ^{1}H NMR spectra of rumen samples were collected on a either a 500 MHz (Varian Inc., Palo Alto, CA) spectrometer using the first transient of the tnnoesy-presaturation pulse sequence. The resulting ^{1}H NMR spectra were processed and analyzed using the Chenomx NMR Suite Professional software package version 6.0 (Chenomx Inc., Edmonton, AB, Canada), as previously described (*199)*.

2.1.4.1. Rumen Fluid Sample Preparation for NMR Spectroscopy

Rumen fluid samples were thawed at room temperature and subsequently, 300 μL aliquot of ruminal fluid transferred to a 1.5 mL Eppendorf tube followed by the addition of 35 μL D_2O and 15 μL of a standard NMR buffer solution [11.667 mM DSS (disodium-2, 2-dimethyl-2-silapentane-5-sulphonate)], 730 mM imidazole, and 0.47% NaN_3 in H_2O (Sigma-Aldrich, Mississauga, ON). The rumen samples (350 μL) were then transferred to a standard Shigemi microcell for subsequent NMR spectral analysis. In total, 64 rumen samples were prepared in this manner at a pH of 7.3-7.7.

2.1.4.2 ^{1}H-NMR Spectral Acquisition

All ^{1}H-NMR spectra were collected on a 500 MHz Inova (Varian Inc., Palo Alto, CA) spectrometer equipped with either a 5 mm HCN Z-gradient pulsed-field gradient (PFG) room-temperature probe or a Z-gradient PFG Varian cold-probe. ^{1}H-NMR spectra were acquired at 25 °C using the first transient of the tnnoesy-presaturation pulse sequence, which was chosen for its high degree of quantitative accuracy. Spectra were collected with 256 transients using a 4 s acquisition time and a 1 s recycle delay. Spectra were processed using the processor module of Chenomx NMR Suite 6.0.

2.1.4.3. ^{1}H-NMR Compound Identification and Quantification

Prior to spectral analysis, all FIDs were zero-filled to 64k data points, and a line broadening of 0.5 Hz was applied. The methyl singlet of the buffer constituent

DSS served as an internal standard for chemical shift referencing (set to 0 ppm) and for quantification. All ^{1}H-NMR spectra were processed and imported into the Chenomx NMR Suite 6.0 software for quantification as previously described (*29*). Each spectrum was processed and analyzed by at least two experienced NMR spectroscopists to minimize compound mis-identification and mis-quantification. We also used sample spiking to confirm the identity of several spectral signatures seen in our NMR spectra. This was conducted by adding 50-500 μM of the presumptive compound to selected rumen samples to test if the corresponding ^{1}H-NMR signals changed as expected.

2.1.5. GC-MS Compound Identification and Quantification

Prior to analysis by GC-MS, rumen fluid samples were extracted to separate polar metabolites from non-polar (i.e., lipophilic) metabolites. The rumen extraction and derivatization protocol for the GC-MS work was adapted from previously described methods (*174*). For polar metabolites, an aliquot of 100 μL of ruminal fluid containing 2 μL of ribitol in water (20 μg/mL), as an internal standard, was extracted with 800 μL of cold HPLC grade methanol: double-distilled water (8:1 vol/vol) and vortexed for 1 minute. The sample was kept at 4°C for 20 min and then centrifuged at 6,000 rpm for 8 min. After centrifugation, 200 μL of the supernatant were evaporated to dryness using a speedvac concentrator (Savant Instruments Inc., SDC-100-H, Farmingdale, NY).

After speedvac evaporation, to the extracted residue was added 40 μL of 20 mg/mL methoxyamine hydrochloride (Sigma-Aldrich) in ACS grade pyridine and

incubated at room temperature for 16 h. After methoximation, 50 µL of MSTFA (N-Methyl-N-(trimethyl- silyl)trifluoroacetamide) with 1% TMCS (trimethylchlorosilane) derivatization agent (Pierce) followed by incubation at 37°C for 1 h on a hotplate derivatization agent (Sigma-Aldrich). GC-MS samples were then vortexed twice throughout incubation to ensure complete dissolution. Samples were analyzed immediately after derivatization.

Derivatized extracts were analyzed using an Agilent 5890 Series II GC-MS operating in electron impact (**EI**) ionization mode. One µL aliquots were injected with splitless mode onto a 30 m × 0.25 mm × 0.25 µm DB-5 column (Agilent Technologies) with the helium carrier gas set to a flow rate of 1 mL/min and an initial oven temperature of 70°C. The oven temperature was increased at 10°C/min to final temperature 310°C, and final run time of 45 min. Samples were run using full scan at a mass range of spectra 50-500 m/z (1.7 scans/s) with a solvent delay of 12 min. Retention indices (RIs) were calculated using an internal and a C8-C20 alkane mixture solution (Fluka, Sigma-Aldrich) as external alkane standard (*175*).

Quantification and identification of trimethylsilated metabolites was performed as previously described (*176*). The Automated Mass Spectral Deconvolution and Identification System (**AMDIS**) spectral deconvolution software (version 2.62) from National Institute of Standards and Technology (**NIST**) was used to process the total ion chromatogram and the EI-MS spectra of each GC peak. After deconvolution, the purified mass spectrum of each of the trimethylsilylated metabolites was identified using the NIST MS Search program (version 2.0 d)

linked to the 2008 NIST mass spectral library. Metabolites were identified by matching the EI-MS spectra with those of reference compounds from the NIST library. In AMDIS, each search produces a list of library spectra ("hits"), which is ranked by the similarity to the target spectrum according to a mathematically computed "match factor". The match factor indicates the likelihood that our spectrum and the reference NIST spectrum arose from the same compound. In the current case, we considered hits with a match factor of >60% and a probability >20% to be probable compound matches. These cut-off values have been shown to yield consistent results with synthetic mixtures containing known compounds and with samples independently analyzed by ^{1}H-NMR. In addition, authenticity checks were performed by using additional published retention index libraries. The absolute concentrations of most metabolites were determined by comparison with standard calibration curve response ratios of various concentrations of standard substance solutions, including the internal standard ribitol that was also derivatized concomitantly with rumen samples.

2.1.6. Direct Flow Injection MS/MS Compound Identification and Quantification

To determine concentrations of amino acids, sugars, acylcarnitines, sphingolipids, and glycerophospholipids in the rumen samples, the Absolute*IDQ* kit p150 (Biocrates Life Sciences AG, Innsbruck, Austria) was prepared as described in the manufacturer's protocol. The method involves derivatization and extraction of analytes from the rumen samples, along with selective mass-spectrometric detection and quantification via multiple reaction monitoring. Isotope-labeled

internal standards are integrated into the kit plate filter to facilitate metabolite quantification. Briefly, rumen samples were thawed on ice and 10 µL from each rumen fluid sample was loaded onto the center of the filter on the upper 96-well kit plate and dried in a stream of nitrogen. Subsequently, 20 µL of a 5% solution of phenyl-isothiocyanate was added for derivatization. After incubation, the filter spots were dried again using an evaporator. Extraction of the metabolites was then achieved by adding 300 µL methanol containing 5 mM ammonium acetate. The extracts were obtained by centrifugation into the lower 96-deep well plate, followed by a dilution step with 600 µL of kit MS running solvent. Mass spectrometric analysis was performed on an ABI4000 Qtrap® tandem mass spectrometry instrument (Applied Biosystems/MDS Analytical Technologies, Foster City, CA) equipped with a solvent delivery system. A standard flow injection protocol consisting of two 20 µL injections (one for the positive and one for the negative ion detection mode) was applied for all measurements. MRM detection was used for quantification. The Biocrates MetIQ software was used to control the entire assay workflow, from sample registration to automated calculation of metabolite concentrations to the export of data into other data analysis programs. A targeted profiling scheme was used to quantitatively screen for known small molecule metabolites using multiple reaction monitoring, neutral loss, and precursor ion scans. The kit was originally validated for plasma/serum samples but cross validation with other techniques (^{1}H-NMR, GC-MS) also showed excellent concordance with the kit's results with rumen fluid.

2.1.7. Statistical Analyses

Metabolite concentrations determined by endotoxin assays, ^{1}H NMR, GC-MS, and DFI-MS/MS experiments were compiled and cross-checked (to ensure that compound concentrations measured by 2 or more analytical platforms were consistent). For all statistical analyses, we only included those metabolites that were quantified in every rumen sample. Parametric analysis of the data was conducted using the MIXED procedure of SAS (SAS Institute Inc., Cary, NC; version 9.1.3) according to the following model:

$$Y_{ijklmn} = \mu + p_i + a_j + a(s)_{jk} + d_l + t_m + (dt)_{lm} + e_{ijklmn},$$

where Y_{ijklmn} is the observation for dependent variables, μ represents the population mean, p_i is the fixed effect of period i (i = 1 to 4), a_j is the fixed effect of cow j (j = 1 to 8), $a(s)_{jk}$ is the random effect of cow j within the square k (k = 1 to 2), d_l is the fixed effect of measurement day l (l = 1 to 2), t_m represents the fixed effect of diet m (m = 1 to 4), $(dt)_{lm}$ is the diet by day interaction, and e_{ijklmn} is the residual error assumed to be normally distributed. The covariance structure of the repeated measures at different days for response variables was modeled as first-order autoregressive, which provided the smallest values of the fit statistics based on the Bayesian information criteria. To test linear or quadratic effects of treatment on blood variables, the orthogonal contrasts with the CONTRAST statement of SAS (SAS Institute Inc.) were used. Instead of raw P values, the Bonferroni correction and the false discovery rate (FDR) were applied to counter the effect of multiple hypothesis testing. This is considered to be more appropriate

for analyzing the multivariate results found in metabolomic data (*177*). Data are shown as least squares means with their respective standard errors of the mean also shown. Significance was declared at $P \leq 0.05$; a tendency was considered at $0.05 < P \leq 0.10$.

Integrated concentration tables for 64 samples [n = 8 for each day (d 1 and 10), yielding a total of n = 16 for each of the 4 dietary treatments] were then imported into the MetaboAnalyst web server (http://www.metaboanalyst.ca; (*178*) for multivariate analysis. Data integrity checks and data normalization were performed against the baseline metabolite concentrations measured for the 0%-grain diet. This was done by first creating a dummy baseline sample by averaging all 16 samples collected at 0%. After this normalization step, all samples were normalized against this reference sample using probabilistic quotient normalization procedures (*178, 179*). The compound normalization was conducted using autoscaling, which made all compound variances equal to 1. After this normalization step, the data were analyzed by multivariate statistical analysis using principal components analysis (**PCA**). Principal components analysis is an unsupervised clustering technique that can be used to examine the intrinsic variation in a data set and to reduce the dimensionality or complexity of the data. Scores plots were used to show the similarities and differences among the data sets. In a scores plot, observations (i.e., rumen samples) exhibiting metabolic similarities are clustered closer together, whereas those that are metabolically or chemically different are placed further apart. Loading plots were

also used to reveal which variables (i.e., rumen fluid metabolites) were most responsible for the variation within the data set. Apart from revealing any similarities or separation trends among the data, PCA also removes any unwanted or systematic information (noise) from the data set. The axes of the scores and loading plots represent unique linear independent combinations of the observations and the variables, called principal components (**PC**), which are orthogonal to each other. Usually, the first 2 PC (PC 1 and PC 2) capture most of the intrinsic variation in the data. In addition to this PCA study, another multivariate technique known as partial least squares discriminant analysis (**PLS-DA**) was performed using MetaboAnalyst (*178*). Partial least squares discriminant analysis is a supervised (as opposed to a nonsupervised) pattern recognition method that aims at maximizing any discriminating variation between predefined classes. The PLS-DA results were visualized using the first 2 PC of the scores plot to identify characteristic trends or grouping among cows on the different diets. The corresponding loading plot was used to determine the metabolites most responsible for separation in the PLS-DA scores plot. Based on the PLS-DA results, metabolites were plotted according to their importance in separating the dietary groups and each metabolite received a value called variable importance in the projection (**VIP**). Variable importance in the projection values >1 suggest that the metabolite is significantly involved in the separation of groups (*180*). Hierarchical clustering analysis (**HCA**) with Euclidean distance measures and an average linkage method was also performed to explore the presence of clustering patterns among the rumen fluid metabolites. This was also done via

MetaboAnalyst. The expression patterns and a heat map of each variable were categorized using an average linkage hierarchical clustering program (*181*).

2.2 Results

2.2.1. ^{1}H NMR Compound Identification and Quantification

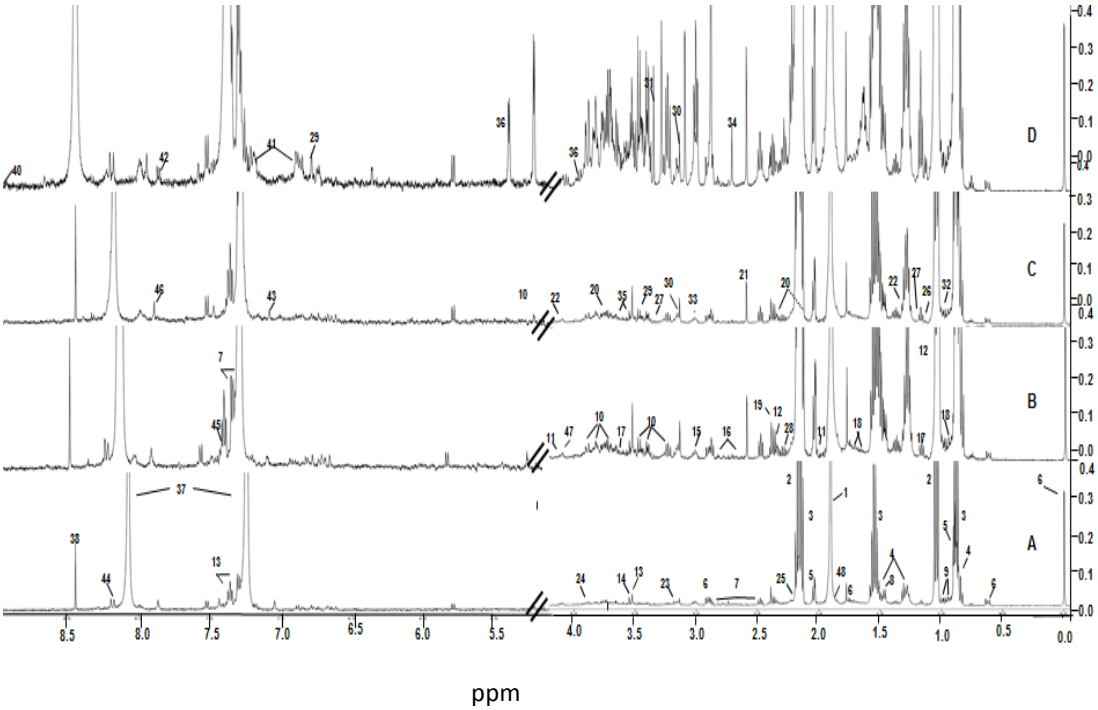

Figure 2.1 shows the characteristic 1H NMR spectra of ruminal fluid corresponding to dairy cows on diets with 0, 15, 30, and 45% barley grain
Key;1 Acetate; 2, Propionate; 3, Butyrate; 4, Valerate; 5, DSS; 6, Isovalerate; 7, 3-Phenylpropionate; 8, Alanine; 9, Isoleucine; 10, Glucose; 11, Proline; 12, Isobutyrate; 13, Phenylacetate; 14, Glycine; 15, Cadaverine; 16, Aspartate; 17, Ethanol; 18, Leucine; 19, Succinate; 20, Glutamate; 21, Methylamine; 22, Lactate; 23, Choline; 24, Fumarate; 25, Acetone; 26, Isopropanol; 27, 3-Hydroxybutyrate; 27, Caffeine; 28, Acetoacetate; 29, 3-Hydroxyphenylacetate; 30, N Nitrosodimethylamine; 31, Methanol; 32, Valine; 33, Lysine; 34, Dimethylamine; 35, Glycerol; 36, Maltose; 37, Imidazole; 38, Formate; 39, Uracil; 40, Nicotinate; 41, Tyrosine; 42, Benzoate; 43, Histidine; 44, Hypoxanthine; 45, Phenylacetylglycine; 46, Xanthine; 47, Ribose; 48, 4-Hydroxybutyrate

All NMR spectra were collected on ruminal fluid samples obtained on d 12 and 21 of the experiment (d 1 and 10 of the measurement period). The NMR spectrum of rumen is remarkably simple and surprisingly uncomplicated, which made the identification and quantification of rumen metabolites relatively easy. Typically 98% of all visible peaks were assigned to a compound and more than 95% of the spectral area could be routinely fitted using the Chenomx spectral analysis software (*169*). Most of the visible peaks can be annotated with a compound name. A total of 64 rumen samples (16 samples from each diet i.e., 0, 15, 30, and 45% barley grain) were analyzed. An average of 48 compounds were unambiguously identified and quantified in each sample. Feeding dairy cows with increasing proportions of barley grain was associated with concentration increases of several rumen metabolites, including ethanol, ethanolamine, 3-hydroxybutyrate, methylamine (**MA**), dimethylamine, N-nitrosodimethylamine, glucose, propionate, butyrate, alanine, maltose, uracil, xanthine, phenylacetylglycine, and phenylacetate ($P < 0.05$). On the other hand, greater proportions of barley grain in the diet resulted in lower concentrations of 1, 3-dihydroxyacetone and 3-phenylpropionate (**3-PP**) in the rumen fluid (Table. 2.1). The complete list of average compound concentrations with their respective standard errors of the means is shown in Table. 2.1.

Table 2.1 Concentration of rumen metabolites determined by direct flow injection NMR. Concentration (μM) of rumen metabolites in dairy cows fed graded amounts of barley grain determined by nuclear magnetic resonance (LSM ± SEM, n = 8).

Metabolites[1]	Metabolic[3] Pathway	Barley grain proportion (% of diet dry matter)					*P*-value[2]	
		0	15	30	45	SEM	Linear	Square
Amino acid Metabolism								
3-Hydroxyphenylacetate	KBM, VM	52	67	65	63	4	0.06	0.02
3-Phenylpropionate	FM	626	523	482	410	25	<0.01	0.54
Alanine	FM, PPM	212	234	323	480	12	<0.01	<0.01
Aspartate	TCA, BM, SMB	126	132	196	179	13	<0.01	0.34
Benzoate	SMB, FM	52	57	72	45	4	0.75	<0.01
Cadaverine	GM, SMB, PDA	65	50	124	122	7	<0.01	0.33
Glutamate	APM,TCA, BM	360	379	490	516.5	20	<0.01	0.82
Glycine	PPM, SMB, GM	119	130	177	190	13	<0.01	0.93
Histidine	PPP, SMB	48	43	55	29	3.5	<0.01	<0.01
Isobutyrate (mM)	PPM, PDA	1.5	1.5	1.67	1.80	0.08	<0.01	0.46
Isoleucine	SMB, TCA	173	152	267	183	13	0.01	0.02
Isovalerate (mM)	PDA	1.09	0.9	1.08	1.13	0.07	0.36	0.11
Leucine	SMB, TCA	126	120	183	192	12	<0.01	0.51
Lysine	TCA, PM	118	119	164	232	9	<0.01	<0.01
Phenylacetate	TM	347	480	582	640	24	<0.01	0.12
Phenylacetylglycine	TM	83	72	135	105	6	<0.01	0.05
Proline	APM, GM, TCA	155	160	220	173	7	<0.01	0.01
Tyrosine	TM, SMB	42	36	49	61	5	<0.01	0.05
Butanoate Metabolism								
3-Hydroxybutyrate	BM	64	78	90	110	6	<0.01	0.65
4-Hydroxybutyrate	BM	206	217	253	240	18	0.08	0.48
Acetoacetate	BM,TM, PM	67	64	78	80	4.5	0.01	0.5
Butyrate (mM)	BM	9	8	10	15	0.5	<0.01	<0.01
Fumarate	BM, BOP, TCA	8	11	7	12	0.7	0.12	0.24
Caffeine Metabolism								
Caffeine	CM	23	16	25	17	1.5	0.19	0.47
Glycolysis / Gluconeogenesis								
1,3-Dihydroxyacetone	GLM, GL	16	6	7	6	0.7	<0.01	<0.01
Acetate (mM)	AM, GL	60	56	55	67	1.5	0.06	<0.01
Ethanol	AM, GL	202	241	355	425	42	<0.01	0.76
Glucose (mM)	GL, GNG	0.5	0.7	1.1	2.5	0.1	<0.01	0.01
Glycerol	GaM, GNG	144	158	236	265	13	<0.01	0.54
Lactate	PM, CC	157	174	282	180	17	0.02	<0.01
Maltose	SSM	71	82	78	133	14	<0.01	0.13

Phospholipid Metabolism								
Choline	GPL	18	13	17	25	2	<0.01	<0.01
Ethanolamine	GPL	86	74	153	184	12	<0.01	0.79
Methane Metabolism								
Dimethylamine	MM	10	21	41	51	7	<0.01	0.6
Methylamine	MM	28	90	108	703	19	<0.01	<0.01
N-Nitrosodimethylamine	MM	88	70	110	120	4.5	<0.01	<0.01
Formate	MM, SMB, NM	160	163	160	275	31	0.02	0.08
Nucleotide Metabolism								
Hypoxanthine	PPM	52	76	85	205	11	<0.01	<0.01
Ribose	PPM, AAM	311	323	406	255	17	0.28	<0.01
Uracil	PPM, CF, MM	113	142	234	270	16	<0.01	0.85
Xanthine	PPM, CF, SMB	60	92	117	178	11	<0.01	0.18
TCA Cycle								
Fumarate	TCA, AAM, PPS	9	11	8	12	0.8	0.12	0.24
Nicotinate	TCA, SMB, AAM	37	43	62	41	3	0.03	<0.01
Propionate (mM)	TCA, PPM, AAM	17	18	23	32	1.5	<0.01	0.01
Succinate	TCA, BSM,BM	112	125	158	118	11	0.32	0.02
Phenylpropanoid synthesis								
Ferulate	PPS, BSM	17	21	14	20	1.5	0.65	0.27

[1]Only metabolites unique to NMR are shown. More metabolites were measured but because their concentrations were also measured by GC-MS and DI-MS and were not found to be statistically different, these data are not given here. Rumen fluid for the analysis was collected shortly before the morning feeding on days 12 and 21 of each experimental period. Cows were fed once daily at 0800.

[2] Linear indicates linear effect of dietary treatment, square indicates a quadratic effect of dietary treatment.

[3]Amino acid metabolism: **AAM**, Glycerolipid metabolism: **GLM**, Acetaldehyde mtabolism: **AM**, Glycolysis: **GL**, Gluconeogensis: **GNG**, Galactose metabolism: **GaM**, Starch and sucrose metabolism: **SSM**, Propanoate metabolism: **PM**, Cori Cycle: **CC**. Butanoate metabolism: **BM**, Tyrosine metabolism: **TM**, Biosynthesis of phenylpropanoids: **BOP**, Citrate cycle: **TCA cycle**, Secondary metabolite biosynthesis: **SMB**, Arginine and proline metabolism: **APM**, Phenylalanine metabolism: **FM**, Protein digestion and absorption: **PDA**, Purine/pyrimidine metabolism: **PPM**, Pentose phosphate pathway: **PPP**, Glutathione metabolism: **GM**, Ketone bodies metabolism: **KBM**, Valine metabolism: **VM**, Glycerophospholipid metabolism: **GPL**, Methane metabolism: **MM**, Nitrogen metabolism: **NM**, Caffeine metabolism: **CM**, Phenylpropanoid synthesis: **PPS**.

2.2.2. GC-MS Compound Identification and Quantification

Typical high-resolution GC-MS total ion chromatograms of the ruminal fluid corresponding to diets with 0, 15, 30, and 45% barley grain are shown in Figure 2.2. As can be seen in this Figure, many of the visible peaks can be annotated with a compound name; however, approximately 40% of these peaks remain unidentified. Whereas some of these peaks may be due to derivatization byproducts or degraded metabolites, the lack of a comprehensive GC-MS library for rumen fluid metabolites [the National Institute of Standards and Technology (NIST) mass spectra library contains only a small portion of metabolically relevant compounds; http://www.nist.gov/srd/nist1a.cfm] also limits the attainable coverage from automated library search algorithms. The use of other commercially available reference libraries for GC-MS (i.e., the Fiehn GC-MS library from Agilent, http://www.agilent.com/chem/fiehnlibrary) might have provided a slightly better and more complete coverage of the rumen metabolites.

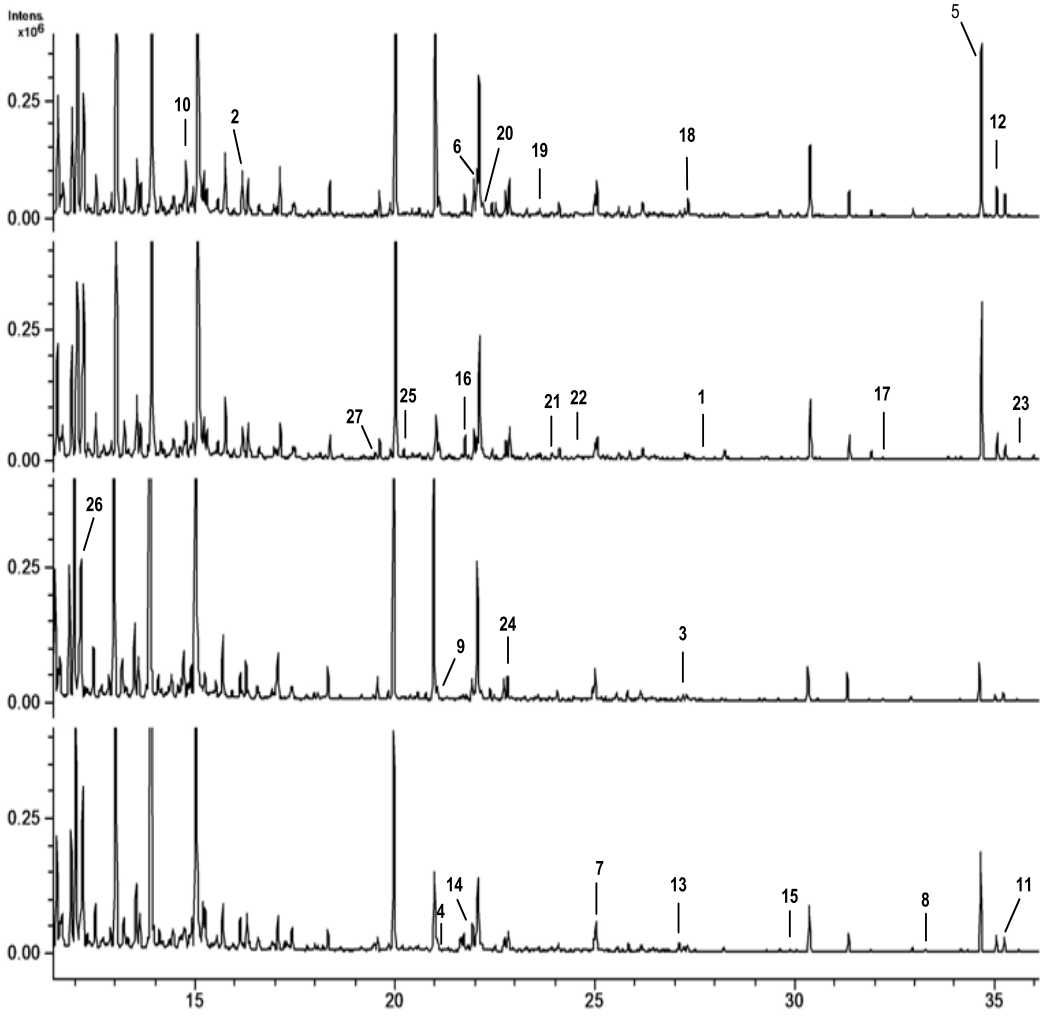

Figure 2.2 Typical GC-MS rumen spectra (0 – 36 RT) from bovine fed A) 0%, B) 15%, C) 30% and D) 45% barley grain

Key; 1: 4-Aminobutyric acid 2, Alanine; 3, Aspartate; 4, Benzoate ; 5, Glucose; 6, Glycine ; 7, 3-Phenylpropionate; 8, Hypoxanthine; 9, Isoleucine; 10, Lactate; 11, Lysine; 12, Mannose; 13, Methionine; 14, Phenylacetate; 15, Phenylalanine; 16, Proline; 17, Putrescine; 18, Pyroglutamate; 19, Serine; 20, Succinate; 21, Threonine; 22, Thymine; 23, Tyrosine; 24, Uracil; 25, Urea; 26, Valerate; 27, Valine; 28, Ribitol

In total, 27 metabolites were quantified via GC-MS of which 10 were unique to this particular platform (Table. 2.2).

Table 2.2 Concentration of rumen metabolites determined by GC-MS. Concentration (μM) of rumen metabolites in dairy cows fed graded amounts of barley grain as determined by gas chromatography-mass spectrometry (LSM ± SEM, n = 8**).**

Metabolites[1]	Metabolic[3] Pathway	Barley grain proportion (% of diet dry matter) 0	15	30	45	SEM	*P*-value[2] Linear	Square
Amino acid Metabolism								
4-Aminobutyrate	AAM, BM	66	76	86	103	5	<0.01	0.46
Hydrocinnamic acid	BM	633	523	488	407	27	<0.01	0.6
Methionine	GM, PM, SMB	20	24	34	47	3	<0.01	0.17
Phenylalanine	SM,TM,S MB	28.	35	65	78	4	<0.01	0.46
Putrescine	APM, SMB, GM	26	52	122	314	12	<0.01	<0.01
Threonine	PDA, MM, SM	23	30	36	41	5	0.01	0.86
Urea (m*M*)	APM, CM, PPM	1	2	3	2.5	0.3	<0.01	0.02
Glutathione Metabolism								
Pyroglutamate	GM	355	384	486	524	20	<0.01	0.8
Nucleotide Metabolism								
Thymine	PPM	40	26	30	30	6	0.4	0.31
Glycolysis								
Mannose	SMB, GL, GaM	123	91	159	210	18	<0.01	0.51

[1]Only metabolites unique to GC-MS are shown. More metabolites were measured but because their concentrations were also measured by NMR and DI-MS and were not found to be statistically different, these data are not given here. Rumen fluid for the analysis was collected shortly before the morning feeding on days 12 and 21 of each experimental period. Cows were fed once daily at 0800.

[2] Linear indicates linear effect of dietary treatment, square indicates a quadratic effect of dietary treatment.

[3]Alanine and aspartate metabolism: **AAM**, Butanoate metabolism: **BM**, Glutathione metabolism:**GM**, Propanoate metabolism: **PM**, Secondary metabolites biosynthesis: **SMB**, Arginine and proline metabolism: **APM**, Phenylalanine metabolism: **FM**, Tyrosine metabolism: **TM**, Protein digestion and absorption: **PDA**, Methane metabolism: **MM**, Sphingolipid metabolism: **SM**, Caffeine metabolism: **CM**, Purine/pyrimidine metabolism: **PPM**, Glycolysis: **GL**, Galactose metabolism: **GaM**.

Comparisons between the NMR and GC-MS measured concentrations (across the 20 compounds that were quantified by both techniques) showed generally good

agreement (within 20 to 30% of each other; data not shown). The ANOVA tests showed 8-fold and 2-fold increases in the rumen concentrations of putrescine and urea ($P < 0.001$), respectively, when feeding cows a 45% barley grain diet (Table. 2.2). Also, increasing the amount of grain in the diet increased the concentrations of 4-aminobutyrate and several amino acids in the rumen fluid, including methionine, phenylalanine, and threonine. In contrast, the concentration of hydrocinnamic acid decreased in cows fed larger amounts of grain (Table. 2.2).

2.2.3. DFI-MS/MS Compound Identification and Quantification

The DFI-MS/MS targeted analysis using the Biocrates Absolute*IDQ* kit provided quantitative results for 45 metabolites (6 acylcarnitines, 12 amino acids, hexose, 15 phospatidylcholines, 9 sphingolipids, and 1 lysophosphatidylcholine; (Table. 2.3). From the 15 measured phospatidylcholines, only 4 provided quantitative data in all samples, whereas the remaining 11 were below the limit of detection in some rumen samples. Note, because bacteria and other microbes do not normally produce sphingolipids (except certain *Sphingomomas spp*) we can be quite certain that most of the detected sphingolipids were from cattle tissues, while the remaining compounds may have their origins from either the rumen microflora and/or the rumen tissue. In our study, the lower limit of quantification by DFI-MS/MS, based on the AbsoluteIDQ kit, was 5 nM for a phospholipid species (PC aa C30:2) and a sphingomyelin SM ((OH) C14:1/d18:1)).Overall, results of ANOVA indicated that increased proportions of barley grain in the diets of dairy cows were associated with decreases in the rumen concentrations of several

phosphatidylcholines and an elevated concentration of rumen fluid hexoses. Our data also showed that feeding dairy cows increasing proportions of barley grain was associated with statistically significant increases of rumen endotoxins and lowering in the ruminal pH (Table 2.4)

Table 2.3 Concentration of metabolites determined by direct flow injection MS/MS

Concentration (μM) of rumen metabolites in dairy cows fed graded amounts of barley grain as determined by direct flow injection MS/MS (LSM ± SEM,n = 8).

Metabolites[1]	Metabolic[3] Pathway	Barley grain proportion (% of diet dry matter)					*P*-value[2]	
		0	15	30	45	SEM	Linear	Square
Amino acid Metabolism								
Arginine	APM,TCA, SMB	18	14	20	44	4	<0.01	<0.01
Glutamine	FM, PPM, NM	830	945	993	907	65	0.25	0.07
Ornithine	APM,GM, SMB	16	16	25	59	4	<0.01	<0.01
Tryptophan	FM, PDA, SMB	8	4	6	10	0.78	0.2	<0.01
Sphingolipid Metabolism								
SM (OH) C14:1	MC, CS, SM	0.002	0.003	0.002	0.002	0.0008	0.76	0.76
SM (OH) C16:1	MC, CS, SM	0.01	0.006	0.007	0.006	0.001	0.07	0.11
SM (OH) C22:1	MC, CS, SM	0.006	0.003	0.005	0.004	0.001	0.47	0.48
SM (OH) C22:2	MC, CS, SM	0.006	0.001	0.001	0.002	0.001	0.04	0.02
SM (OH) C24:1	MC, CS, SM	0.003	0.002	0.002	0.002	0.0005	0.16	0.91
SM C16:0	MC, CS, SM	0.011	0.006	0.003	0.002	0.002	<0.01	0.31
SM C16:1	MC, CS, SM	0.003	0.001	0.001	0.001	0.0006	0.03	0.07
SM C20:2	MC, CS, SM	0.003	0.001	0.001	0.001	0.0008	0.13	0.32
SM C22:3	MC, CS, SM	0.003	0.001	0.003	0.001	0.001	0.43	0.76
SM C24:1	MC, CS, SM	0.009	0.034	0.024	0.006	0.011	0.71	0.05
Glycerophospholipid Metabolism								
PC aa C32:3	GPL, FFAM, MC	0.007	0.01	0.007	0.021	0.003	<0.01	0.06
PC aa C34:1	GPL, FFAM, MC	0.3	0.027	0.03	0.034	0.021	<0.01	<0.01
PC aa C34:2	GPL, FFAM, MC	0.73	0.041	0.028	0.038	0.054	<0.01	<0.01
PC aa C34:3	GPL, FFAM, MC	0.026	0.019	0.015	0.006	0.003	<0.01	0.78
PC aa C36:2	GPL, FFAM, MC	0.642	0.263	0.104	0.019	0.116	<0.01	0.17
PC aa C36:3	GPL, FFAM, MC	0.214	0.029	0.033	0.021	0.025	<0.01	0.01
PC ae C30:2	GPL, FFAM, MC	0.006	0.004	0.004	0.005	0.0009	0.36	0.11
PC ae C34:1	GPL, FFAM, MC	0.021	0.007	0.01	0.012	0.0025	0.03	<0.01
PC ae C34:2	GPL, FFAM, MC	0.011	0.004	0.004	0.008	0.0019	0.27	<0.01
PC ae C36:1	GPL, FFAM, MC	0.057	0.017	0.011	0.015	0.004	<0.01	<0.01
PC ae C36:2	GPL, FFAM, MC	0.044	0.009	0.004	0.008	0.004	<0.01	<0.01
PC ae C38:5	GPL, FFAM, MC	0.016	0.012	0.007	0.007	0.002	0.02	0.043
PC ae C38:6	GPL, FFAM, MC	0.014	0.003	0.002	0.002	0.001	<0.01	<0.01
PC ae C40:2	GPL, FFAM, MC	0.004	0.003	0.003	0.004	0.0009	0.88	0.1
PC ae C40:3	GPL, FFAM, MC	0.005	0.002	0.002	0.004	0.0009	0.56	0.02
lysoPC a C6:0	GPL, FFAM, MC	0.032	0.031	0.026	0.07	0.005	0.36	0.85

Fatty acid Metabolism								
C14:2-OH	FFT, LC	0.013	0.013	0.014	0.013	0.0008	0.9	0.61
C16	FFT, LC	0.029	0.028	0.027	0.036	0.002	0.14	0.07
C16:2	FFT, LC	0.004	0.003	0.005	0.003	0.0008	0.94	0.5
C18:1-OH	FFT, LC	0.015	0.012	0.009	0.013	0.001	0.21	0.05
C3	FFT, LC	0.017	0.016	0.011	0.023	0.002	0.14	<0.01
C3-DC (C4-OH)	FFT, LC	0.166	0.106	0.108	0.135	0.02	0.29	0.03

[1] Only metabolites unique to direct flow injection MS/MS are shown. Rumen fluid for the analysis was collected shortly before the morning feeding on days 12 and 21 of each experimental period. Cows were fed once daily at 0800 h.

[2] Linear indicates linear effect of dietary treatment, square indicates a quadratic effect of dietary treatment.

[3]Arginine and proline metabolism: **APM**, Citrate cycle: **TCA cycle**, Secondary metabolites biosynthesis: **SMB**, Phenylalanine metabolism: **FM**, Purine/pyrimidine metabolism: **PPM**, Nitrogen metabolism: **NM**, Glutathione metabolism:**GM**, Protein digestion and absorption: **PDA**, Sphingolipid metabolism: **SM**, Membrane component: **MC**, Cell signaling: **CS**, Glycerophospholipid metabolism: **GPL**, Free fatty acid metabolism **FFAM**. Lipid catabolism: **LC**, Fatty acid transport: **FFT.**

Table 2.4 Concentration of Ruminal endotoxins determined by LAL assay and ruminal pH

Concentration of rumen endotoxins in dairy cows fed graded amounts of barley grain as determined by LAL assay (LSM ± SEM, n = 8).

Endotoxins and Ruminal pH	Barley grain proportion (% of diet dry matter)				SEM	*P*-value[1]	
	0	15	30	45		Linear	Square
Endotoxin (mg/mL)	0.77	0.94	7.2	9	0.9	<0.01	0.001
Ruminal pH	6.71	6.4	6.1	5.9	0.08	0.12	0.01

Rumen fluid for the analysis was collected shortly before the morning feeding on days 12 and 21 of each experimental period. Cows were fed once daily at 0800 h.

[1] Linear indicates linear effect of dietary treatment, square indicates a quadratic effect of dietary treatment

2.2.4. Diet-Dependent Multivariate Analysis of Rumen Metabolites

Our data show that feeding dairy cows increasing proportions of barley grain was associated with changes in the concentrations of several metabolites. To visualize the difference among the metabolites data, we carried out PCA. A PCA analysis of the complete set of 93 metabolites that were quantified in 64 rumen samples showed that the first 2 PC cover 32% of the observed variance in the sample set (Figure 2.3a). The PCA scores plot revealed the differences corresponding to cows fed different amounts of barley grain, which appeared to be well separated in both PC 1 and PC 2. The clusters corresponding to rumen metabolite profiles from diets with 0 and 15% grain strongly overlapped with each other. However, the clusters representing the 45% grain diets were spaced further apart from those corresponding to the 0, 15, and 30% grain diets. However, the cluster of cows fed 30% grain is located relatively far from the 0% cluster but very close to the 15% cluster (Figure 2.3a).

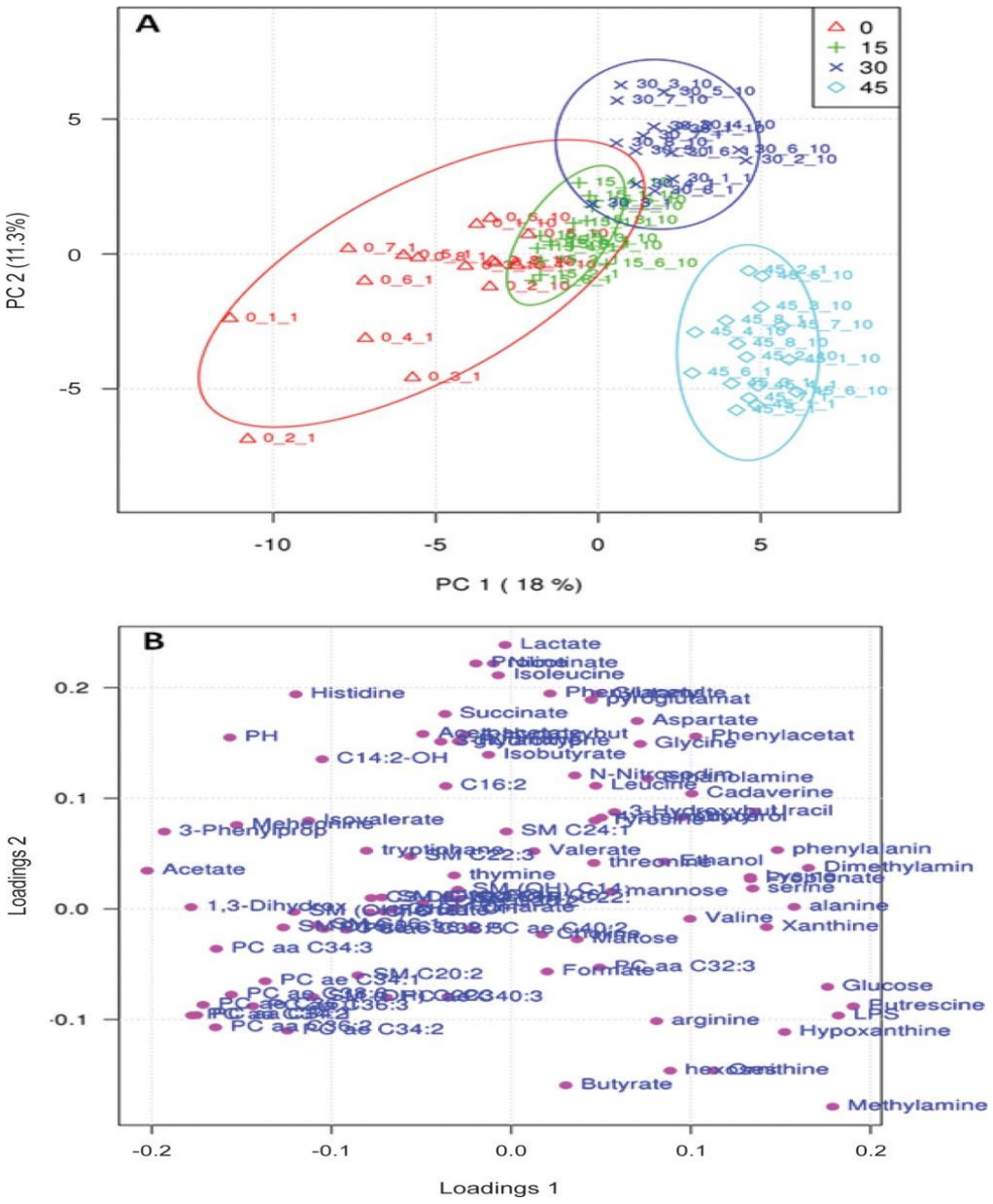

Figure 2.3 Principal component analysis (PCA) based on the rumen metabolites profile data.

A) PCA scores plots discriminating between the rumen fluid of cows fed 0% (open triangle), 15% (+), 30% (X), and 45% (open diamond) rolled barely grain in the diet. The first number in the data points represents the diet (0, 15, 30, and 45), the second is the cow number (1–8 cows), and the third indicates the sampling day (1 and 10). **B)** Scores plot of the 93 commonly detected metabolites projected into the PCA model. Metabolites are labeled by the names used in

Tables 1, 2 and 3. Variables with the same distance from 0 with similar positions are positively correlated. Those in the opposite direction are negatively correlated.

To visualize the individual rumen fluid metabolites responsible for the variation of the first PC (PC 1 and PC 2), we used the corresponding loading plot (Figure 2.3b). This scatter plot gives a graphical representation of the extent to which each metabolite accounts for the variance in the data and shows the relationships/correlations between the different rumen metabolites. Metabolites with the same distance from 0 and with similar directions are positively correlated, whereas those in the opposite direction are negatively correlated. For example, MA, putrescine, hypoxanthine, glucose, and the bacterial membrane component LPS (or endotoxin) are positively correlated to each other with the 45% diet. These metabolites, on the other hand, are negatively correlated with pH and acetate. Those rumen metabolites that are positively associated with each other in the 45% diet appear to play an important role in the separation along the PC 1 axis. The metabolic consequences of the various diets (i.e., 0, 15, 30, and 45% barley grain) were more clearly visible using PLS-DA. The PLS-DA scores plot revealed that it was possible to discriminate not only the 30 and 45% barley grain diets form each other, but more interestingly to separate the 0 and 15% diets (Figure 2.4). The corresponding PLS-DA loading plot indicates that MA, putrescine, hypoxanthine, glucose, and bacterial endotoxin were found to have contributed most to the results of PLS-DA scores plot. The *P*-value for 2,000 permutations was $P < 0.001$.

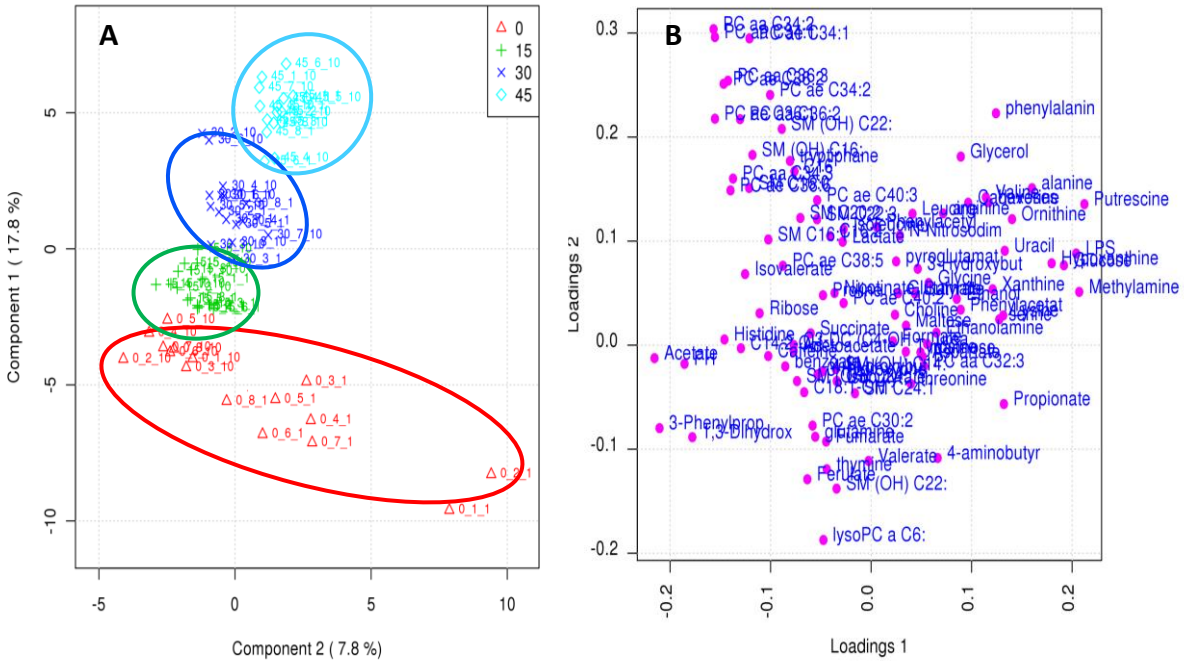

Figure 2.4 Partial Least Squares Discriminant Analysis (PLS-DA) base on the rumen metabolites profile data

A) PLS-DA scores plots discriminating between the rumen fluid of cows fed 0% (open triangle), 15% (+), 30% (X), and 45% (open diamond) rolled barely grain in the diet. The first number in the data points represents diet (0, 15, 30, and 45), the second is about the cow number (1–8 cows), and the third indicates sampling day (1 and 10). **B**) Scores plot of the 93 commonly detected metabolite projection into the PCA model. Metabolites are labeled by their names used in Table 1, 2 and 3. Variables with the same distance from 0 with similar positions are positively correlated. Those in the opposite direction are negatively correlated. The following metabolites were important for the separation as observed in the score plots, with VIP values >1; Putrescine, Lipopolysaccharide, 3-Phenypropionate, Methylamine, Acetate, rumen pH, Glucose, Hypoxanthine, Alanine, Ornitine, 1,3-Dihydroxyacetone, Histidine, Acetoacetate, C 14:2-0H, Phenylalanine.

In addition, PLS-DA allowed the identification of the metabolites that were most important for the separation observed in the scores plots, which are shown in

Figure 2.5 (variables with VIP values >1). Those metabolites that were the most important for the separation of 4 diets (i.e., VIP values >1) were putrescine, 3-PP, MA, acetate, glucose, hypoxanthine, alanine, ornithine, 1, 3-dihydroxyacetone, histidine, acetoacetate, acylcarnitine 3-hydroxytetradecadienoylcarnitine (C14:2-OH), and phenylalanine. Bacterial endotoxin (LPS) and ruminal pH were also found to be important (Figure 2.5).

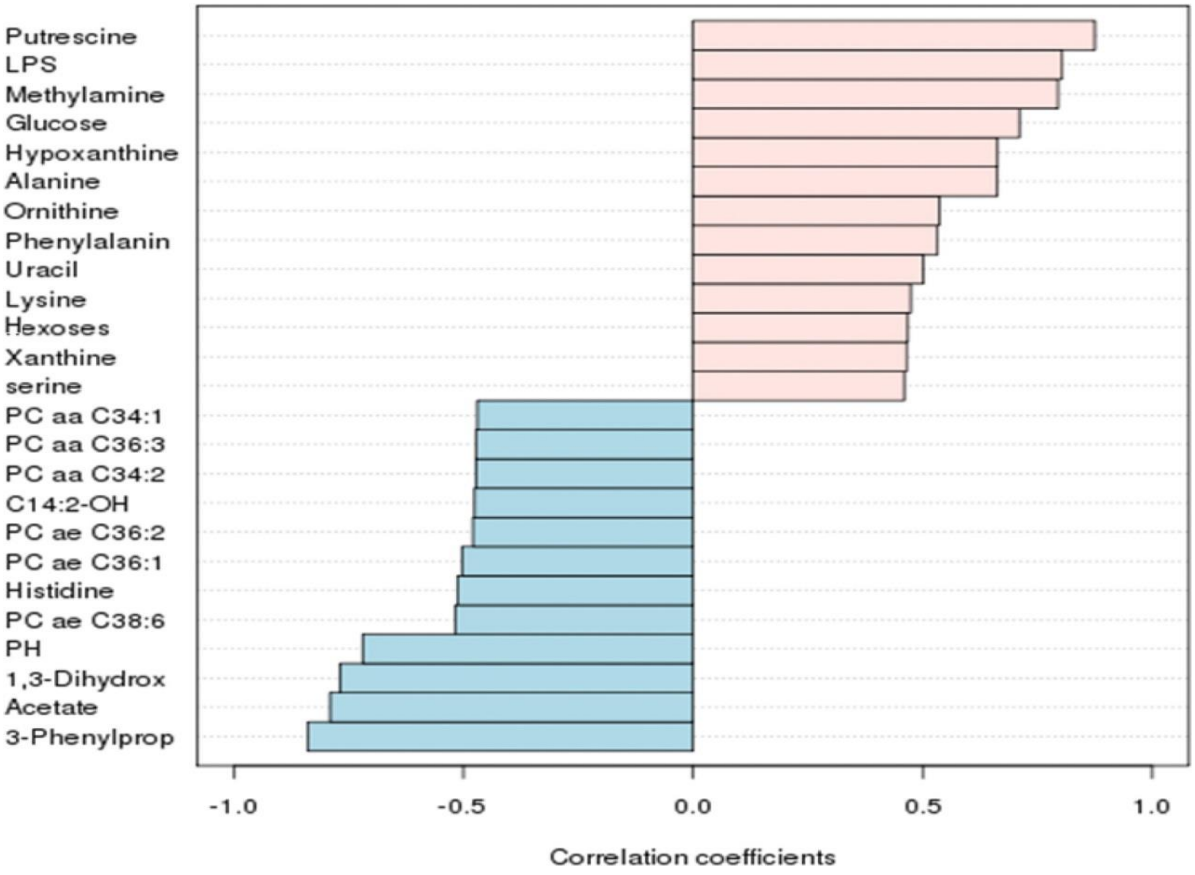

Figure 2.5 A bar graph showing the top 23 ruminal metabolites.
A bar graph showing the top 23 metabolites (along with bacterial endotoxin and ruminal pH) correlating with diet (0, 15, 30, and 45% barley grain). Variables with the same distance from 0 with similar positions are positively correlated. Those in the opposite direction are negatively correlated.

We observed that as the pH increased with feeding high proportion of barley grain, the levels of various organic acids or VFA (acetate, 3-PP, benzoate, and lactate) also. On the other hand, as the level of LPS increased (and the pH decreased), the quantity of amine-containing compounds (methylamine and putrescine) and bases or base derivatives (uracil and hypoxanthine) increased in ruminal fluid. This indicates that a self-regulating ruminal buffering effect exists arising from the production of acids in high-pH conditions and the production of amines or bases in low-pH conditions. To visualize the relationship and differences in the concentrations of rumen metabolites among each sample, we used HCA and a heat map representation (Figure 2.6).

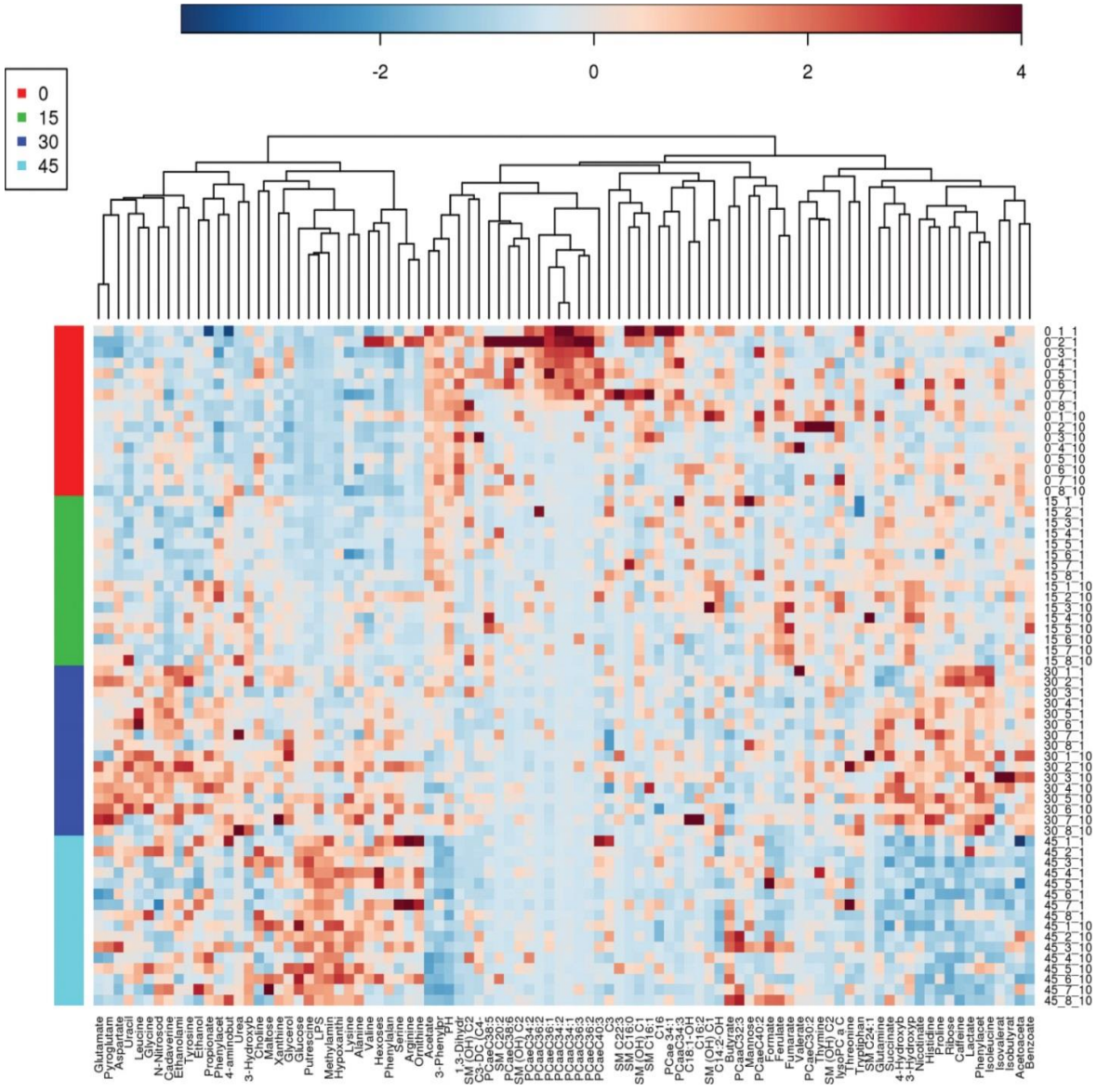

Figure 2.6 Hierarchical clustering analyses for different rumen fluid metabolites.

Metabolites measured before morning feeding in dairy cows fed with four different diets (0, 15, 30, and 45% barley grain inclusion in dry matter). The expression patterns of each parameter (shown in each row) were categorized by an average linkage hierarchical clustering program (*181*). Cells are colored based on the signal intensity measured in rumen. Dark brown represents high rumen levels and blue showed low signal intensity and gray cells showing the intermediate level (see color scale above the heat map).

The dendrogram in Figure 2.6 shows the presence of different subclusters corresponding to different numbers of metabolites with various degrees of similarity.The responses of each variable to the 4 diets are indicated with changes in the color intensity on the heat map. Interestingly, the HCA revealed the presence of 1 cluster consisting of a group of phosphatidylcholines (**PTC**) including PTC ae C36:1, PTC aa C34:2, PTC aa C34:1, PTC aa C36:3, PTC ae C36:2, and PTC ae C40:3, where ae = acyl-alkyl and aa = diacyl. An additional subcluster with the HCA that is associated with high-grain diets comprised glucose, putrescine, MA, hypoxanthine, lysine, and alanine, xanthine and glycerol as well as bacterial endotoxin. Another subcluster revealed by HCA was formed by nicotinate along with histidine, proline, caffeine, lactate, phenylacetate, and isoleucine. A distinct feature of the HCA was that rumen metabolites positioned in the top 2 clusters (i.e., from glutamate to 3-hydroxyphenylacetate along with choline to ornithine) of the heat map showed a clear increase with a higher level of grain in the diet. On the other hand, clusters including phosphatidylcholines, in the middle of the heat map, showed a clear decrease with increased grain in the diet. The heat map for the remaining metabolites seemed to be independent of the amount of dietary grain (2.6).

To visualize the relationship and differences in the concentrations of rumen metabolites among each sample, we used HCA and a heat map representation. The dendrogram in F shows the presence of different subclusters corresponding to different numbers of metabolites with various degrees of similarity. The responses

of each variable to the 4 diets are indicated with changes in the color intensity on the heat map. Interestingly, the HCA revealed the presence of 1 cluster consisting of a group of phosphatidylcholines (**PTC**) including PTC ae C36:1, PTC aa C34:2, PTC aa C34:1, PTC aa C36:3, PTC ae C36:2, and PTC ae C40:3, where ae = acyl-alkyl and aa = diacyl. An additional subcluster with the HCA that is associated with high-grain diets comprised glucose, putrescine, MA, hypoxanthine, lysine, and alanine, xanthine and glycerol as well as bacterial endotoxin. Another subcluster revealed by HCA was formed by nicotinate along with histidine, proline, caffeine, lactate, phenylacetate, and isoleucine. The heat map for the remaining metabolites seemed to be independent of the amount of dietary grain (Figure 2.6).

2.2.5. Multivariate Data Analysis of Different Measurements Days

Multivariate data analysis was also used to differentiate between ruminal fluid groups collected at d 1 and 10 of the measurement period (Figure 2.7). These data revealed interday variations of the rumen metabolite profiles based on the collection day of the ruminal fluid samples (d 1 and 10). The 0 and 30% barley grain diets did not seem to exhibit any separation of the corresponding clusters, as shown in Figures 2.7A and 2.7C, respectively. However, the 15 and 45% diets revealed 2 distinctive patterns in the corresponding scores plot on Figures 2.7B and 2.7D, respectively, which was more evident in the 15% diet (Figure 2.7B). The PLS-DA allows for the identification of the metabolites that were important for the separation of these 2 groups at d 1 and 10.

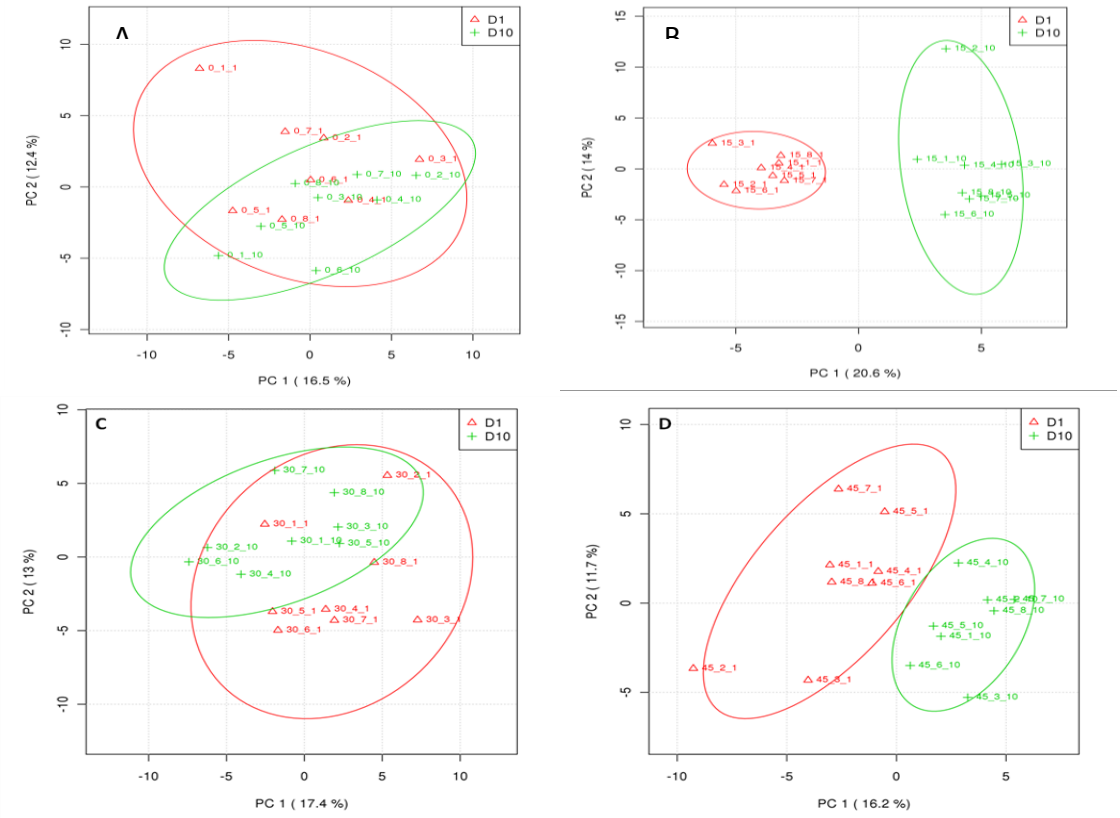

Figure 2.7. Principal component analysis (PCA) of rumen metabolites on different sampling days.

The open triangle shows the rumen fluid of cows collecting at day 1 and "+" shows the rumen fluid of cows collecting at day 5. The first number in the data points represents diet (0, 15, 30, and 45), the second is the cow number (1–8 cows), and the third indicates sampling day (1 and 10); a, b, c, and d show PCA score plots discriminating between rumen fluid metabolites collected from cows on days 1 and 10 of the measurements period that were fed 0, 15, 30, and 45% rolled barely grain in the diet, respectively. The following metabolites were important for the separation observed in the score plots, with VIP values >1; diet with 15% grain: Aspartate, Alanine, Hypoxanthine, Methylamine, Glucose, Putrescine, 3-Phenypropionate, Lipopolysaccharide, Ferulate, 3-Hydroxyphenylacetate, Xanthin, Formate, Succinate, Histidine, 1,3-Dihydroxyacetone; diet with 45% grain: Aspartate, 3−Phenylpropionate, Methylamine, Putrescine, pH, Hypoxanthine, Alanine, Glucose, Ferulate, Formate, Valerate, Xanthin, 3-Hydroxyphenylacetate, Histidine.

2.3 Discussion

Previously, we reported that feeding graded amounts of barley grain to dairy cows was associated with major changes in the concentrations of various rumen fluid metabolites (*169*). In that study we used ^{1}H NMR to identify and quantify 46 different metabolites in the rumen fluids of dairy cows. Here, we used 2 more metabolomics platforms (GC-MS and DFI-MS/MS) along with ^{1}H NMR to analyze rumen fluid samples. By using a quantitative, multiplatform approach, the number of measured rumen metabolites was increased to 93. To our best knowledge, this study is the first comprehensive report that used multiple quantitative metabolomic approaches coupled with multivariate analyses to identify a large number of metabolites and their patterns in the rumen fluid of dairy cows fed graded amounts of grain in their diet. In our discussion, we will focus on metabolite differences between the 4 different grain diets and their potential contribution to the etiopathology of metabolic disorders in dairy cattle due to the feeding of grain-rich diets.

Results from this study confirmed our previous findings that feeding cows 4 different diets (0, 15, 30, and 45% rolled barley grain) is associated with major shifts in the profile of common as well as uncommon rumen metabolites including SCFA, amino acids, ethanol, endotoxin, and MA (*169*). In addition, the present study revealed major changes in other metabolites that are not typically seen in rumen fluid. These new data both complement and further advance our knowledge regarding the effects of grain-rich diets on rumen metabolism, especially with regard to rumen and host health.

For example, in this study, a multifold increase in the concentrations of many other biogenic amines besides MA such as putrescine, cadaverine, and dimethylamine was observed. Also, feeding increasing amounts of grain augmented the concentrations of ethanol, N-nitrosodimethylamine, and ethanolamine in the ruminal fluid of dairy cows. Interestingly, these data showed that rumen concentrations of the biogenic amines were greater on d 10 (end of the experiment) as compared with d 1 of the measurement period. The source of biogenic amines in the rumen of cattle is related to diet and most importantly to the ruminal pH and rumen microbiota (*182*). Rumen biogenic amines derive from the decarboxylation of amino acids by the activity of certain types of rumen microbiota (*183*). The most common biogenic amines (i.e., MA, cadaverine, and putrescine) in ruminants are produced from decarboxylation of arginine, lysine, and arginine/ornithine, respectively. Feeding diets rich in grain lowers ruminal pH, and the pH level in the lumen of the gastrointestinal tract is an important factor that influences the amino acid decarboxylase activity of microbiota. Indeed, amino acid decarboxylase activity has been reported to be greater when the pH is decreased to an acidotic level (*184*). Data from our study show that cows fed 30 and 45% barley grain had a rumen pH below 5.8 for up to 6 to 12 h postfeeding (*7*). Such low pH levels are typically associated with SARA in cows (*170*). The association between low rumen pH and a release of large amounts of glucose and amine-containing compounds (MA, putrescine, hypoxanthin, and ornithine) can also be attributed to the effects of low pH on the diversity of microbiota in the rumen. The sudden availability of easily degradable starch from barley grain,

acting as a specific substrate to amylolytic microbiota, lowers rumen pH and induces a selective and explosive proliferation of certain bacteria species in the rumen. Recent research has demonstrated that switching diets from forage to cereal grains, as done in our study, is associated with increasing counts of starch- and sugar-degrading bacteria in the rumen, such as *Streptococcus bovis* and *Lactobacillus* spp.(*168*). Results of in vitro studies, using equine cecal contents and starch as the carbohydrate source, have shown that streptococci and lactobacilli are the main species having the capacity to decarboxylate certain amino acids and produce biogenic amines (*185*).

The precise pathophysiological functions of biogenic amines are not yet fully understood. However, due to their structural similarities with endogenous amines, such as the catecholamines, many of the biogenic amines generated in the gastrointestinal tract are hypothesized to have effects on vascular function, if they are translocated into the circulation (*97*). The latter authors also discussed involvement of gastrointestinal tract-derived biogenic amines in the etiopathology of laminitis in horses fed starch-and fructan-rich diets. Cattle fed large amounts of grain typically are affected by laminitis (*5*) but the exact mechanisms behind bovine laminitis in cattle fed grain-rich diets are not well understood. A potential implication of large amounts of biogenic amines produced in the rumen of cows fed large amounts of grain in bovine metabolic disorders such as laminitis needs to be investigated in the future.

Other studies indicate also that biogenic amines are involved in other pathological processes in the host. Intriguingly, studies of putrescine metabolism in animals indicate that the absorbed putrescine is degraded through oxidative deamination, catalyzed by amine oxidases, resulting in the production of aldehyde and hydrogen peroxide (*186, 187*). Putrescine serves as a precursor to spermidine and spermine (*188*), and ruminant animals express plasma amine oxidase, which oxidizes both spermidine and spermine (*189*) into aldehyde and hydrogen peroxide. Aldehydes and hydrogen peroxide are known as extremely toxic compounds for a variety of eukaryotic cells and can cause oxidative stress, which may contribute to periparturient disorders and may be associated with metabolic diseases (*190*). Besides the toxicity in the systemic circulation, the release of putrescine might also be harmful for the rumen itself. Because the rumen is deficient in catalases, hydrogen peroxide tends to accumulate in the rumen, a result that might be very toxic to ruminal protozoa and rumen epithelial cells (*191*).

One of the most interesting findings from this study is the concentration of ethanolamine and maltose that linearly increased with increasing amounts of barley grain in the diet. To our knowledge, this is the first report demonstrating a direct relationship between feeding large amounts of grain and the release of large amounts of ethanolamine in the rumen fluid of dairy cows. Ethanolamine is a nutrient derived from phosphatidylethanolamine, which is the most abundant phospholipid in membranes of shed enterocytes (*192*). The exact mechanism(s)

regarding how ethanolamine is released in the rumen fluid of cows fed large amounts of grain is not known; however, we hypothesize that the shifts occurring in the microbial activity (*168*), and changes in the turnover of epithelial cells (*193*) as well as the cell lysis of ruminal microbiota (*194*), might also be a source of ethanolamine in the rumen in response to grain-rich feeding. Intriguingly, new research has indicated that ethanolamine can be used by pathogenic gram-negative bacteria (enterohemorrhagic *E. coli* strain O157:H7) as a nitrogen source, conferring a growth advantage over other commensal microbiota. For example, the studies by (*195*) and (*196*) showed that a burst of 2 major pathogenic bacteria such as *Salmonella enterica* and enterohemorrhagic *E. coli* was promoted by the presence of ethanolamine in the lumen. So, the ability of enterohemorrhagic *E. coli* strain O157:H7 to use ethanolamine as a nitrogen source provides it with the nutritional and competitive advantage to survive during nutritional stress that leads to human illnesses such as diarrhea, hemolytic-uremic syndrome, and hemorrhagic events (*197*). These diseases are often associated with direct contact through the dairy farm environment, fecal contamination of meat at slaughter, and vegetables that have been fertilized with cattle manure (*198, 199*). These data indicate that the release of such metabolites during periods of nutritional stress might be critical for multiplication of certain pathogenic bacteria with relevance for both animal health and food safety. The fate of ethanolamine is its degradation by bacteria to ethanol and acetate (*195*). As might be expected, the concentrations of ethanol and acetate were also increased in cows fed large amounts of grain as seen in the current study.

Barley grains are the main source of starch in ruminant diets. Starch is normally hydrolyzed to maltose, a disaccharide (glucose-α-glucoside) by enzymatic activity. Catabolism of the disaccharide maltose provides a competitive advantage in vivo to pathogenic *E. coli* O157:H7 during the initiation stage of colonization in intestine that used maltose for its growth (*200*). A specific maltose-binding protein, as a part of maltose transport system is located in the periplasmic space of the cell wall of *E. coli*. The 2-fold increase in the concentration of ethanolamine and maltose in the rumen of cows fed 45% barley grain in diets may explain why cattle fed grain had higher populations of this pathogenic *E. coli* than in cattle fed only hay (*201*). This may also explain the observation that when these cattle were abruptly switched from a high-grain diet to an all-forage diet, the total populations of *E. coli* decreased 1,000-fold within 5 d. These questions had never been conclusively answered to date.

Another interesting observation arising from this study was the increased rumen concentrations of urea, hypoxanthine, xanthine, uracil, ornithine, LPS, and alanine. These metabolites were associated with feeding of high-grain diets to cows and we found that their concentrations were elevated with increasing proportions of barley grain. All 6 metabolites are degradation products of rumen bacteria as discussed previously (*202*) demonstrated that bacterial nucleic acids (i.e., RNA or DNA) incubated with rumen fluid rapidly degrade into xanthine, hypoxanthine, and uracil. It is also known that the death of gram-negative bacteria is associated with the release of LPS and alanine (*203*). It is well

established that the decrease in the rumen pH in dairy cows fed high-grain diets is associated with major changes in microbiota composition, as many microbial species are not able to survive the stress of the low pH (*204*).

Still another interesting observation from our study that is tied to the low pH conditions in the rumen is that the rumen fluid concentration of urea rose with increasing levels of grain in the diet. In fact, the concentration of urea peaked at 3 m*M* when cows were fed a 45% barley grain diet. This is consistent with data collected by (*205*) who observed high concentrations of urea in the ruminal fluid of sheep fed grain diets. The presence of urea can be quite problematic, due to its rapid hydrolysis to NH_3 by microbial enzymes in the rumen (*206, 207*). This is because NH_3 can be absorbed through the rumen wall into blood and tissues, where it is toxic. Urea toxicity or high levels of NH_3 in the blood can lead to dyspnoea, excessive salivation, frothing, ataxia, weakness, abdominal pain, violent struggling, and bellowing (*208*). Because the concentrations of CP were similar among the 4 diets of the current study, higher urea concentration in the rumen fluid of dairy cows fed large amounts of grain can be explained either by a higher rate of bacterial degradation or by a more rapid conversion of ammonia to urea as a result of the lower rumen pH (*209*).

Ornithine also has been shown to be produced by ornithine carbamoyltransferase in the catabolic pathway of arginine in many microorganisms (*210*) including rumen bacteria and protozoa (*211*). For example, ciliates are known to release ornithine into the ruminal fluid (*212*). Altogether, the increased concentrations of

hypoxanthine, xanthine, uracil, alanine, ornithine, ethanolamine, and endotoxin in the rumen fluid of cows on a high-grain diets appears to be a result of the induction of widespread bacterial cell lysis and a fundamental change in the rumen microflora.

We also found high concentrations of glucose in the rumen of dairy cows fed the greatest amounts of barley grain (i.e., 30 and 45%). Normally, glucose levels are very low in ruminal fluids but higher levels can be found in cattle fed diets high in starch or other rapidly fermentable carbohydrates (*213*). Furthermore, the presence of glucose in the rumen fluid of cows fed large amounts of grain might explain why those cows had greater concentrations of lactate in the rumen. Lactate is produced by lactate-producing bacteria such as *Streptococcus bovis* and *Lactobacillus* spp., which are more tolerant to the acidic (low pH) conditions. Consequently, these microbes gradually replace other normal rumen microorganisms and tend to become the major components of the rumen microbial population by using glucose as their main substrate (*214*). In our study, besides lactate and propionate, the concentration of butyrate was also increased in the rumen of cows fed large amounts of grain. Butyrate is also produced by the catabolism of lactate in the rumen fluid of cattle fed grain-rich diets in response to a decrease in ruminal pH. In contrast to lactic acidosis, which is characterized by low pH and increased lactate levels only, SARA is an intermediate state where microbial fermentation is instable and oriented to the production of butyrate, propionate, or both at the expense of acetate as observed in this study. The

changes in the SCFA profile in favor of lactate, propionate, and butyrate in response to feeding large amounts of grain arise from changes in the propionate and valerate anabolic pathways of rumen bacteria (*215*). This also arises from shifts in the populations of bacteria and protozoa. For example, (*216*) suggested that the increase in ruminal protozoa concentration could play a central role in butyric SARA by promoting butyrate production from lactate. Greater rumen concentrations of lactate, propionate, and butyrate in response to feeding large amounts of grain found in this study were expected and also agree with previously reported studies (*164, 169, 170*).

In addition to substantial changes in the organic acid and pH profile of rumen fluid from cows on grain-rich diets, we also found a 2-fold increase in the rumen concentration of ethanol in cows fed 30 and 45% barley grain diets. This increase in ethanol is due to the high abundance of fermentable carbohydrates in grain that first give rise to glucose, which later converts to ethanol (*217*). Another route to the generation of ethanol in the rumen is also from the degradation of ethanolamine (*195*). Because ethanolamine also was increased in this study with increasing amounts of grain, it is reasonable to suggest that ethanolamine during SARA is also a source of ethanol in the rumen. This is in agreement with previously reported data on ruminants that indicate that overfeeding them with grain is associated with ethanol concentrations in rumen as high as 8 m*M* (*218*). One study also reported rumen ethanol concentrations above 2 m*M* in dairy cows fed a TMR containing 54% corn silage and 13.5% rolled barley grain (*219*).

Exposure to high concentrations of ethanol in the lumen of the gastrointestinal tract has been reported to have significant consequences for the host. For example, alcohol exposure can promote the growth of gram-negative bacteria in the intestine, which may result in accumulation of endotoxins (*220*). In addition, alcohol metabolism by gram-negative bacteria and intestinal epithelial cells can result in the accumulation of acetaldehyde, which in turn can increase intestinal permeability to endotoxins. Further research is warranted to elucidate the role of ethanol accumulation in the rumen on the permeability of the rumen epithelia to rumen LPS and other toxic compounds that build up in the rumen during SARA. These compounds might have major consequences to the host health.

An interesting metabolite that was revealed by our HCA is nicotinate or niacin. It should be pointed out that nicotinate did not increase with higher proportions of barley grains in the diet (i.e., 45%). (*221*) found that nicotinate is widely distributed in feeds as niacin in cereals has limited availability for some animal species. Furthermore, the availability of niacin for both host and rumen microbes may be limited when cattle are fed low-roughage diets. Many bacterial species, capable of synthesizing nicotinate, have been identified in rumen contents (e.g., *Bacterium ruminicola* spp., *Bacteroides succinogenes, Ruminococcus flavefaciens, Lachnospira multiparus, Streptococcus bovis,* and *Butyrivibrio*; (*222*). Dietary nicotinate tends to be converted to dinucleotide coenzymes NAD and NADP, which serve as co-substrates in many energy-yielding oxidation-reduction processes. In particular, Hino and Russell in 1985_found that NAD

favors the deamination of amino acids. Oxidation of NADH to NAD had a marked effect on the deamination of branched-chain amino acids, whereas neutral and charged amino acids tended to be unaffected (*223*). So our data suggest that the presence of nicotinate in the rumen favors the deamination of amino acids, which may partly explain the elevated ruminal levels of biogenic amines noted earlier.

Whereas many rumen metabolites increased with increasing levels of grain in the diet, a few compounds were found to decrease. In particular, our data indicated that the concentration of 3-PP linearly decreased with increasing proportions of grain in the diet. In contrast, the opposite effect was observed with regard to ruminal fluid concentrations of phenylacetate. This result confirms previous findings by our team where feeding cows large amounts of grain was associated with lowered levels of 3-PP (*169*). Research conducted in forage-fed sheep has shown that the latter 2 compounds are important aromatic acids in ruminal fluid, with 3-PP and phenylacetate accounting for about 50.8 and 13.5% of total aromatic acids in the rumen fluid, respectively (*224*). Our results demonstrated that the ratio between these aromatic compounds could change with increasing amounts of grain in the diet. Phenylacetate and 3-PP in the rumen are generated by the hydrogenation activity of ruminal microbes on plant phenolic compounds such as *p*-coumaric, ferulic, and caffeic acids, followed by a dehydroxylation process (*225*). An alternative origin of 3-PP and phenylacetate is also possible via the deamination of aromatic amino acids such as tyrosine and phenylalanine (*226,*

227), but to our knowledge no studies have linked the concentration changes of 3-PP and phenylacetate to the overall health of the dairy cattle.

Another interesting cluster of metabolites, as revealed by HCA and associated with high-grain diets was a group of 6 PTC compounds (i.e., PTC aa C34:1, PTC aa C34:2, PTC ae C36:2, PTC ae C36:1, and PTC ae C38:6), where ae = acyl-alkyl and aa = diacyl. Concentrations of these compounds decreased with increasing amounts of barley grain in the diet. The very low concentrations of PTC in the ruminal fluid could be related to the time of sampling, which was performed before the morning feeding. Phosphatidylcholine is a major phospholipid in ruminants and it is critical for lipid absorption and transport, cell membrane structure, cell signaling, and synthesis of lipoproteins(*228*). Phosphatidylcholine is needed for the synthesis of very low-density lipoproteins, which are responsible for the export of triacylglycerol from hepatocytes. Low levels of choline are often blamed for the accumulation of triglycerides in the liver and development of fatty liver disease in dairy cattle (*229*). The main dietary source of choline in ruminant diets is PTC from plant membrane material (*230*) microbial choline, and choline supplements.

Choline that reaches the small intestine of cows is in the form of PTC, the main phospholipid in the rumen protozoa (*231*). Phosphatidylcholine is present in rumen protozoa as a major component of their cell membranes. Phosphatidylcholines comprise about 3% of the total phospholipids, whereas protozoal biomass accounts for 20 to 50% of the total microbial biomass in the

rumen (*232*). It is assumed that most of the PTC metabolites in the rumen fluid come from protozoa. The density of protozoa in the rumen is correlated with the diet of the animals. It has been reported that grain-rich diets are associated with lowered counts of protozoa in the rumen (Jouany et al., 1989). Results of another two studies showed decreases in the number of protozoa in cows during SARA (*233*), (*168*). Thus, it is suggested that concentration of rumen PTC compounds could be used as biomarkers indicating a decrease of rumen protozoa counts when cows are fed diets with high grain content.

Our study also revealed a temporal variation in the rumen concentration of metabolites occurring between d 1 and 10 of the measurement period, particularly for the diets with the highest levels of grain. Multivariate analysis demonstrated that ruminal fluid collected on d 1 and 10 from cows fed 15 and 45% barley grain could be easily separated on the basis of their metabolite concentrations. The 10 most important metabolites that contribute to this inter-day separation were aspartate, methylamine, putrescine, LPS, alanine, glucose, ferulate, and formate. Their concentrations were increased at d 10 compared with d 1, whereas the concentration of 3-PP and the pH were found to be lower at d 10. These data suggest that high-grain diets (>30%) require longer periods of physiological adaptation than low-grain diets. In a previous study, in which yearling steers were fed 70, 75, 80, and 85% concentrate diets based on steam-flaked corn for 5 d each followed by a 90% concentrate, the ruminal fluid metabolic profiles showed a clear separation at d 1 and 10 (*234*). Bevans et al. (2005) transitioned heifers from

a 40% concentrate diet to a 90% concentrate diet by feeding a diet containing 65% concentrate for 3 d only (*235*). The mean ruminal pH did not differ during the first day but pH became more acidic on d 2 and 3 after introduction of the 65% concentrate diet. The results from our current study indicate that 21 d of feed intake from 45% barley grain was not enough for full diet adaptation and might lead to rumen acidosis in cows.

2.4 Conclusions

As high productivity is expected from dairy cows, the use of readily fermentable diets becomes necessary to meet their very high energy and protein requirements. However, this comes at a cost that leads to significant metabolic imbalances in the rumen and surrounding tissues, which likely contribute to the observed increase in periparturient diseases. Our data show, unequivocally, that increasing amounts of cereal grain in the diet of lactating cows leads to marked increases in the rumen fluid concentrations of putrescine, methylamines, and other biogenic amines. It also leads to increased ruminal acidity and increased levels of endotoxin. High grain consumption also leads to high levels of glucose, alanine, maltose, ornithine, propionate, uracil, valerate, xanthine, and phenylacetate as well as to potentially increased concentrations of *N*-nitrosodimethylamine (NDMA), urea, ethanolamine, maltose, and dimethylamine (DMA). These changes indicate that significant alterations to the rumen microflora are taking place and that these are reflected by widespread cell death (manifested by altered levels of purine metabolites and certain amino acids), the release of harmful or proinflammatory

compounds (endotoxin, urea/NH_3, ethanol, and biogenic amines) into the rumen, and the production of VFA (leading to the acidification of the rumen). The acidification of the rumen also increases intestinal permeability to these compounds. Ruminal acidification due to high grain consumption also leads to further cell death, further microfloral changes, and the release of even more harmful compounds, thereby setting up a vicious cycle not unlike that seen in human gastrointestinal diseases or chronic inflammatory conditions such as ulcerative colitis and Crohn's disease. In addition to these metabolic changes, we have also highlighted how some rumen-derived metabolites (particularly those associated with high-grain diets) have been previously associated with elevated risks or higher incidences of certain periparturient diseases such as SARA, acute rumen acidosis, urea toxicity, fatty liver disease, as well as inflammatory diseases such as mastitis, laminitis, milk fever, and other conditions. These data certainly underline the importance of gaining a better understanding of the biochemical function of rumen as a whole ecosystem. Improvements in our understanding between diet and rumen health, as well as improved methods for monitoring these changes, will enable us to maintain the fine balance between high milk productivity and good herd health.

Chapter 3

The Bovine Ruminal Fluid Metabolome[1]

---

[1]A version of this chapter has been published previously: Saleem, F., Bouatra, S., Guo, A., Psychogios, N., Mandal, R., Dunn, S., Ametaj, B., and Wishart, D. (2013) The Bovine Ruminal Fluid Metabolome, *Metabolomics 9*, 360-378.

Author Contributions

I conducted most of the experiments, analyzed the data and wrote the first draft of the manuscript. The DFI-MS experiments were conducted by R. Mandal. A. Guo, created the bovine ruminal metabolome database (BRDB), S. M. Dunn, provided me with ruminal sample. D. S Wishart, (supervisor and Co-PI), B. N. Ametaj, (co-supervisor and PI) and N. Psychogios, edited this paper.

Introduction

Ruminants, which include cattle, goats, sheep, yaks, water buffalo and llamas, represent one of the most populous and economically important groups of animals in the world. Serving as sources of milk, meat, leather and mechanical assistance (draft animals), domestic ruminants, or livestock, were among the first animals to be domesticated (*236-238*). Now they are found in every continent and number more than 3.5 billion (*239*). Ruminants are distinctive for having a four-chambered stomach, for chewing their cud and for their ability to efficiently process plant material (cellulose) into digestable sugars. This capacity to process cellulose depends completely on the unique microflora found in their rumen. The rumen, or hindgut, serves as the primary site for microbial fermentation of ingested feed for ruminants. It is essentially a large fermentation vat that contains hundreds of different microbial species. Indeed, estimates are that just 1 mL of ruminal fluid contains 10-50 billion bacteria, 1 million protozoa and 1000's of yeast or fungi (*240*). Because the environment inside the rumen is anaerobic, most ruminal microbes are obligate or facultative anaerobes capable of decomposing complex plant material such as cellulose, hemicellulose and starch into simple sugars, which are further fermented to small organic acids, carbon dioxide and methane.

Rumen gives ruminants the ability to digest cellulose-rich feedstuffs and to convert them into a wide range of metabolites that are not only used by the microbes for their own proliferation, but also enable ruminants to absorb these

nutrients for muscle/meat production, milk production and body maintenance. The health of many ruminants, especially cattle, depends critically on the health of their rumen and on efficient rumen metabolism. Several lines of evidence support a role for altered rumen metabolism (due to the feeding of high grain/low fiber diets) leading to a pathological condition in cattle commonly referred to as acute or sub-acute rumen acidosis (ARA or SARA; (*5*). ARA is often accompanied by a greater incidence of metabolic diseases, such as acidosis, fatty liver, laminitis, liver abscesses, displaced abomasum and systemic inflammation (*241*). In dairy cattle, almost 50% of the cows in a given herd can be affected by one or more of these rumen-associated or metabolic diseases (*242*, *243*). Since cattle health, meat quality and milk quality are directly dependent on metabolite production in rumen, a comprehensive analysis of the chemical composition of bovine ruminal fluid (the fluid that bathes the rumen) could offer important biochemical insights into the role that rumen-diet interactions have on cattle health as well as milk and meat quality. Furthermore, because the bovine rumen is a remarkably efficient fermenter capable of converting "waste" cellulose to higher value products (sugar, ethanol, organic acids), further biochemical insights into ruminal fluid composition could potentially help in the development of more efficient biofuel reactors (*244*).

While, comprehensive metabolomic studies of certain human biofluids have been undertaken (*86, 87*), only a few studies have used modern metabolomic technologies to characterize the ruminal fluid in ruminants. One recent study investigated the effects of intra-rumen infusion of short chain fatty acids (SCFA)

in non-lactating heifers by using ^{1}H NMR spectroscopy. More recently, another study looked into the metabolism of rumen epithelial tissue of newborn calves using the same NMR techniques (*245*). Two other studies used ^{1}H NMR to quantify the volatile fatty acid (VFA) concentrations (*246*) and carbohydrate metabolism by *Fibrobacter spp*. in ruminal fluid (*247*). Typically these studies reported on the presence of no more than 10-12 metabolites. As yet, no study has been attempted to comprehensively characterize bovine ruminal fluid. Furthermore, most published studies addressing rumen metabolism or rumen chemistry have focused on dietary effects on a single class of ruminal fluid compounds, such as amino acids, carbohydrates, volatile fatty acids (VFA) and short chain fatty acids (SCFA).

To facilitate future research into rumen chemistry and biochemistry, we believe it is crucial to establish a "baseline" that comprehensively describes the chemical composition of ruminal fluid. Furthermore, we believe it would be particularly helpful for livestock researchers to have a centralized, comprehensive, electronically accessible database of the detectable metabolites found in ruminal fluid. In an effort to address these issues we have decided to comprehensively characterize the bovine ruminal fluid metabolome and to assemble a ruminal fluid metabolome database. In doing so, we have used a combination of both experimental and literature-based research. Experimentally, we used high-resolution NMR spectroscopy, GC-MS, ICP-MS, and DFI-MS/MS, lipidomics and endotoxin (pyrochrome Limulus amebocyte lysate) assays to identify, quantify and validate more than 200 different ruminal fluid metabolites. To

complement these experimental metabolic profiling efforts, we also surveyed and extracted metabolite and diet-association data from more than 1000 journal articles that had been identified through computer-aided literature and in-house developed text-mining software. This "bibliomic" effort yielded data for another 87 metabolites. The resulting Bovine Rumen Database **(BRDB)** (http://www.rumendb.ca) is a comprehensive, web-accessible resource containing these 246 positively identified and quantified rumen metabolites or metabolite species (corresponding to 334 unique structures), their respective concentrations and their diet/disease associations.

3.1 Materials and methods

All experimental procedures were approved by the University of Alberta Animal Policy and Welfare Committee, and animals were cared for in accordance with the guidelines of the Canadian Council on Animal Care (*13*).

3.1.1. Rumen Collection

Ruminal fluid (100 mL) was obtained from 8 healthy cows and 8 cows with rumen acidosis that were fed a basic food ration as per the Nutrient Requirements of Dairy Cattle - NRC (2001) guidelines. All rumen fluid samples were collected through a cannula using a tube fitted with a strainer and a syringe into a 140 mL plastic container. The pH of each rumen fluid sample was determined immediately after collection by a mobile pH meter (Accumet AP61, Fischer Scientific, Ottawa, Ontario, Canada). Subsequently, rumen fluid samples were centrifuged at 6,000 × g for 15 min and the supernatant filtered through a

disposable 0.22-μm sterile, pyrogen-free filter (Fischer Scientific, Fairlawn, NJ). This was done to remove particulate matter, such as undigested feed and cell debris. All rumen fluid samples were frozen to -20 °C within 2 h to minimize any possible metabolite degradation. All rumen fluid samples were thawed on ice for approximately 2 h before use.

3.1.2. Rumen Endotoxin Measurement

The concentration of cell-free endotoxin (or lipopolysaccharide) in the ruminal fluid supernatant was determined by the pyrochrome Limulus amebocyte lysate assay (Associates of Cape Cod Inc., East Falmouth, MA), as described previously (*29*). After thawing, the supernatant (1.5 mL) was diluted 1,000-fold using pyrogen-free Limulus amebocyte lysate reagent water and pyrogen-free test tubes (Associates of Cape Cod Inc.). Commercially available kits (Associates of Cape Cod Inc.) were used for the assay. The method and the quantity of reagents described in the kit were modified to have standard ranges of 0.625-10 ng/mL. Control endotoxin samples containing 10 ng of endotoxin per vial (Associates of Cape Cod Inc.) were used to prepare the standard solutions. Samples were tested in duplicate, and the optical density values read on a microplate spectrophotometer (Spectramax 190, Molecular Devices Corporation, Sunnyvale, CA) at a wavelength of 405 nm. The intra-assay CV was <10% for all assays.

3.1.3. NMR Spectroscopy

Rumen samples were thawed at room temperature whereupon after thawing, 300 μL of ruminal fluid was transferred to a 1.5 mL eppendorf tube followed by

the addition of 35 μL D_2O and 15 μL of a standard NMR buffer solution (11.667 mM DSS (disodium-2, 2-dimethyl-2-silapentane-5-sulphonate)], 730 mM imidazole, and 0.47% NaN_3 in H_2O (Sigma-Aldrich, Mississauga, ON). These samples (350 μL) were then transferred to a standard Shigemi microcell NMR tube for spectral analysis. All ^{1}H-NMR spectra were collected on a 500 MHz Inova (Varian Inc., Palo Alto, CA) spectrometer equipped with a 5 mm Z-gradient PFG Varian cold-probe. ^{1}H-NMR spectra were acquired at 25 °C using the first transient of the tnnoesy-presaturation pulse sequence, which was chosen for its high degree of quantitative accuracy (*248*). Spectra were collected with 256 transients using a 4 s acquisition time and a 1 s recycle delay.

3.1.3.1 NMR Compound Identification and Quantification

Prior to spectral analysis, all FIDs were zero-filled to 64k data points and a line broadening of 0.5 Hz was applied. The methyl singlet of the added DSS served as an internal standard for chemical shift referencing (set to 0 ppm) and for quantification. All ^{1}H NMR spectra were processed and imported into the Chenomx NMR Suite 6.0 software for quantification (*249, 250*) as previously described (*29*). Each spectrum was processed and analyzed by at least two experienced NMR spectroscopists to minimize compound mis-identification and mis-quantification. We also used sample spiking to confirm the identity of several spectral signatures seen in our NMR spectra. This was conducted by adding 50–500 μM of the presumptive compound to selected rumen samples to test if the corresponding ^{1}H-NMR signals changed as expected.

3.1.4. GC-MS compound Identification and Quantification

Prior to analysis by GC-MS the rumen samples were extracted to separate polar metabolites from non-polar (lipophilic) metabolites. The rumen extraction and derivatization protocol for our GC–MS work was adapted from previously described methods (*174*). For polar metabolites, an aliquot of 100 µL of rumen fluid containing 2 µL of ribitol in water (20 µg/mL) was subsequently added as a quantification standard. In order to separate polar and non-polar metabolites the mixture was extracted with 800 µL of cold HPLC grade methanol: double-distilled water (8:1 v/v) and vortexed for 1 min. The sample was kept at 4 °C for 20 min and then centrifuged at 6,000 rpm for 8 min. After centrifugation, 200 µL of the supernatant was evaporated to dryness using a Speedvac concentrator (Savant Instruments Inc., SDC-100-H, Farmingdale, NY).

After evaporation, 40 µL of 20 mg/ml methoxyamine hydrochloride (Sigma–Aldrich) in ACS grade pyridine was added to the extracted residue and incubated at room temperature for 16 hours. After methoximation, 50 µL of MSTFA (N-Methyl-N-trifluoroacetamide) with 1% TMCS (trimethylchlorosilane) derivatization agent (Pierce) was added followed by incubation at 37 °C for 1 h on a hotplate (*251*). GC–MS samples were then vortexed twice throughout incubation to ensure complete dissolution. Derivatized extracts were analyzed using an Agilent 5890 Series II GC-MS operating in electron impact (EI) ionization mode. One µL aliquots were injected (splitless) onto a 30 m × 0.25 mm × 0.25 µm DB-5 column (Agilent Technologies) with helium carrier gas set to a

flow rate of 1 mL/min and initial oven temperature of 70 °C. The oven temperature was increased at 10 °C/min to a final temperature 310 °C, and final run time of 45 min. Samples were run using full scan at a mass range of 50-500 m/z (1.7 scans/sec) with a solvent delay of 12 min. Retention indices (RIs) were calculated using a C8-C20 alkane mixture solution (Fluka, Sigma-Aldrich) as an external standard (*174*). Quantification and identification of trimethylsilated metabolites were performed as previously (*86, 250*)

3.1.5. Direct Flow Injection MS/MS Compound Identification and Quantification

To determine the concentration of amino acids, sugars, acylcarnitines, sphingolipids and glycerophospholipids in these rumen samples, we applied a targeted quantitative metabolomics approach using a combination of direct injection mass spectrometry with a reverse-phase LC-MS/MS. The kit (Absolute*IDQ*™) is a commercially available assay from BIOCRATES Life Sciences AG (Austria). This kit, in combination with an ABI 4000 Q-Trap (Applied Biosystems/MDS Sciex) mass spectrometer, can be used for the targeted identification and quantification of 160 different endogenous metabolites including amino acids, acylcarnitines, biogenic amines, glycerophospholipids, sphingolipids and sugars. The method used combines the derivatization and extraction of analytes, with selective mass-spectrometric detection using multiple reaction monitoring (MRM) pairs. Isotope-labeled internal standards and other internal standards are integrated into the kit's 96-well plate filter for metabolite quantification. The kit was originally validated for plasma/serum samples

although more recently it has been validated for urine and cerebrospinal fluid. The first 14 wells in the kit are used for quality control and standardization, with the remaining 82 being available for sample analysis. A total of eight normal rumen samples were analyzed using the protocol described in the Absolute*IDQ* user manual. Briefly, ruminal fluid samples were thawed on ice and then vortexed and centrifuged at 13,000 x g. Ten µL of each rumen fluid sample were loaded onto the center of the filter on the upper 96-well plate and dried in a stream of nitrogen. Subsequently, 20 µL of a 5% solution of phenyl-isothiocyanate were added for derivatization. After incubation, the filter spots were dried again using an evaporator. Extraction of the metabolites was then achieved by adding 300 µL methanol containing 5 mM ammonium acetate. The extracts were obtained by centrifugation into the lower 96-deep well plate, followed by a dilution step with 600 µL of the kit's MS running solvent. Mass spectrometric analysis was performed on an API4000 Qtrap® tandem mass spectrometer (Applied Biosystems/MDS Analytical Technologies, Foster City, CA) equipped with a solvent delivery system. The samples were initially delivered to the mass spectrometer by LC followed by direct injection (DI). The Biocrates MetIQ software was used to control the entire assay workflow, from sample registration to automated calculation of metabolite concentrations to the export of data into other data analysis programs.

3.1.6. Trace Element Analysis Using ICP-MS

Before trace elemental analysis by ICP-MS was performed, rumen fluid samples were processed as described previously (*252*). In particular, a total of 2 mL (±0.1 mL) of rumen fluid was collected and sonicated in an ultrasound water bath for 10 min in order to obtain a homogeneous dispersion. The sample was then diluted to 10 mL with 2% HNO_3. Trace element concentrations were determined on a Perkin-Elmer Sciex Elan 6000 quadrupole ICP-MS operating in a dual detector mode. Blank subtraction was applied after internal standard correction. A four point calibration curve was used to quantify compounds (0, 0.025, 0.050, and 0.100 ppm for Na; 0, 0.25, 0.50, and 1.00 ppm for Ca, Mg, Fe, K; 0, 0.005, 0.010, and 0.020 ppm for the remaining elements). A typical count rate for a 10 ppb Pb solution would be 150,000 to 200,000 cps. The sample uptake rate was approximately 1 mL/min with 35 sweeps per reading using one reading per replicate and three replicates. Dwell times were 10 to 20 ms for all elements with the exception of As (which was 100 ms). The relative standard deviation (2σ level) for As, Ni, Pb, and Zn were between 5 and 10%. The accuracy of the ICP-MS analytical protocol was periodically evaluated via the analysis of certified reference standard materials (whole rock powders) BE-N and DR-N available from the SARM laboratory at the CRPG (Centre de Recherches Pétrographiques et Géologiques).

3.1.7. Lipidomics - Identification and Quantification

Lipids were extracted from rumen fluid according to the procedure of Bligh and Dyer (*253*). The total lipid extract was partitioned into neutral lipid, glycolipid

and phospholipid fractions on silica Sep-Pak cartridges (Supelco, MO, USA) according to the method of Hamilton and Comai (*254*). Briefly, the cartridge was first washed with 15 mL of chloroform. Total lipid extracts were evaporated to near dryness under a stream of N_2, brought to a volume of 2 mL with chloroform and transferred to the Sep-Pak cartridge. After the sample was loaded onto the cartridge, 2 mL of chloroform was used to wash residual lipid from the original container and transfer it to the cartridge. Subsequently, 10 to 12 mL of chloroform was added to remove the neutral lipids. Glycolipids were eluted by the sequential addition of 15 mL acetone: methanol (9:1 v/v). Finally, 10 mL methanol was added to elute the phospholipids. Subsequently, sterol esters, free fatty acids, triacylglycerols and hydrocarbons were separated from neutral lipid fractions on silica Sep-Pak cartridges (Supelco, MO, USA) using the method described by Christie (*255*). Each fraction was evaporated to near dryness under a stream of N_2.

Fatty acid methyl esters (FAMES) were prepared according to the method of Christie (*255*). A known amount of free fatty acids and cholesterol ester in 2:1 chloroform: methanol (v/v) was taken together with heptadecanoic acid (17:0, used as an internal standard). The mixture was evaporated under a stream of N_2 and to this 1 mL of the methylating reagent (2% sulphuric acid in methanol, v/v) was added. The mixture was incubated at 80 °C for 1 h, cooled on ice for 10 min after incubation and neutralized by 0.5 mL of a 0.5% sodium chloride solution. FAMEs were extracted by the addition of 2 x 2 mL aliquots of hexane and vortexing for 2 min. The two layers were allowed to separate and the upper

hexane layer was collected, and subjected to GC-MS analysis for quantification of fatty acids.

Gas chromatographic analysis of FAMEs was done using heptadecanoic acid as internal standard. Analyses were performed using an Agilent 7890-5975 GC-MS (Agilent technologies) in an Electron Impact (EI) mode. Separation of fatty acids was achieved by injecting 2 µL of the FAMEs mixture onto a cyanopropyl-containing polysiloxane HP 88 column (Agilent technologies). The initial oven temperature was 70 °C (1 min), which was raised to 76 °C at 1 °C/min and then ramped to 250 °C at a rate of 6.1 °C/min. The carrier gas (helium) flow rate was set to 11.6 cm /sec. The injector was programmed to be either splitless or split with a split ratio set 10:1. The quadrupole temperature and the detector temperature were set at 185 °C and 250 °C, respectively. Confirmation of each AME's identity was performed by comparing EI-MS spectra and retention times to laboratory standards (Sigma-Aldrich, St. Louis, MO, USA). Quantification of the lipids and fatty acids was achieved using defined fatty acid methyl ester standards.

3.1.8. Literature Survey of Rumen Metabolites

In addition to the experimental studies of the ruminal fluid metabolome described above, a complete literature review of known metabolites and metabolite

concentrations in ruminal fluid was also conducted. This literature survey was also facilitated by several computational text-mining tools, which were originally developed for the Human Metabolome Database (*79*) One of the most useful programs was an in-house text-mining tool called PolySearch (*256*). This program was used to generate a hyperlinked list of abstracts and papers from PubMed containing relevant information about rumen fluid metabolites and their corresponding concentration data. Specifically, PolySearch compiled a ranked list of metabolites based on the frequency of word co-occurrence with terms such as "rumen", "ruminal", "cow", "bovine" and "cattle" in conjunction with words such as "concentration", "identification", "quantification", "mM", or "micromol". PolySearch also extracted key sentences from the abstracts, then labelled and hyperlinked the metabolites mentioned in the text. From the resulting ~1000 papers and abstracts, we manually extracted metabolite information (metabolite identities, concentrations, and disease states.) and entered the data into our database. The resulting list of literature-derived rumen metabolites helped confirm metabolites found in our experimental analyses. The literature-derived concentration values also simplified some of the searches for putative metabolite matches.

3.2 Results and Discussion

In this study, using a combination of both experimental and literature-based approaches, we have attempted to identify and quantify the endogenous metabolites that can be detected in bovine ruminal fluid. We have deposited this

information into the Bovine Rumen Database or BRDB (http://www.rumendb.ca). This freely available, easily queried, web-enabled database provides a list of the metabolite names, level of verification (confirmed or probable), normal and diet-associated changes and references for all (to the best of our knowledge) bovine rumen metabolites that have ever been identified and quantified in the literature. The BRDB also contains the concentration data compiled from the experimental studies described here. Each rumen metabolite entry in this database is linked to a separate MetaboCard, which provides additional information on the metabolite (up to 110 data fields). The BRDB itself is searchable and supports general text queries including names, synonyms, conditions and diet associations. Clicking on the browse button (on the BRDB navigation panel) generates a tabular view that allows users to casually scroll through the database or re-sort its contents by compound name or by concentration. Clicking on a given MetaboCard button brings up the full data content (from the BRDB) for the corresponding metabolite. The ChemQuery button allows users to draw or write (using a SMILES string) a chemical compound to search the BRDB for chemicals similar or identical to the query compound. ChemQuery also supports chemical formula and molecular weight searches. The BRDB is also capable of performing searches on the basis of NMR chemical shifts (NMRSearch), mass spectra (MS-Search) and GC–MS data (GCMS-Search). Currently the BRDB contains information on 246 metabolites or metabolite species which could be further resolved to 334 metabolites with precisely defined structures. This is not a number that will remain unchanged. Rather it reflects the total number of ruminal fluid metabolites (organic and

inorganic) that have ever been identified and quantified by ourselves and others. Certainly as technology improves, it is anticipated that this number will increase as other, lower abundance metabolites will be detected and will be added to future versions of the BRDB.

3.2.1. The Composition of Bovine Ruminal Fluid

Overall, the composition of bovine ruminal fluid is dominated by phospholipids, inorganic ions and gases, amino acids, dicarboxylic acids, short chain fatty acids, volatile fatty acids, diglycerides, triglycerides, carbohydrate and cholesterol esters. Many of these metabolites are microbial in origin. In the rumen, fermentation occurs under anaerobic conditions. As a result, sugars are metabolized predominantly to volatile fatty acids (VFAs). The principle VFAs are acetic, butyric and propionic acids, which collectively provide the majority of the energy needs for ruminants. A more detailed description of our findings is given in the following 6 sections covering: 1) Literature Review/Text Mining; 2) NMR; 3) GC-MS; 4) FAMEs/GC-MS Lipid Profiling; 5) DFI MS/MS; and 6) ICP-MS.

3.2.2. Literature Survey of Ruminal Fluid Metabolites

The BRDB provides both concentration averages and concentration ranges for 246 rumen fluid metabolites or metabolite species (corresponding to 334 unique structures). In addition to the measured values obtained from our own experimental studies, the BRDB also presents literature-derived concentrations of the metabolites with references to either PubMed IDs or to other texts. In many cases, multiple concentration values are given. This is done to provide

users/readers with a better estimate of the potential concentration variations that different laboratories or technologies may measure. As a general rule, there is very good agreement between most methods and most laboratories. Other than the inorganic ions and gases such as sodium (116 mM), chloride (25 mM), potassium (20 mM), carbon dioxide (16 mM), methane (6 mM), calcium (1 mM), and oxygen (3 μM), the 13 most abundant organic metabolites found in rumen are acetate (55 mM), propionate (30 mM), butyrate (9 mM), tricarballylic acid (8 mM), valerate (3.5 mM), isobutyrate (1.5 mM), glucose (2 mM), isovalerate (1mM), glutamate (830 μM), methylamine (600 μM), formate (500 μM), phenylacetate (300 μM), and hypoxanthine (220 μM). The least abundant metabolites in ruminal fluid include several phosphatidylcholines (PCs), (1-40 nM), lysophosphatidylcholines (40-90 nM), sphingomyelins (SM), (1-40nM), and acylcarnitines (1-7 nM). These data suggest that the current limit of detection for metabolites in ruminal fluid is in the low nanomolar range. As might be expected, many of the least abundant compounds are phospholipids and sphingolipids (likely of endogenous origin from the rumen tissue) while the most abundant molecules, such as CO_2, acetate, propionate, butyrate and isobutyrate are most certainly microbial in origin, representing the main catabolic breakdown products of plant material (such as celluloses, fibre, starches and sugars) being fermented by the rumen microflora. One point that is particularly interesting is the fact that the concentration of the average metabolite in rumen fluid varies by about +/- 50% (such as arginine, fumarate, glycine and hydroxytetradecadienylcarnitine). Therefore, drawing conclusions about potential diet or disease biomarkers without

properly taking into account this variation would be ill advised. Clearly more studies on the contributions to the observed variations in ruminal fluid are warranted, although with hundreds of metabolites to measure for dozens of conditions, these studies will obviously require significant technical resources.

3.2.3. Compound Identification and Quantification by NMR

Figure 3.1 illustrates a typical high-resolution NMR spectrum of ruminal fluid. As seen in this figure it is remarkably simple and surprisingly uncomplicated.

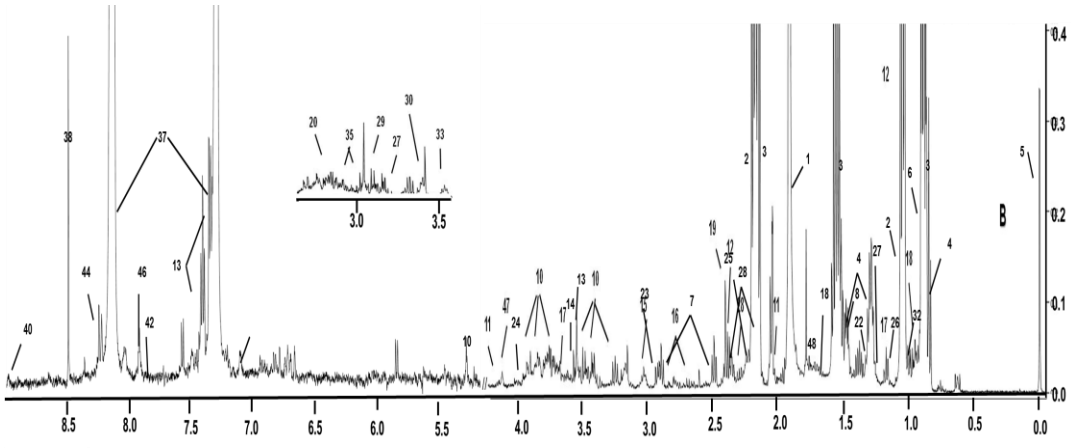

Figure 3.1 Typical 500 MHz 1H-NMR spectra of ruminal fluid.
Key: 1: Acetate; 2: Propionate; 3: Butyrate; 4: Valerate; 5: DSS ; 6: Isovalerate ; 7: 3-Phenylpropionate; 8: Alanine; 9: Isoleucine; 10: Glucose; 11: Proline; 12: Isobutyrate; 13: Phenylacetate; 14: Glycine; 15: Cadaverine; 16: Aspartate; 17: Ethanol; 18: Leucine; 19: Succinate; 20: Glutamate; 21: Methylamine; 22: Lactate; 23: Choline; 24: Fumarate; 25: Acetone; 26: Isopropanol; 27: 3-Hydroxybutyrate; 27: Caffeine; 28: Acetoacetate; 29: 3-Hydroxyphenylacetate; 30: N-Nitrosodimethylamine; 31: Methanol; 32: Valine; 33: Lysine; 34: Dimethylamine; 35: Glycerol; 36: Maltose; 37: Imidazole; 38: Formate; 39: Uracil; 40: Nicotinate; 41: Tyrosine; 42: Benzoate; 43: Histidine; 44: Hypoxanthine; 45: Phenylacetylglycine; 46 ppm line; 47: Ribose; 48: 4-Hydroxybutyrate; 49: Ornithine; 50: Serine; 51: Phenylalanine.

This made the identification and quantification of rumen metabolites relatively easy. Typically 98% of all visible peaks were assigned to a compound and more than 95% of the spectral area could be routinely fitted using the Chenomx spectral analysis software. In other words, the level of spectral assignment is essentially complete. From the ruminal fluid samples of the 8 healthy dairy cows, a total of 50 compounds were positively identified and quantified. The most abundant compounds were propionate (16 mM), acetate (6 mM), butyrate (9 mM), valerate (3 mM), isobutyrate (1.5 mM), ammonia (2.7 mM) and isovalerate (1 mM). The lowest concentration that could be reliably detected using NMR was 8 µM (for ferulate), 10 µM (for dimethylamine) and 18 µM (for choline).

The complete list of compound concentrations (including averages, standard deviations and the frequency of their occurrence) is shown in Table 3.1. Inspection of Table 3.11 also reveals the generally good agreement between the NMR-measured concentrations and those reported in the literature. In total, 47 out of the 50 compounds identified in the healthy control dairy cows, had

concentration values previously reported in the literature. More than 95% (45/47) of these compounds exhibited good agreement with literature values (i.e., meaning the average values from our own experiments fell within one standard deviation of the literature value). In addition, 4 compounds had concentrations somewhat higher than previously reported values (glycerol, L-tyrosine, L-valine, and valerate), while one compound had a concentration lower than previously reported (formate).

Table 3.1 Concentration of metabolites in ruminal fluid samples.

Metabolites	µM; (%Occurrence)	Literature Value	Metabolites	µM; (%Occurrence)	Literature Value
Amino Acids			**Organic acids**		
Alanine[a, b]	220 ± 51 (100%)	205 ± 10*	Fumarate[a]	9±4 (100%)	4 ± 3.0*
Arginine[c]	19 ± 14 (100%)	160 ± 5*	Isobutyrate[a]	1430 ± 228(100%)	1285 ± 235*
Aspartate[a,b, c]	115 ± 47 (100%)	160 ± 5*	Isovalerate[a]	1094 ± 207 (100%)	805 ± 121*
Citrulline[c]	37 ± 20 (100%)	NA	Lactate[a, b]	134 ± 17 (100%)	123 ± 11*
Glutamate[a, c]	333 ± 12 (100%)	330 ± 18*	Nicotinate[a]	37 ± 8 (100%)	24 ± 13*
Glycine[a, b, c]	113 ± 27 (100%)	105 ± 7*	Phenylacetate[a, b]	317 ± 62 (100%)	302 ± 86*
Histidine [a, c]	32 ± 10 (100%)	31 ± 12*	Propionate[a]	16860 ± 5180(100%)	16000±2000*
Isoleucine[a, b, c]	147 ± 42 (100%)	134 ± 14*	Succinate[a, b]	124 ± 21 (100%)	83 ± 12*
Leucine[a,c]	145 ± 46 (100%)	104 ± 7*	Valerate[a]	3044 ± 1092 (100%)	1700 ± 400*

Glutamine[c]	831 ± 251 (100%)	NA	**Misc**		
Lysine[a, b, c]	177 ± 79 (100%)	111 ± 8*	1,3-DHA	17± 5 (100%)	112 ± 6*
Metheonine [b, c]	19 ± 10 (100%)	NA	Cadaverine[a]	66 ± 23 (100%)	65 ± 12
Ornithine[a, c]	19 ± 12 (100%)	NA	Caffeine[a]	23 ± 8 (100%)	13 ± 3*
Phenylalanine[a, b, c]	34 ± 17 (100%)	NA	Choline[a]	18 ± 7 (100%)	16 ± 2*
Proline[a, b, c]	158 ± 24 (100%)	124 ± 9*	Dimethylamine[a]	10 ± 2 (100%)	6 ± 2*
Pyroglutamate[b]	356 ± 45 (100%)	NA	Ethanol[a]	202 ± 55 (100%)	154 ± 32*
Serine[b, c]	49 ± 25 (100%)	NA	Ethanolamine[a]	86 ± 33 (100%)	NA
Threonine[b, c]	25 ± 8 (100%)	NA	Glycerol[a]	144 ± 55 (100%)	97 ± 4*
Tryptophan[a, b, c]	11 ± 5 (100%)	NA	Hypoxanthine[a,b]	63 ± 25 (100%)	111 ± 33*
Tyrosine[a, b, c]	49 ± 12 (100%)	44 ± 4*	Methylamine[a]	49 ± 12 (100%)	85 ± 72*
Valine[a, b, c]	143 ± 52 **(**100%**)**	128 ± 33	NADMA[a]	88 ± 13 (100%)	67 ± 2*
4-aminobutyrate	66 ± 13 **(**100%**)**	NA	PAG[a]	82 ± 9 (100%)	59 ± 5*
Carbohydrates			Thymine[b]	40 ± 23 (100%)	NA
Glucose[a,b]	549 ± 97 (100%)	490 ± 127*	Uracil[a, b]	104 ± 25 (100%)	121 ± 40*
Maltose[a]	71 ± 21 (100%)	52 ± 13*	Xanthine[a]	60 ± 16 (100%)	85 ± 23*
Mannose[b]	125 ± 25 (100%)	NA	Endotoxin(mg/mL	0.77 ± 0.21 (100%)	0.67 ± 0.17*
Ribose[a]	312 ± 40(100%)	258 ± 38*	**Trace elements**		
Organic acids			Copper[d] (Cu)	2.59 ± 0.5 (100%)	1.5
3-hydroxybutyrate[a]	63 ± 13 (100%)	53 ± 12*	Beryllium[d] (Be)	0.06 ± 0.05 (100%)	NA
3-HPA[a]	53 ± 10 (100%)	47± 15*	Boron[d] (B)	1187 ± 105 (100%)	NA
3-phenylpropionate[a, b]	613 ± 100 (100%)	421 ± 35*	Sodium[d] (Na)	113362±3434(100%)	99347[§]
4-hydroxybutyrate[a]	206 ± 82 (100%)	NA	Magnesium[d] (Mg)	102.0 ± 6.0 (100%)	NA
Acetate[a]	61000±5800(100%)	45000 ±2700*	Aluminum[d] (Al)	157.0 ± 5.0 (100%)	NA
Acetoacetate[a]	68 ± 9 (100%)	48 ± 17*	Phosphorus[d] (P)	9202 ± 64 (100%)	6333[§]
Benzoate[a, b]	49 ± 10(100%)	37 ± 4*	Potassium[d] (K)	18120 ± 153 (100%)	27333[§]
Butyrate[a]	9386±1367 (100%)	7400 ± 800*	Calcium[d] (Ca)	931.0 ± 27.0 (100%)	1050[§]
Ferulate[a]	17 ± 8 (100%)	8 ± 5*	Thallium[d] (Ti)	0.430 ± 0.01(100%)	NA

Table 3.1 Continued

Metabolites	**(µM); (% Occurrence)**	**Metabolites**	**(µM); (% Occurrence)**
Ions		**Acylcarnitines**	
Chromium[d] (Cr)	0.34± 0.02 (100%)	Hexadecadienylcarnitine[c]	0.009 ± 0.001 (72%)
Manganese[d] (Mn)	2.5 ± 0.7 (100%)	Octadecadienylcarnitine[c]	0.071 ± 0.001 (13%)
Nickel[d] (Ni)	0.12 ± 0.08 (100%)	Propionylcarnitine[c]	0.036 ± 0.006 (82%)
Lithium[d] (Li)	3.8 ± 0.5 (100%)	Hydroxybutyrylcarnitine[c]	0.140 ± 0.097 (94%)
Vanadium[d] (V)	0.042 ± 0.01 (100%)	Hydroxypropionylcarnitine[c]	0.038 ± 0.004 (19%)
Gallium[d] (Ga)	5.2 ± 0.8 (100%)	Butenylcarnitine[c]	0.037 ± 0.002 (37%)
Rhenium[d] (Re)	0.082 ± 0.001 (100%)	Valerylcarnitinec	0.046 ± 0.011 (24%)
Rubidium[d] (Rb)	5.82 ± 0.08 (100%)	Methylglutarylcarnitine[c]	0.187 ± 0.013 (29%)

Strontium[d] (Sr)	1.43 ± 0.02 (100%)	Tiglylcarnitine[c]	0.053 ± 0.012 (25%)
Yttrium[d] (Y)	0.0053 ± 0.001 (100%)	Glutaconylcarnitine[c]	0.042 ± 0.003 (10%)
Zirconium[d] (Zr)	0.050 ± 0.012 (100%)	Hexenoylcarnitine[c]	0.096 ± 0.001 (5%)
Molybdenum[d] (Mo)	0.0187 ± 0.008 (100%)	Pimelylcarnitine[c]	0.05 ± 0.02 (60%)
Palladium[d] (Pd)	0.023 ± 0.012 (100%)	**Free Fatty acids**	
Antimony[d] (Sb)	0.006 ± 0.001 (100%)	FFA14:0[e]	3.3 ± 0.6 (100%)
Cesium[d] (Cs)	0.005 ± 0.004 (100%)	FFA15:0[e]	1.5 ± 0.3 (100%)
Barium[d] (Ba)	0.58 ± 0.019 (100%)	FFA16:0[e]	243.0 ± 35.0 (100%)
Lanthanum[d] (La)	0.02 ± 0.004 (100%)	FFA16:1(9)[e]	0.6 ± 0.2 (100%)
Cerium[d] (Ce)	0.44 ± 0.23 (100%)	FFA18:0[e]	186.0 ± 27.0 (100%)
Gold[d] (Au)	0.02 ± 0.01 (100%)	FFA18:1(isomer)[e]	12.6 ± 3.4 (100%)
Biogenic amines		FFA18:1(9)[e]	1.1 ± 0.3 (100%)
Dimethylarginine[c]	0.33 ± 0.14 (25%)	FFA18:2(9,11)[e]	3.5 ± 2.6 (100%)
Acetylornithine[c]	1.24 ± 1.24 (100%)	FFA20:0[e]	1.3 ± 0.2 (100%)
Carnosine[c]	0.47 ± 0.24 (100%)	FFA18:3(9,12,15)[e]	0.5 ± 0.4 (100%)
Histamine[c]	5.07 ± 6.37 (100%)	**Cholesterol esters**	
Kynurenine[c]	20.23 ± 0.03 (100%)	CE12:0[e]	2.3 ± 3.1 (100%)
Methioninesulfoxide[c]	20.84 ± 15.4 (100%)	CE14:0[e]	7.3 ± 4.1 (100%)
Phenylethylamine[c]	20.2 ± 6.0 (100%)	CE15:0[e]	3.6 ± 2.3 (100%)
Sarcosine[c]	36.9 ± 30.5 (100%)	CE16:0[e]	107 ± 70 (100%)
Taurine[c]	1.07 ± 0.007 (50%)	CE16:1[e]	1.7 ± 1.3 (100%)
Serotonin[c]	1.02 ± 0.04 (50%)	CE18:0[e]	54.0 ± 34.0 (100%)
Putrescine[b]	28.0 ± 12.0 (100%)	CE18:1(isomer)[e]	23.5 ± 15.7 (100%)
Acylcarnitines		CE18:2(9,11)[e]	15.1 ± 7.3 (100%)
Tetradecenoylcarnitine[c]	0.09 ± 0.001 (13%)	CE20:0[e]	4.4 ± 2.4 (100%)
Tetradecadienylcarnitine[c]	0.02 ± 0.003 (32%)	CE22:0[e]	2.4 ± 1.8 (100%)
Hydroxytetradecadienylcarnitine[c]	0.02 ± 0.012 (54%)	CE22:1(13)[e]	1.1 ± 0.26 (100%)
Hexadecanoylcarnitine[c]	0.03 ± 0.004 (97%)	CE24:0[e]	1.2 ± 0.77 (100%)
Hydroxyhexadecanoylcarnitine[c]	0.01 ± 0.001 (22%)		

Table 3.1 Continued

Metabolites	**(µM); (% Occurrence)**	**Metabolites**	**(µM); (% Occurrence)**
Lysophosphatidylcholines		**Phosphatidylcholines**	
lysoPC a C16:1[c]	0.08 ± 0.02 (24%)	PC ae C32:1[c]	0.012 ± 0.004 (72%)
lysoPC a C17:0[c]	0.07 ± 0.01 (56%)	PC ae C32:2[c]	0.039 ± 0.002 (16%)
lysoPC a C18:0[c]	0.11 ± 0.02 (16%)	PC ae C34:0[c]	0.022 ± 0.004 (13%)
lysoPC a C18:1[c]	0.14 ± 0.04 (27%)	PC ae C34:1[c]	0.025 ± 0.015 (96%)
lysoPC a C18:2[c]	0.16 ± 0.04 (17%)	PC ae C34:2[c]	0.018 ± 0.011 (94%)
lysoPC a C20:4[c]	0.09 ± 0.02 (24%)	PC ae C34:3[c]	0.014 ± 0.006 (44%)
lysoPC a C26:0[c]	0.84 ± 0.03 (16%)	PC ae C36:1[c]	0.06 ± 0.05 (96%)
lysoPC a C16:0[c]	0.14 ± 0.02 (94%)	PC ae C36:2[c]	0.048 ± 0.05 (78%)

Phosphatidylcholines		PC ae C36:3[c]	0.012 ± 0.05 (60%)
PC aa C28:1[c]	0.064 ± 0.005 (19%)	PC ae C36:4[c]	0.023 ± 0.014 (85%)
PC aa C30:2[c]	0.009 ± 0.002 (47%)	PC ae C36:5[c]	0.022 ± 0.003 (10%)
PC aa C32:0[c]	0.040 ± 0.03 (47%)	PC ae C38:1[c]	0.022 ± 0.03 (43%)
PC aa C32:2[c]	0.034 ± 0.003 (54%)	PC ae C38:2[c]	0.055 ± 0.03 (18%)
PC aa C32:3[c]	0.011 ± 0.003 (43%)	PC ae C38:3[c]	0.015 ± 0.019 (47%)
PC aa C34:1[c]	0.312 ± 0.284 (50%)	PC ae C38:4[c]	0.034 ± 0.026 (25%)
PC aa C34:2[c]	0.781 ± 0.666 (100%)	PC ae C38:5[c]	0.024 ± 0.018 (50%)
PC aa C34:3[c]	0.038 ± 0.021 (78%)	PC ae C38:6[c]	0.011 ± 0.013 (82%)
PC aa C34:4[c]	0.009 ± 0.003 (13%)	PC ae C40:2[c]	0.015 ± 0.004 (57%)
PC aa C36:1[c]	0.157 ± 0.135 (29%)	PC ae C40:3[c]	0.018 ± 0.003 (69%)
PC aa C36:2[c]	0.601 ± 0.735 (82%)	PC ae C42:1[c]	0.017 ± 0.002 (10%)
PC aa C36:3[c]	0.211 ± 0.19 (79%)	PC ae C42:3[c]	0.008 ± 0.001 (25%)
PC aa C36:5[c]	0.018 ± 0.019 (57%)	PC ae C44:4[c]	0.030 ± 0.001 (23%)
PC aa C36:6[c]	0.017 ± 0.007 (50%)	PC ae C44:5[c]	0.022 ± 0.004 (14%)
PC aa C38:1[c]	0.091 ± 0.003 (16%)	**Sphingomyelins**	
PC aa C38:4[c]	0.033 ± 0.008 (25%)	SM (OH) (d18:1/14:1)[c]	0.031 ± 0.002 (50%)
PC aa C38:5[c]	0.015 ± 0.007 (32%)	SM (OH) (d18:1/C16:1)[c]	0.01 ± 0.01 (72%)
PC aa C38:6[c]	0.020 ± 0.014 (82%)	SM (OH) (d18:1/22:1)[c]	0.01 ± 0.01 (44%)
PC aa C40:3[c]	0.008 ± 0.002 (31%)	SM (OH) (d18:1/22:2)[c]	0.01 ± 0.01 (40%)
PC aa C40:6[c]	1.81 ± 0.451 (12%)	SM (OH) (d18:1/24:1)[c]	0.043 ± 0.003 (46%)
PC aa C42:2[c]	0.007 ± 0.002 (44%)	SM (d18:1/16:1)[c]	0.043 ± 0.014 (37%)
PC aa C42:4[c]	0.008 ± 0.004 (60%)	SM (d18:1/20:2)[c]	0.018 ± 0.011 (50%)
PC aa C42:5[c]	0.076 ± 0.013 (22%)	SM (d18:1/22:3)[c]	0.013 ± 0.01 (29%)
PC ae C30:2[c]	0.83 ± 0.003 (65%)	SM (d18:1/24:1)[c]	0.04 ± 0.01 (69%)

[a] Metabolites measured by NMR, [b] Metabolites measured by GC-MS, [c] Metabolites Measured by DFI-MS/MS,[d] Metabolites measured by ICP-MS, [e] Metabolites measured by FAMEs/GC-MS and [f]Metabolites measured by pyrochrome Limulus amebocyte lysate assay. **NADMA**: N-Nitrosodimethylamine, **1, 3-DHA**: 1, 3-Dihydroxyacetone, PAG: Phenylacetylglycine, **3-HPA**: 3-Hydroxyphenylacetate. Literature values of metabolites from healthy cows are derived from: *Ametaj et al. (2010b) and [§]Kegley et al. (1990).

Compounds exhibiting the greatest discrepancy between experimental measured values and literature derived values include: glycerol, L-tyrosine, formate and valerate. These discrepancies may be explained by their inherent volatility or chemical instability (esp. valerate and formate). Other discrepancies may be due to sample collection/preservation effects. A third source of variation may be technical problems with the separation or extraction methods being used to obtain

‘‘clean’’ ruminal fluid. In contrast to the healthy controls, the NMR spectra of the rumen fluid isolated from dairy cows suffering from rumen acidosis tended to be somewhat more variable. The same level of spectral coverage (98% peak identification, 95% spectral area) was achieved with these cows as with the healthy cows. The complete list of compound concentrations comparison for the cows with rumen acidosis and healthy cows along with their literature values are shown in Table 3.2. Inspection of Table 3.2 again shows the generally good agreement between the NMR-measured concentrations and those reported in the literature, although there are clear and significant differences between the normal cows and those with rumen acidosis. The most strongly differentiating compounds were D-glucose, butyrate, propionate, phenylactetate, butyrate, formate, hypoxanthine, cadaverine, methylamine, putrescine and L-alanine. The concentrations of these metabolites are significantly higher in ruminal fluid of cows with rumen acidosis as compared to healthy cows.

Table 3.2 Comparison of ruminal metabolites conc. in cows fed graded amounts of grain.

	Barley grain proportion (% of diet dry matter)					*P*-value[§]	
	0	15	30	45	SEM[¶]	Linear	Quadratic
[1]Metabolites conc. (µM)							
1,3-Dihydroxyacetone*	17 ± 5	7 ± 2	7 ± 3	7 ± 2	0.68	<0.01	<0.01
3-Hydroxybutyrate	63 ± 13	77 ± 13	90 ± 23	110 ± 40	5.7	<0.01	0.65
3-Hydroxyphenylacetate	53 ± 10	67 ± 13	65 ± 13	63 ± 25	3.57	0.06	0.02
3-Phenylpropionate	613 ± 100	513 ± 58	475 ± 64	411 ± 115	25.7	<0.01	0.54
4-Aminobutyrate	66 ± 13	76 ± 12	87 ± 14	103 ± 33	4.84	<0.01	0.46
4-Hydroxybutyrate	206 ± 82	217 ± 22	253 ± 94	239 ± 48	17.5	0.08	0.48

Acetate	60100 ± 5800	56350± 7280	54620 ± 7940	64280 ± 6040	1.47	0.06	<0.01
Acetoacetate	68 ± 9	64 ± 9	78 ± 15	80 ± 27	4.33	0.01	0.5
Alanine*	220 ± 51	244 ± 40	314 ±84	441 ± 74	12.1	<0.01	<0.01
Arginine*	19 ± 14	14 ± 7.	20 ± 10	44.5 ± 35.6	4.37	<0.01	<0.01
Aspartate	115 ± 47	122 ± 35	185 ± 50	180 ± 69	12.3	<0.01	0.34
Benzoate	49 ± 10	53 ± 21	70 ± 23	52 ± 33	3.54	0.75	<0.01
Butyrate*	9386 ± 1367	8100 ± 1350	8103 ± 1631	15131 ± 2957	0.45	<0.01	<0.01
Cadaverine*	66 ± 23	51 ± 10	125 ± 24	122 ± 44	6.71	<0.01	<0.01
Caffeine	23 ± 8	16 ± 4	26 ± 6	17 ± 7	1.58	0.19	0.47
Dimethylamine	10 ± 2	22 ± 6	47 ± 45	52 ± 31	7.07	<0.01	0.6
Ethanol	202 ± 55	241 ± 96	355 ± 148	425 ± 259	42.4	<0.01	0.76
Ethanolmine	86 ± 33	73 ± 15	152 ± 55	134 ± 55	11.8	<0.01	0.79
Ferulate	17 ± 8	20 ± 4	13 ± 3	20 ± 11	1.48	0.65	0.27
Formate	160 ± 46	163 ± 33	160 ± 45	276 ± 104	31.5	0.02	0.08
Fumarate	9 ± 4	11 ± 4	8 ± 2	12 ± 4	0.72	0.12	0.24
Glucose*	549 ± 97	523 ± 130	996 ± 334	1806 ± 1305	0.11	<0.01	0.01
Glutamate	333 ± 12	380 ± 59	490 ± 92	517 ± 115	19.9	<0.01	0.82
Glutamine	831 ± 252	946 ± 239	994 ± 358	907 ± 255	64.5	0.25	0.07
Glycerol	144 ± 55	158 ± 11	236 ± 61	265 ± 71	12.8	<0.01	0.54
Glycine	113 ± 27	129 ± 17	165 ± 55	168 ± 70	12.5	<0.01	0.93
Histidine*	32 ± 10	43 ± 9	55 ± 14	29 ± 11	3.46	<0.01	0.01
Hypoxanthine*	63 ± 25	80 ± 24	90 ± 49	205 ± 61	11.5	<0.01	<0.01
Isobutyrate	1430 ± 228	1450 ± 180	1670 ± 530	1815 ± 194	0.08	<0.01	0.46
Isoleucine	147 ± 42	137 ± 40	235 ± 62	183 ± 74	13	0.01	0.02
Isovalerate	1094 ± 207	900 ± 140	1180 ± 420	1133 ± 192	0.07	0.36	0.11
Lactate	134 ± 17	159 ± 22	252 ± 61	180 ± 118	17.2	0.02	<0.01
Leucine	146 ± 46	119 ± 17	183 ± 76	191 ± 44	12.4	<0.01	0.51
Lysine*	177 ± 79	122 ± 26	165 ± 30	232 ± 67	8.28	<0.01	0.01
Mannose	125 ± 25	91 ± 49	159 ± 83	211 ± 86	18.3	<0.01	0.051

Table 3.2 Continued

	Barley grain proportion (% of diet dry matter)					*P*-value[§]	
	0	15	30	45	SEM[¶]	Linear	Quadratic
Methionine	19 ± 10	22 ± 8	32 ± 10	47 ± 19	3.21	<0.01	0.17
Methylamine*	49 ± 12	90 ± 33	108 ± 104	703 ± 119	19.1	<0.01	<0.01
Nicotinate	37 ± 8	43 ± 11	62 ± 17	41 ± 12	3.07	0.03	<0.01
N-Nitrosodimethylamine	88 ± 13	70 ± 11	110 ± 22	121 ± 43	4.52	<0.01	0.02
Ornithine	19 ± 12	17 ± 7	25 ± 12	38 ± 13	3.76	<0.01	0.016
Phenylacetate*	317± 62	462 ± 121	541 ±118	640 ± 101	23.6	<0.01	<0.01
Phenylacetylglycine	82 ± 9	73 ± 14	136 ± 33	104 ± 35	5.85	<0.01	0.05
Phenylalanine	34 ± 17	36 ± 13	64 ± 17	65 ± 20	3.8	0.01	0.46

Proline*	158 ± 24	158 ± 33	220 ± 31	173 ± 29	7.21	<0.01	0.01
Propionate*	16860 ± 5180	18210 ± 3210	22630 ± 8030	31835 ± 6795	1.49	<0.01	<0.01
Putrescine*	28 ± 12	52 ± 17	122 ± 29	214 ± 89	12..0	<0.01	<0.01
Pyroglutamate	356 ± 45	384 ± 59	486 ± 94	525 ± 120	19.9	<0.01	0.8
Ribose	312 ± 40	323 ± 70	406 ± 95	255 ± 78	17.8	0.28	<0.01
Serine*	49 ± 25	50 ± 14	85 ± 29	123 ± 57	5.92	<0.01	<0.01
Succinate	124 ± 21	147 ± 35	178 ± 65	118 ± 52	10.8	0.32	0.02
Threonine	25 ± 8	28 ± 7	35 ± 22	41 ± 29	5.52	0.01	0.86
Thymine	40 ± 23	27± 12	30 ± 14	35 ± 30	6.52	0.4	0.31
Tryptophan	11 ± 5	7 ± 3	10 ± 3	17 ± 9	0.78	0.2	<0.01
Tyrosine	49 ± 12	35 ± 13	50 ± 24	61 ± 21	4.5	<0.01	0.05
Uracil	104 ± 25	122 ± 127	199 ± 91	246 ± 48	16.7	<0.01	0.85
Urea	898 ± 84	1872 ± 1191	2928 ± 1634	1977 ± 792	0.35	<0.01	0.02
Valerate	3044 ± 1092	2932 ± 433	4033 ± 557	3000 ± 807	0.52	0.52	0.81
Valine*	144 ± 72	139 ± 34	199 ± 60	248 ± 55	11.5	<0.01	<0.01
Xanthine	60 ± 16	92 ± 20	117 ± 71	178 ± 60	10.6	<0.01	0.18
SM (OH) (d18:1/14:1)	0.031 ± 0.002	0.003 ± 0.004	0.002 ± 0.003	0.002 ± 0.003	0.0008	0.76	0.76
SM (OH) (d18:1/22:1)	0.01 ± 0.01	0.03 ± 0.014	0.04 ± 0.001	0.04 ± 0.014	0.001	0.47	0.48
SM (OH) (d18:1/22:2)	0.01 ± 0.01	0.021 ± 0.012	0.015 ± 0.006	0.012 ± 0.008	0.001	0.04	0.02
SM (OH) (d18:1/24:1)	0.043 ± 0.003	0.002 ± 0.003	0.002 ± 0.002	0.002 ± 0.003	0.0005	0.16	0.91
SM (d18:1/16:0)	0.04 ± 0.01	0.01 ± 0.01	0.003 ± 0.01	0.002 ± 0.006	0.002	<0.01	0.31
SM (d18:1/16:1)	0.043 ± 0.014	0.001 ± 0.002	0.001 ± 0.003	0.001 ± 0.002	0.0006	0.03	0.07
SM (d18:1/20:2)	0.018 ± 0.01	0.010 ± 0.003	0.011 ± 0.002	0.009 ± 0.003	0.0008	0.13	0.32
SM (d18:1/22:3)	0.013 ± 0.01	0.001 ± 0.002	0.003 ± 0.004	0.001 ± 0.004	0.001	0.43	0.76
SM (d18:1/24:1)	0.04 ± 0.01	0.03 ± 0.06	0.02 ± 0.07	0.01 ± 0.005	0.011	0.71	0.05
PC aa C34:1*	0.312 ± 0.284	0.227 ± 0.120	0.231 ± 0.165	0.14 ± 0.145	0.021	<0.01	<0.01
PC aa C34:2*	0.781 ± 0.66	0.535 ± 0.32	0.431 ± 0.41	0.345 ± 0.22	0.054	<0.01	<0.01
PC aa C34:3	0.038 ± 0.021	0.009 ± 0.01	0.01 ± 0.01	0.06 ± 0.003	0.003	<0.01	0.78
PC aa C36:2	0.601 ± 0.735	0.564 ± 0.381	0.501 ± 0.341	0.531 ± 0.436	0.116	<0.01	0.17

Table 3.2 Continued

	Barley grain proportion (% of diet dry matter)					*P*-value[§]	
	0	15	30	45	SEM[¶]	Linear	Quadratic
PC aa C36:3*	0.211 ± 0.19	0.02 ± 0.06	0.04 ± 0.09	0.04 ± 0.09	0.025	<0.01	0.01
PC ae C30:2	0.83 ± 0.013	0.44 ± 0.012	0.24 ± 0.014	0.21 ± 0.012	0.0009	0.36	0.11
PC ae C34:1	0.025 ± 0.015	0.01 ± 0.005	0.01 ± 0.005	0.01 ± 0.009	0.0025	0.03	<0.01
PC ae C34:2	0.018 ± 0.011	0.004 ± 0.003	0.004 ± 0.002	0.01 ± 0.01	0.0019	0.27	<0.01
PC ae C36:1	0.06 ± 0.05	0.04 ± 0.01	0.02 ± 0.005	0.01 ± 0.02	0.004	<0.01	0.02
PC ae C36:2*	0.048 ± 0.05	0.01 ± 0.01	0.02 ± 0.07	0.01 ± 0.01	0.004	<0.01	<0.01
PC ae C38:5	0.024 ± 0.018	0.01 ± 0.01	0.01 ± 0.01	0.01 ± 0.005	0.002	0.02	0.043

PC ae C38:6	0.011 ± 0.013	0.003 ± 0.003	0.002 ± 0.003	0.002 ± 0.002	0.001	<0.01	0.016
PC ae C40:2	0.015 ± 0.004	0.002 ± 0.003	0.003 ± 0.002	0.004 ± 0.004	0.0009	0.88	0.1
PC ae C40:3	0.018 ± 0.003	0.012 ± 0.004	0.012 ± 0.006	0.014 ± 0.005	0.0009	0.56	0.02
lysoPC a C16:0	0.14 ± 0.02	0.03 ± 0.018	0.02 ± 0.019	0.03 ± 0.02	0.005	0.36	0.85
C14:2-OH	0.01 ± 0.002	0.013 ± 0.003	0.01 ± 0.003	0.01 ± 0.004	0.0008	0.9	0.61
C16	0.02 ± 0.01	0.03 ± 0.011	0.03 ± 0.01	0.04 ± 0.015	0.002	0.14	0.07
C16:2	0.004 ± 0.002	0.003 ± 0.01	0.005 ± 0.01	0.003 ± 0.001	0.0008	0.94	0.5
C18:1-OH	0.01 ± 0.01	0.012 ± 0.01	0.01 ± 0.02	0.01 ± 0.005	0.001	0.21	0.05
C3	0.02 ± 0.01	0.017 ± 0.01	0.01 ± 0.01	0.02 ± 0.01	0.002	0.14	<0.01
C3-DC (C4-OH)	0.2 ± 0.13	0.11 ± 0.02	0.11 ± 0.05	0.14 ± 0.09	0.02	0.29	0.03

[1]Rumen fluid for the analysis was collected shortly before the morning feeding on days 12 and 21 of each experimental period. Cows were fed once daily at 0800 h. § Linear indicates a linear effect of dietary treatment, while quadratic indicates a quadratic effect of dietary treatment. *Indicates the most strongly differentiating compounds among the 4 diets ($p \leq 0.01$). ¶SEM: Standard error of the mean.

Rumen acidosis is a ruminal fermentation disorder that is characterized by a reduction in ruminal fluid pH below 5.5-5.6 for extended periods of time (8-12 hours). It has been found to be most prevalent after engorgement of large amounts of starch or other rapidly fermentable carbohydrates by cattle. Starch-rich diets increase the availability of free glucose in the rumen, and enhance the growth of most bacteria, which leads to higher production of VFAs (including acetate, propionate and butyrate) in ruminal fluid. This situation exceeds the ability of the ruminal papillae to absorb them and thus VFAs accumulate in the ruminal fluid and, as a result, decrease ruminal pH (*58*). In addition to glucose and VFAs, rumen acidosis is also characterised by higher concentrations of other microbial products including ethanol, methanol, histamine, tyramine, L-alanine, endotoxin, methylamine and hypoxanthine in ruminal fluid and can exert systemic effects (*29, 204*).

3.2.4. Compound Identification and Quantification by GC–MS

Figure 3.2 illustrates a typical high resolution GC-MS total ion chromatogram of the polar extracts from a ruminal fluid sample of a healthy cow.

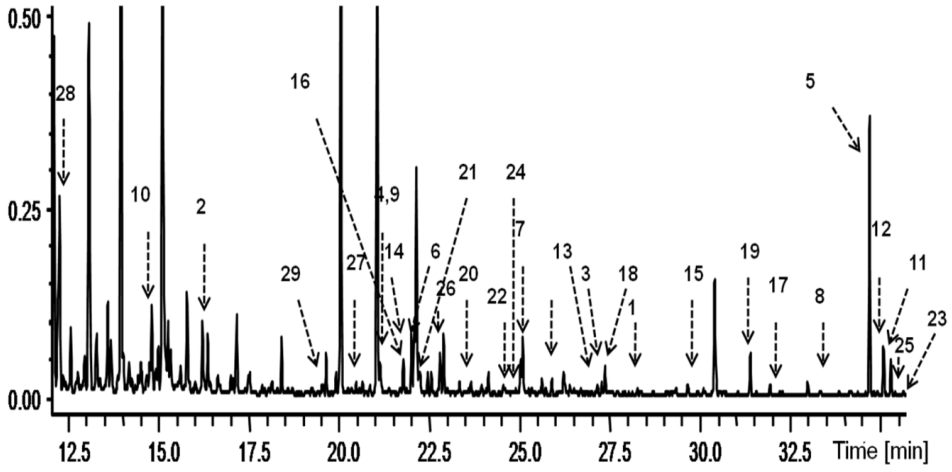

Figure 3.2 Typical GC-MS spectrum of ruminal fluid.
Key: 1: 4-Aminobutyric acid 2: Alanine; 3: Aspartate; 4: Benzoate ; 5: Glucose; 6: Glycine ; 7: 3-Phenylpropionate; 8: Hypoxanthine; 9: Isoleucine; 10: Lactate; 11: Lysine ; 12: Mannose ; 13: Methionine; 14: Phenylacetate; 15: Phenylalanine; 16: Proline;17: Putrescine; 18: Pyroglutamate; 19: Ribitol (standard); 20: Serine; 21: Succinate; 22: Threonine; 23: Tryptophan; 24: Thymine; 25: Tyrosine; 26: Uracil; 27:Urea; 28:Valerate; 29: Valine.

As can be seen in this Figure, many of the visible peaks can be annotated with a compound name; however, 40% of these peaks remain unidentified. This relatively low level of coverage is a common problem in global or untargeted GC-MS metabolomics studies. While some of these peaks may be due to derivatization by-products or degraded metabolites, the lack of a comprehensive GC-MS library for rumen metabolites (the NIST mass spectral library contains only a small portion of metabolically relevant compounds), also limits the attainable coverage from automated library search algorithms. All peaks

corresponding to an identified metabolite were verified with pure standards and correlated to literature values. In total we identified and quantified 28 polar metabolites using GC-MS (Table 3.1). This list includes 8 additional metabolites that were not detected/quantified by NMR but could be quantified by GC MS using ribitol as an internal standard (Table 3.1). Comparisons between the NMR and GC-MS measured concentrations (across the 20 compounds that were quantified by both techniques) showed generally good agreement (within 20-30% of each other). GC-MS methods typically gave higher concentrations of proline, hypoxanthine, lysine, succinate, tyrosine and valerate compared to the corresponding NMR results. Compound concentrations below 1 μM were associated with low signal-to-noise ratio responses, limiting accurate quantification. However these compounds were identified based on previously described methods (*257*). Interestingly, NMR detects 30 compounds that GC-MS methods cannot detect while GC-MS detects 8 compounds that NMR cannot routinely detect, including 2 very high abundance compounds (urea and 4-aminobutyric acid). 4-aminobutyric acid formed by the microbial metabolism of amino acids in rumen (*258*) while urea is a non-protein nitrogen (NPN) source that is naturally present in forages. In the rumen, urea is rapidly degraded by resident microbes into ammonia which can be utilized by the bacteria for synthesis of amino acids required for their own growth. High-quality microbial protein also contributes a large portion of the protein that cows digest in the small intestine.

There are many possible reasons for these differences in instrumental detection. A compound might be found by NMR, but not by GC-MS, if it is too volatile/non-volatile for GC-MS detection, lost in sample preparation or eluted during the solvent delay. A compound might be found by GC-MS, but not by NMR, if its protons are not detectable by NMR (uric acid), or if its concentration is below detectable limits. In all cases, the existence of NMR detectable metabolites was explicitly checked in our GC-MS analyses and vice versa. Together, NMR with targeted and global GC-MS identified and quantified 58 mostly polar metabolites. Overall, GC-MS and NMR appear to be complementary techniques for the identification and quantification of small molecules in ruminal fluid.

3.2.5. Direct Flow Injection MS/MS Compound Identification and Quantification

The DFI combined with MS/MS using the Biocrates Absolute*IDQ* kit provided quantitative results for 116 metabolites (18 acylcarnitines, 19 amino acids, glucose, 50 phosphatidylcholines, 10 sphingolipids, 10 biogenic amines and 8 lyso-phosphatidylcholines (Table 3.1). Note that each phosphatidylcholine species identified by the Biocrates Absolute*IDQ* kit typically corresponds to 2-3 possible unique structures. Consequently the total number of phosphatidylcholine structures identified by this method was 135. Each of the possible phosphatidylcholine structures are listed in the RMDB with two concentration values, one assuming equal distribution of the measured concentration of the given lipid species to all possible unique structures and the other providing the combined species concentration. From the 50 measured phosphatidylcholine

species, 27 consistently yielded quantitative data, whereas the remaining 23 were below the limit of detection (LOD) in some rumen samples. Because bacteria and other microbes do not normally produce sphingolipids (except for *Sphingomonads)*, we can be certain that all of the detected sphingolipids were from cattle tissues, while the remaining compounds may have their origins from either the rumen *Sphingomonads*, and/or the rumen tissue. As far as we are aware, this is the first study of ruminal fluid using the BiocratesIDQ system. Overall, where we found compound overlap, the results agreed very well with reported literature values. This suggests that the Biocrates system is compatible with analyzing filtered rumen fluid. In our study, the lower limit of quantification by DFI-MS/MS, based on the AbsoluteIDQ kit, was 5 nM for a phospholipid species (PC aa C30:2) and a sphingomyelin SM ((OH) C14:1/d18:1).

DFI-MS/MS detected 98 compounds or compound species that GC-MS and NMR methods could not detect while GC-MS detected 15 compounds and NMR detected 36 compounds that DFI-MS/MS could not routinely detect. Interestingly, the DFI-MS/MS, NMR and GC-MS measured concentrations across the 10 amino acids that were quantified by all three techniques showed generally good agreement (within 15-30% of each other). Combined, the DFI-MS/MS, NMR and GC-MS techniques identified and quantified 156 metabolites or metabolite species. Overall, DFI-MS/MS, GC-MS and NMR appear to be complementary techniques for the identification and quantification of small molecules in ruminal fluid.

3.2.6. Lipidomics - Identification and Quantification

The targeted identification and quantification of a wide array of lipids within a single analytical sample (i.e. lipidomics) is a rapidly developing sub-field of metabolomics (*259*). Traditional lipidomics involves separating lipid classes individually, quantifying the lipid classes, hydrolyzing the lipids into their constituent acyl chains and then identifying the fatty acids using GC-MS. Using this approach for 8 rumen fluid samples from healthy cows, we identified and quantified 22 lipids including: 12 cholesterol esters (CE) and 10 free fatty acids (FFA). These results are shown in Table 3.1. We suspect the 12 cholesterol esters are likely of bovine origin while the free fatty acids are most likely of microbial origin. Because the rumen is the site of intense microbial lipid metabolism the lipolysis of dietary glycolipids, phospholipids, and triglycerides readily leads to free fatty acids that are hydrogenated by microbes to more saturated end products (*260*) Most rumen microbes cannot utilize fatty acids as an energy source, and so their use is only limited to cell incorporation and synthetic purposes. Our data show that ruminal fluid contains relatively high concentrations of palmitic acid (243 μM) and stearic acid (185 μM). This is consistent with early studies noting that the lipid material leaving the rumen consists primarily of highly saturated free fatty acids, with the saturated fatty acids being about one-third palmitic and two-thirds stearic acid (*261*). A greater concentration of C18:0 fatty acids in ruminal fluid has been reported from cows fed fish oil and extruded soybean meal (*262*). The lower limit of quantification using the FAMEs/GC-MS technique was 9.8 nM

for the α-linolenic acid. Comparison of our lipid results with literature data was difficult as relatively few papers report rumen lipid concentration data.

3.2.7. ICP-MS Trace Element Identification and Quantification

To determine the trace elemental composition of a ruminal fluid, we used inductively coupled plasma mass spectrometry (ICP-MS). ICP-MS is one of the best techniques for the characterisation of the elemental composition of biological samples. The multi-elemental analysis of rumen fluid using the ICP-MS provided quantitative results for 30 metabolites or trace minerals shown in Table 3.1. As far as we are aware, this is the first multi-elemental study of rumen fluid by ICP-MS and only a few of the compounds measured here, have been previously reported elsewhere. However, among those compounds with published values (sodium, phosphorus, potassium and calcium) there appears to be good agreement with the literature values. In our studies, the lower limit of quantification by ICP-MS was 5 nM for Cesium (Cs) and Yttrium (Y). Many trace minerals are essential for metabolism, skeletal growth, reproduction and health of many living organisms. However, in the rumen these metals are likely involved in the activation (as cofactors) of bacterial enzymes that play an important role in rumen fermentation, as well as in bacterial growth (*263*). All of these trace minerals originate from dietary sources. It is also important to note that ruminant saliva is also rich in minerals, particularly sodium, phosphate, and bicarbonate, which serve as buffering agents in the rumen and serve to keep the rumen environment ideal for microbial growth (*253*).

3.2.8. Method Comparison

We used 6 different metabolic profiling methods to experimentally characterize as much of the known ruminal fluid metabolome as possible: 1) NMR; 2) GC-MS; 3) FAMEs/GC-MS lipidomics profiling; 4) DFI MS/MS, 5) ICP-MS and 6) Pyrochrome *Limulus* amebocyte lysate assay. Using these 6 methods, we were able to identify a total of 212 distinct metabolites or metabolite species. NMR spectroscopy was able to identify and quantify 50 compounds, GC-MS was able to identify and quantify 28 compounds, lipidomics was able to identify and quantify 22 compounds, the pyrochrome Limulus amebocyte lysate assay identified and quantified 1 compound, ICP-MS identified and quantified 30 compounds while DFI MS/MS identified and quantified 116 metabolites or metabolite species, corresponding to 201 unique compounds with well-defined structures. NMR and GC-MS were able to identify a common set of 20 metabolites while NMR, GC-MS and DFI- LC-MS/MS were able to identify a common set of 10 metabolites (9 amino acids and hexose/glucose). These data are summarized in the Venn diagram shown in Figure 3.3. These differences in metabolite coverage from the different technologies are largely due to differences in sensitivity, in detection/instrument biases as well as in separation protocols, compound stability, compound solubility, compound volatility and other factors.

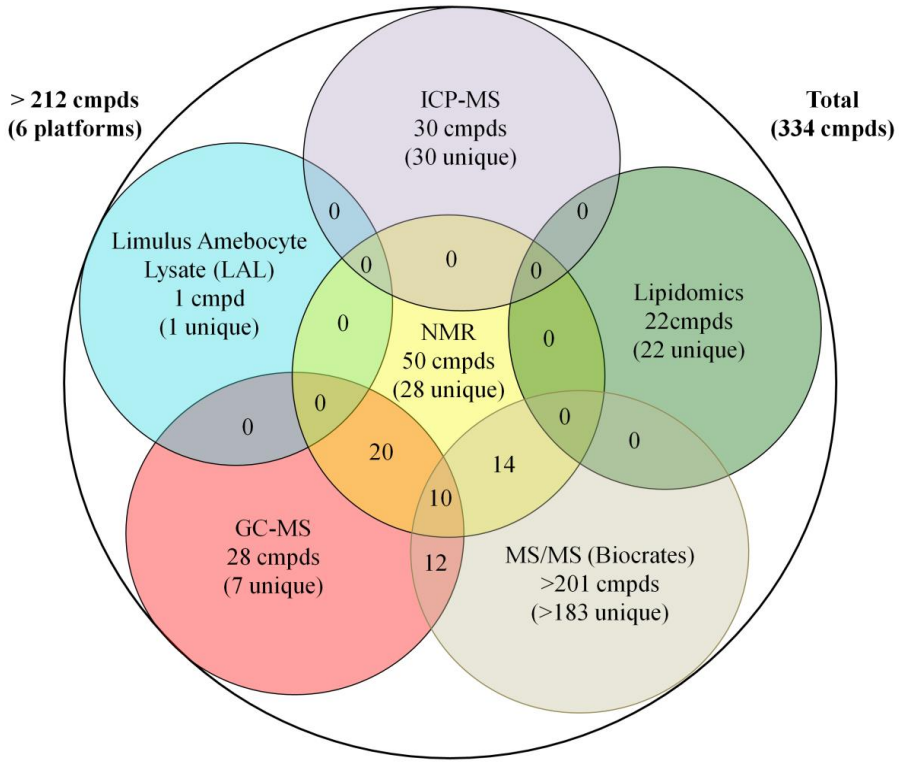

Figure 3.3 Venn diagram showing the overlap of rumen metabolites detected by different analytical methodes.

Venn diagram showing the overlap of rumen metabolites detected by global NMR, GC–MS, FAMEs/GC-MS, ICP-MS, Limulus Amebocyte Lysate, ICP-MS and DFI MS/MS methods compared to the detectable rumen metabolome.

While several pairwise platform comparisons have already been discussed, it is perhaps instructive to look at how three different platforms did in the identification and quantification of the one group of compounds that all three platforms measured: amino acids. Comparison of amino acid concentrations as measured by NMR, GC-MS and DFI-LC-MS/MS showed that while the quantitative results were in relatively good agreement (Figure 3.4), a few exceptions were evident.

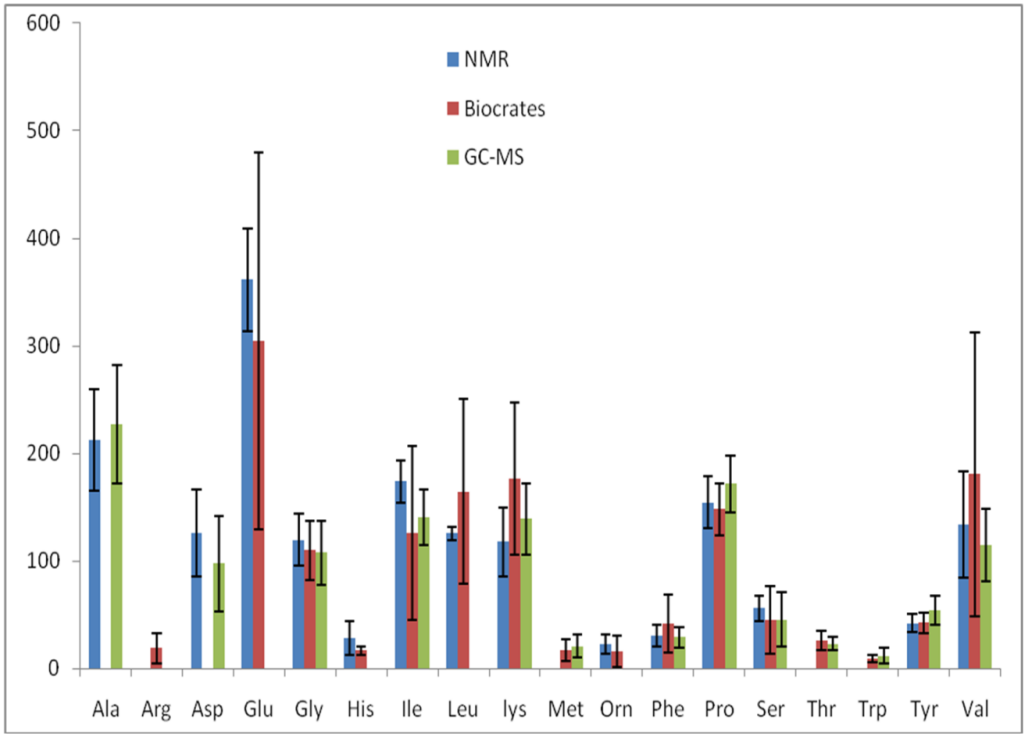

Figure 3.4 Graphical representation of ruminal fluid concentrations of amino acids by NMR, GC/MS and MS/MS.
The error bars reflect 1 standard deviation

For example, the NMR concentration of L-alanine is lower than the GC-MS value. This may be due to the short GC retention time of L-alanine (7 min), which overlaps with non-specified ionized fragments and so an accurate quantification by GC-MS is difficult. The considerably higher concentration of L-glutamic acid by NMR relative to DFI-MS/MS may be due to the hydrolysis of L-glutamine to L-glutamic acid during the DFI-MS/MS sample preparation step (*264*). It has been reported that the distinction of L-glutamine and pyroglutamic acid with GC-MS is very difficult, while the identification of L-glutamic acid and pyroglutamic acid can be complicated (*264*). While side-by-side platform comparisons for the

quantification of specific metabolites can be quite informative, it is also instructive to compare the different platforms on the basis of their level of metabolitle coverage. Given that the “detectable” bovine rumen fluid metabolome consists of 246 known and probable metabolites or metabolite species, we can calculate that NMR is able to access 20.3 % (50/246) of the rumen metabolome, GC-MS is able to measure 11.3 % (28/246), GC-MS-FAMES (general lipidomics) is able to measure 8.9% (22/246), the pyrochrome Limulus amebocyte lysate assay is able to measure 0.4% (1/246), ICP-MS is able to detect 12.1% (30/ 246) while DFI-MS/MS is able to measure 47.1% (116/246) of the ruminal fluid metabolome. When combined, the 6 methods are able to obtain data on 86.2% of the endogenous rumen metabolome (212/246).

It is important to emphasize that not all of the experimental approaches used here were ‘‘global’’ in their intent. Indeed some methods were quite targeted. In particular, the DFI-MS/MS was highly targeted, while the lipidomics method was generally targeted to lipids and fatty acids. Likewise, it is also important to emphasize that not all possible metabolomics platforms or the latest metabolomics technologies were assessed in this study. The use of more sophisticated or targeted detection and separation protocols (e.g., immunodetection and chemical derivatization) along with the use of more sensitive instruments (GC-TOF, FT-MS and Orbitraps) would likely have led to the experimental detection of more compounds. However, for this particular study, we wanted to address the question of how well a cross-section of commonly accessible metabolomic technologies or platforms could perform in identifying and quantifying metabolites in bovine

ruminal fluid. Overall, DFI-MS/MS appears to be the most suitable method for ruminal fluid characterization, especially in terms of its broad coverage (primarily of lipids) and amenability to quantification. While NMR, GC-MS and ICP-MS do provide information on many water-soluble metabolites, we believe that these methods are still insufficiently sensitive to compensate for their lack of coverage. Overall, it appears that the DFI-MS/MS method may be the best choice for ruminal fluid lipid analysis but NMR, GC-MS and ICP-MS are also necessary for the comprehensive analysis of water-soluble metabolites in ruminal fluid. Comparison of the bovine ruminal fluid metabolome to other published and unpublished biofluid metabolomes characterized by our lab or compiled through literature surveys (Table 3.3) shows that ruminal fluid is somewhat simpler than milk, serum, urine or cerebrospinal fluid, as it lacks many of the lipids found in these other fluids. While bovine ruminal fluid has a number of metabolites in common with human serum, urine and bovine milk i.e. amino acids, organic acids, fatty acids and trace elements, the concentrations of these compounds are often substantially different.

Table 3.3 Comparison of the bovine ruminal fluid metabolome with other biofluid metabolomes as measured using different metabolomic methods.

Metabolomic Techniques	No. of compounds in bovine milk*	No. of compounds in bovine ruminal fluid	No. of compounds in human cerebrospinal fluid	No. of compounds in human serum	No. of compounds in human urine*
DFI-MS/MS	108	116	—	139	186
Endotoxins	—	1	—	—	—
GC-MS	—	28	41	99	94

HPLC	—	—	—	—	4
ICP-MS	20	31	—	—	45
LC-ESI-MS/MS	—	—	17	96	93
Lipidomics	> 2000	22	—	3381	—
NMR	20	50	53	49	190
Total number of metabolites measured and reported in literature	~2200	246	308	4229	840

*Unpublished data.

According to our data, bovine ruminal fluid consists of at least 246 detectable metabolites or metabolite species, corresponding to 334 unique structures. Based on the existing literature and our knowledge of metabolic pathways or dietary sources concerning these metabolites, we estimate that approximately 5-7 % of the ruminal fluid metabolome is of clear microbial origin (i.e. purine derivatives, VFAs and endotoxin) while 40-45% of the ruminal fluid metabolome is of clear bovine origin (primarily longer-chain organic acids, sphingolipids, biogenic amines, trace elements, cholesterol esters and most acylcarnitines). The remaining 50-55% of the ruminal fluid metabolome, which includes amino acids, free fatty acids and phosphatidylcholines, is of both microbial and bovine origin.

This study is part of a longer-term study to establish a comprehensive metabolome database of multiple tissues and biofluids for cattle. The rumen fluid metabolome database is the first of these to be completed and is intended to provide an idea of what kind of compounds can be routinely identified and quantified in bovine ruminal fluid using conventional metabolomic techniques. This database is intended to allow livestock researchers and veterinarians to easily

evaluate and compare the “normal” bovine ruminal fluid metabolome with rumen fluid metabolomic profiles collected on other cattle herds. This resource should allow them to assess cattle health or detect or predict the development of different conditions (rumen toxicity, milk fever, bloat, rumen acidosis and ketosis) that may affect herd productivity or herd health. Ultimately it is hoped that this work on the bovine ruminal fluid metabolome could help lead to the identification of new disease biomarkers and the development of new treatments for rumen-related diseases in both dairy and beef cattle.

3.3 Conclusion

Combining our experimentally derived values with our computer-aided literature survey data allowed us to identify and quantify a total of 246 metabolites or metabolite species (corresponding to 334 unique structures) in bovine ruminal fluid. This list constitutes the “detectable” bovine ruminal fluid metabolome. In assessing this metabolite list we found that ruminal fluid is a metabolically diverse biofluid, with representative metabolites spanning 28 different compound categories. More specifically we found the composition of bovine ruminal fluid is dominated by phospholipids, inorganic ions and gases, amino acids, dicarboxylic acids, short chain fatty acids, volatile fatty acids and carbohydrates. Detectable ruminal metabolites range in concentration from 1 nanomolar (for certain sphingomyelins and phospholipids) to 116 mM (for sodium). More than 100 metabolites in ruminal fluid appear to have normal concentrations above 1 μM. While clear differences do exist in the number and type of compounds detected by

the analytical technologies employed in this study, our intent was to characterize the ruminal fluid metabolome with a cross-section of commonly available metabolomics tools or platforms. Overall, our results suggest that comprehensive metabolite profiling of bovine ruminal fluid requires multiple platforms and multiple methods as no single method can offer (nor likely will offer) complete metabolite coverage.

Obviously, this study is not the ‘‘final’’ word on ruminal fluid metabolomics. Rather, it should be viewed as a starting point for future studies and future improvements in this field. Indeed, our primary objective for undertaking these studies and compiling these data was to help advance the fields of quantitative metabolomics. Experimentally, our data should serve as a useful benchmark from which to compare other technologies and to assess coming methodological improvements in bovine ruminal fluid characterization. From a biochemical standpoint, we think the information contained in the bovine ruminal fluid metabolome database (BRDB) should provide a convenient, centralized resource from which veterinarians could exploit to help in livestock disease detection and diagnosis. We also believe it could be a valuable resource for livestock researchers wanting to learn more about the bovine rumen and its unique biochemical functions.

Chapter 4

Lipopolysaccharide Induced Conversion of Recombinant Prion Proteins

---

Manuscript in preparation.

Author Contributions

I conducted most of the experiments, analyzed the data and wrote the initial draft of the manuscript. The RENAGE experiments were originally by C. Ladner, and ^{15}N-HSQC NMR experiment was conducted by T. C. Bjorndahl and he also oversaw and designed the experimental set up with me. D. S Wishart, (supervisor and PI) C. Ladner and T. C. Bjorndahl edited this paper.

Introduction

Prion diseases or transmissible spongiform encephalopathies (**TSEs**), including Kuru, variant Creutzfeldt Jakob disease (**vCJD**), bovine spongiform encephalopathy (**BSE**), chronic wasting disease (**CWD**), and scrapie are all examples of incurable and uniformly fatal neuro-degenerative diseases that arise

from the self-propagation of misfolded prion protein. The current working hypothesis is that small numbers of misfolded, β-rich prions (called PrP^{Sc}) are able to catalytically convert native, monomeric, helix-rich cellular prion protein (PrP^{C}) to large numbers of misfolded prions (*265*), which aggregate into larger, uniformly organized, oligomeric substructures that can further assemble into fibrilar, macrostructures. In this way, the misfolded prions are able to spread exponentially leading to widespread cell death wherever PrP^{C} is highly expressed. PrP^{C} is found in all mammalian cells; however, the highest level of expression is in neurological tissues (*266, 267*), which largely explain the neuro-degenerative nature of prion diseases.

The native prion protein, PrP^{C}, is a water soluble, monomeric, ~24 kDa protein with an unstructured N-terminal region containing roughly 70 residues and a globular core consisting primarily of alpha helical secondary structure (*268*) (42% α-helix and about 5% β-sheet). This unstructured N-terminus consists of a number of octa-repeat segments that have been shown to bind divalent metal ions (Cu^{2+},Fe^{2+}, Zn^{2+}) (*269, 270*). The core contains two N-linked glycosylation sites at Asn181 and Asn197 (*271, 272*) while the C-terminus is linked to a lipid glycosylphosphatidylinositol (**GPI**) anchor that secures the protein to the cellular membrane. PrP^{Sc} contains 10% α-helix and 30% β-sheet (*265, 273, 274*) and tends to form large oligomers, insoluble aggregates and fibril like structures. As a result, PrP^{Sc} is protease-resistant, oligomeric and substantially less soluble than PrP^{C}. These divergent features allow the two isoforms to be easily differentiated biochemically.

After many decades of investigation, much is known of the prion protein's (i.e. PrP^{C}) native structure; however, less is known about the beta rich isoform. Likewise, very little is known about the α-helix to β-sheet conversion process, the precise mechanisms behind self-seeded propagation or the potential causative agents that might induce sporadic prion disease. As prion protein misfolding and aggregation is believed to be a major contributor to prion disease etiology, a more detailed molecular understanding of the ordered aggregation and amyloid fibril formation process is critical for designing strategies to prevent or treat these conditions.

To help better understand biochemical aspects of the PrP conversion, several groups have used *in vitro* or test tube systems in which recombinant PrP^{C} molecules are converted into to β-rich PrP^{Sc}-like molecules (called PrP^{β}) using a number of chemical and/or physical agents such as guanidine hydrochloride (*275*), urea (*276*), SDS (*277*), high temperature (*276, 278*), low pH (*279*) that cause complete or partial protein denaturation. Most of these protocols not only cause the conformational change of PrP^{C} into PrP^{β} but also generate "synthetic prions" that exhibit many of the physiochemical properties seen in PrP^{Sc} molecules isolated from diseased tissues. However, unlike brain-derived prions, the conversion and apparent propagation of these synthetic prions is dependent on continued exposure to denaturing conditions rather than the prions themselves. Despite the widespread belief in the "protein-only" hypothesis concerning prion conversion and infectivity, controversies over whether other molecules beside

PrP^{Sc} are also required for prion conversion and replication *in-vivo* still remain. In particular, the role of a number of naturally occurring, non-proteinaceous molecules such as nucleic acids (*280-282*), polyanions (*283*, *284*), lipids (*285-287*) sulfated glycans (*288*) and metals (*289*) are actively being investigated in the pathogenesis of prion diseases.

Recently, it was shown that recombinant prions could be rendered seed-competent (and infectious) with the addition of total liver RNA and synthetic 1-palmitoyl-2-oleoyl-phosphatidylglycerol (**POPG**) lipid molecules. Even more recently it was reported that phosphatidylethanolamine (**PE**) is an essential cofactor for prion conversion and infectivity. These findings strongly suggest that a non-protein molecular component may be responsible for facilitating or augmenting the prion conversion process (*290*). Given these emerging results, we began screening for a "prion converting molecule" among naturally occurring, exogenous molecules. The recent discovery that prions have broad spectrum antibacterial properties (*291*) mediated by membrane-prion interactions directed our screen towards analyzing bacterial components and specifically looking at lipopolysaccharide (LPS), an outer membrane component of Gram-negative bacteria. In particular, LPS is a temperature resistant, amphipathic molecule that consists of both lipid (lipid A) and carbohydrate (core and O-antigen) components. Lipopolysaccharide acts as an immunogen and a strong pyrogen in healthy mammals. It binds the CD14/TLR4/MD2 receptor complex which resides in lipid rafts where the prion protein co localizes. It promotes the secretion of pro-inflammatory cytokines in many cell types, but especially in macrophages. Given that both PrP^{C} and the

LPS/CD14/TLR4 receptor complex are localized to the same membrane domains via their GPI anchors and the structural similarity of LPS to polyanoinic molecules like POPG that have been associated with prion conversion, we decided to investigate LPS's potential effects on PrP^{C} *in-vitro.*

Interestingly, we found that native, recombinant prion protein incubated with modest concentrations of LPS (15µg/mL) at physiologic pH and temperature lead to their rapid conversion to oligomers that were rich in beta-sheet structure (PrP^{β}) compared to the native PrP^{C}. Not only did we confirm that LPS can, in fact, initiate conversion of the prion protein, but also that this converted beta-rich isoform could partially self-propagate by inducing the conversion of freshly added unconverted protein (PrP^{C}) (serial dilution of prion/LPS mixtures) – as long as the LPS concentration in the conversion solution remained above the critical micelle concentration (CMC). Even more interestingly, this serial conversion and propagation phenomenon was not seen with other known prion conversion reagents (including SDS, urea, POPG or PE). Given the ubiquity of LPS in both recombinant prion preparations and the abundance of LPS in many animal pens, cages and feed, these results may have some interesting implications regarding prion propagation – both *in vitro* and *in vivo*.

4.1 Materials and Methods

4.1.1. Materials

For the experiments described here, several recombinant mammalian prion variants were studied, including Syrian hamster, mouse, cervid and bovine prions.

All of the studies were conducted with the recombinant Syrian hamster prions initially and later the results were confirmed using recombinant mouse, cervid and bovine prions. Since the methods and results were essentially identical for all mammalian prions studied, to reduce space and prevent duplication, we shall focus on describing the methods and results from the Syrian hamster prions only. The expression and purification of a truncated form (residues 90-232) of the Syrian hamster prion protein (ShPrP) linked to a 22-residue N-terminal fusion tag containing a 6x-His and a thrombin cleavage site has been described elsewhere (*279*). Lipopolysaccharide from *Escherichia coli* O111:B4 (L3012: 10-20% nucleic acid; L3024: <1% nucleic acids), SDS and proteinase K were purchased from Sigma-Aldrich. Palmitoyl-oleoyl-phosphatidyl-glycerol or POPG (catalog number 840457) and Dioleoyl-phosphatidyl-ethanolamine or DOPE (catalog number 852758P) was acquired from Avanti Polar Lipids (Alabaster, AL).

4.1.2. LPS, SDS, POPG and Urea Induced Conversion of PrPC to PrPβ.

Lyophilized LPS was reconstituted with milliQ H_2O to provide an initial working concentration of 5 mg/mL. To assess LPS-mediated prion conversion and propagation, this stock solution was diluted and used to reconstitute lyophilized ShPrP(90-232) to ~0.5 mg/mL (500 μL in 1.5 mL Eppendorf tubes), providing milligram ratios (w/w) of ShPrP:LPS of 1:6, 1:3, 1:1.5, 1:0.75, 1:0.38, 1:0.17, 1:0.09 and 1:0.01. Sodium chloride (150 mM) and 0.1% NaN_3 were subsequently added to each sample and the samples were incubated (without shaking) at 37 ºC

for 1 week. Given that the average molecular weight of LPS is about 10 kDa or half that of the prion protein, these mg ratios equate to twice that of the molar ratio. Because an exact molecular weight does not exist for LPS, mg ratios were used in this study for comparison and consistency.

SDS, urea, POPG and DOPE directed prion conversions were done using the same protocol outlined for LPS. Briefly, a stock solution of 10% SDS was prepared and diluted into prion protein (0.5 mg/mL) with a final SDS concentration of 0.02% w/v. Subsequently, for propagation experiments, this converted material was diluted with fresh ShPrP(90-232) such that the final SDS w/v concentrations were 0.01%, 0.005%, 0.0025%, 0.00125% and 0.000625%. These values correspond to mg ratios (w/w) of ShPrP:SDS: 1:5, 1:2.5, 1:1.25, 1:0.625, 1:0.315 and 1:0.15. For POPG mediated conversion and propagation experiments, a stock suspension of 1 mg/mL in 20 mM $NaHPO_4$ (pH 7.2) was prepared and added to the protein (0.4 mg/mL) providing ShPrP:POPG mg:mg ratios of 1:0.5, 1:0.25, 1:0.125 and 1:0.0625 and 1:0.0375 in the presence of 150 mM NaCl with 0.01% NaN_3. For DOPE mediated conversion and propagation experiments, a stock suspension of 20 mg/mL in 0.04% Triton-X100 (sonicated for 30 minutes) was prepared and added to the protein (0.4 mg/mL) providing ShPrP: DOPE mg:mg ratios of 1:65, 1:32.5 and 1:16.25 in the presence of 150 mM NaCl with 0.01% NaN_3 . The experiments were carried out in 1.5 mL Eppendorf tubes with 0.5 mL of sample volume. For urea mediated conversion and propagation experiments, a stock suspension of shPrP protein (0.4 mg/mL) was added to different molar concentrations of urea yielding urea solutions of 5

M, 2.5 M, 1.25 M and 0.625 M in the presence of 20 mM sodium acetate with 200 mM NaCl at pH 4.0.. The experiments were carried out in 1.5 mL Eppendorf tubes with 0.5 mL of sample volume. The samples were incubated at 37 ºC and continuously followed by circular dichroism (CD) spectroscopy for up to 1 week.

Urea-induced oligomerization of the prion protein was performed by reconstituting lyophilized ShPrP(90-232) prion protein into 20 mM sodium acetate buffer containing 3 M urea and 200 mM NaCl at pH 4.0. To form fibrils under denaturing conditions, a stock solution of previously denatured $ShPrP^{C}$ (100 µM) in 6 M guanidinium was diluted to 20 µM in 50 mM Hepes buffer (1 M guanidinium hydrochloride, 3 M urea, 150 mM NaCl, pH 7.0) and shaken at 500 RPM for 18 hours prior to dialyzing into milliQ H_2O.

4.1.3. CD Spectroscopy and Data Processing

The prion conversion reactions were followed using CD spectroscopy recorded in the far-UV region (190-260 nm) at 25 ºC in a 0.02 cm path-length quartz cell on an Olis DSM 17 spectropolarimeter. Five scans were averaged for each CD spectrum collected. The protein concentrations were 0.5 mg/mL (~25 µM). Reference spectra were collected in the same manner and subtracted from the measured prion spectra prior to molar ellipticity determination. Ellipticity values were calculated using an average amino acid molecular weight of 113.64 g/mol and the secondary structure content was calculated with CDPro (*292*) using the CONTINLL algorithm and the SP22X reference setN (*293*) .

The endpoint to β-sheet conversion was defined when the helical content (as measured by CD) dropped to 15% and the β-sheet content exceeded 25%. These values were derived from the initial LPS directed conversion experiments and are consistent with the secondary structure values calculated for urea/guanidine converted beta oligomers and fibrils. Using these endpoint values, individual components of the secondary structure were normalized from 0 to 1 and averaged to yield a quantitative index for the extent of conversion.

4.1.4. Transmission Electron Microscopy

Typically 4 μL of each prion or prion-LPS sample were spotted onto 300 mesh copper EM grids (TED PELLA INC., Redding, CA, USA) and allowed to adsorb for 5 minutes. The remaining sample was wicked away with a kimwipe and the grid air-dried for 5 minutes, rinsed with 5 μL of milliQ H_2O and then negatively stained for 1 minute with 4 μL of either 1% lead acetate for LPS-containing samples or 4% uranyl acetate for samples containing the prion protein. The excess staining solution was wicked away and the samples were re-rinsed with another 5 μL of mqH_2O and dried for 5 minutes. The grids were analyzed on a Philips/FEI (Morgagni) transmission electron microscope (**TEM**) to look for and assess the structure and morphology of PrP oligomers and fibrils.

4.1.5. Proteinase-K (PK) Resistance Assay

The method used to assess proteinase-K (PK) resistance of the LPS-converted or template converted prions was adapted from Bessen and Marsh (*294*). Specifically, proteinase K (Sigma Aldrich, St. Louis, MO) was dissolved in 100

mM Tris-HCl (pH 8.0) to a concentration of 2.5 mg/mL. Urea was added to each protein sample to a final concentration of 3 M, and the samples were then incubated for 30 minutes at 37°C in the presence of various proteinase K concentrations (250:1 500:1 750:1 and 1000:1 prion:PK ratios). Protein digestion was stopped with the addition of 5 mM phenylmethanesulfonyl fluoride (PMSF) and the reactions analyzed using 12% SDS PAGE stained with Coomassie blue.

4.1.6. Nucleic Acid Control Experiments

Because LPS contains some level of nucleic acid contamination and because it was unclear whether nucleic acids were contributing to the observed prion conversion, we performed additional control experiments with genomic DNA, DNA fragments and dNTPs. Genomic DNA was purified from *E. coli* (BL21DE3) using a Maxiprep kit (Qiagen) while dNTP's were acquired from Fermertas (Thermo Scientific, Burlington, ON., Canada) and mixed to equimolar ratios prior to use. The source of plasmid DNA was the pET15b+ vector constructed with the ShPrP gene used for expression in this study. This plasmid was also fragmented mechanically by raking 10 µL of the plasmid in a 1.5 mL Eppendorf tube over a 90 well Eppendorf flotation rack to provide a source of sheared DNA. Visual confirmation of the random fragmentation was obtained by running the DNA sample on a standard 2% agarose gel prior to use. The concentration of the polynucleic acid was quantified on a Nanodrop ND-1000 spectrophotometer. The molar ratios of protein to nucleic acids were 1:1 in all experiments. The samples (500 µL with 0.1% NaN_3) were incubated at 37 ºC in 1.5 mL Eppendorf tubes and

analyzed by CD spectroscopy at 24-hour intervals for 11 days. For additional control experiments, residual nucleic acids in the LPS samples (L3024) were also pretreated with DNAse and RNAse. The LPS stock solution (5 mg/mL in mqH_2O) was diluted to 1 mg/mL with the addition of 20 mM Tris-HCl (pH 8.3). $MgSO_4$ and $CaCl_2$ were added to concentrations of 2 mM for the RNAse and DNAse samples, respectively, prior to adding the enzymes at working concentrations of 0.2 µg/mL. The resulting stock solutions were left to react at 37 °C for 18 hours prior to use.

4.1.7. NMR Analysis

Recombinant ShPrP(90-232) was expressed in minimal media with ^{15}N ammonium chloride and purified as previously described (*279*). The sample was dialyzed into 20 mM sodium acetate buffer (pH 7.0) with 150 mM NaCl and 0.1% NaN_3 and concentrated using a 3500 MWCO Centricon device (Millipore Inc., Billerica, MA, USA). Ten percent D_2O was added for solvent lock and the sample was transferred to a Shigemi tube. The final concentration was 620 µM (320 µL with 30 µL of D_2O). ^{15}N-HSQC spectra were collected on a 500 MHz Varian INOVA NMR fitted with a z-gradient, triple resonance probe. A total of 1024 points were collected in the t2 dimension with a sweep width of 6000 Hz and 96 points were collected in the t1 dimension with a spectral width of 1800 Hz. Immediately following collection of the control experiment, LPS (123 µL of a 5 mg/mL aqueous solution) was added to achieve roughly a 1:1 (w/w) ratio. The final protein concentration was 460 µM. This spectrum was recollected with the

same parameters outlined above. Forty transients were collected and averaged for each spectrum.

4.1.8. RENAGE Gel Electrophoresis

Separation of prion oligomers by RENAGE was performed as described previously (*295*). Briefly, converted prion protein (8 µg) was loaded onto an 8% RENAGE gel at pH 4.3 with a 3% stacking gel at pH 5.2. The gels were pre-run for 20 minutes prior to loading protein samples. Separation was obtained with a constant current of 30 mA for 72 minutes. The gel was stained with colloidal Coomassie blue for 4 hours and de-stained with water (*296*). Gel lanes were converted to a chromatogram using ImageJ (http://rsbweb.nih.gov/ij/index.html). Chromatograms were then converted to text file and plotted in Origin software. The peaks were then manually chosen and integrated, assuming Gaussian peaks. Percentages were then calculated from the area of the peak compared to the total integrated area

4.2 Results

4.2.1. LPS Mediated Conversion

The strong interaction between the prion protein and bacterial LPS was evident from our initial binding studies performed by NMR (Figure. 4.1).

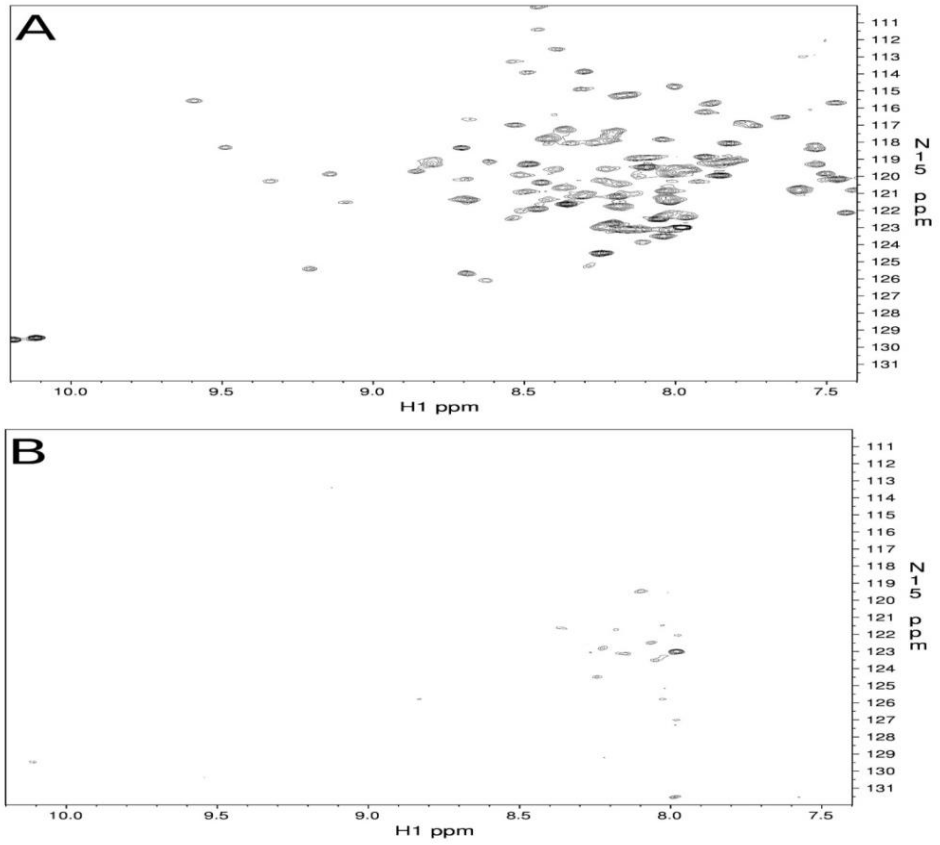

Figure 4.1 Region of the 15N-HSQC NMR spectra for the shPrP90-232 before (A) and after (B) the addition of an equimolar amount of LPS..

Apart from a few N-terminal and 6x-His affinity tag residues, immediate and complete attenuation of shPrP(90-232) ^{15}N-HSQC amide signals resulted upon addition of a 1:1 molar ratio of LPS to the NMR sample. This interaction was also visualized by TEM (Figure 4.2).

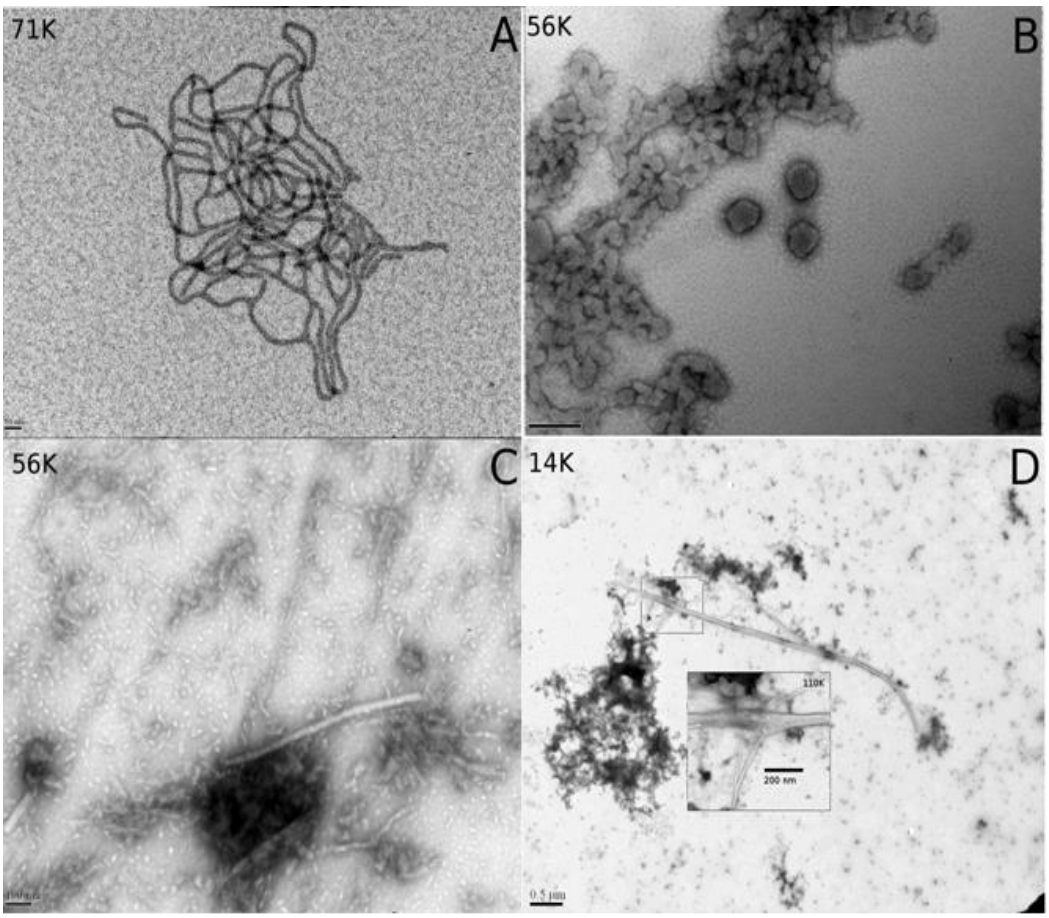

Figure 4.2 Electron microscope images of the LPS mediated conversion of the shPrP (90-232) protein.

A. LPS micelles at 0.5 mg/mL in water, pH 7.0 (magnification 56,000x, bar 50 nm). **B**. The same LPS "micelles" shown in A after addition of 0.5mg/ml ShPrP (magnification 71,000x, bar 200 nm). **C** and **D**. The sample after the addition of 150 mM NaCl, 0.1% NaN_3 and incubated at 37 °C for 48 hours (scale bar: 100 nm in C and 0.5 uM in D). Small fibrils can be seen associated with LPS micelle clusters in **C.**

As seen in the above figure the typical cylindrical micelle structure adopted by LPS in water was disrupted leading to a spherical micelle formation (Figure 4.2B) with diameters ranging between 50 and 150 nanometers. The negative staining achieved with uranyl acetate suggests that protein is adhering to the micelle surface in Figure 4.2B. More interestingly, conversion to a fibril state was

observed upon incubation of this complex at 37 ºC (Fig. 4.2C and 4.2D).

These prion fibrils ranged in length from 100 nm to 1 µm and were associated in pairs and clustered with the LPS micelles. To further characterize this state, a CD spectrum was collected (Figure 4.3B) and a PK digestion assay was performed (Figure 4.3 A). The CD spectrum revealed a high level of beta structure and the PK digestion revealed a 12 kDa proteolytic resistant core, consistent with both oligomeric and fibrillar isotypes of scrapie or infectious prions.

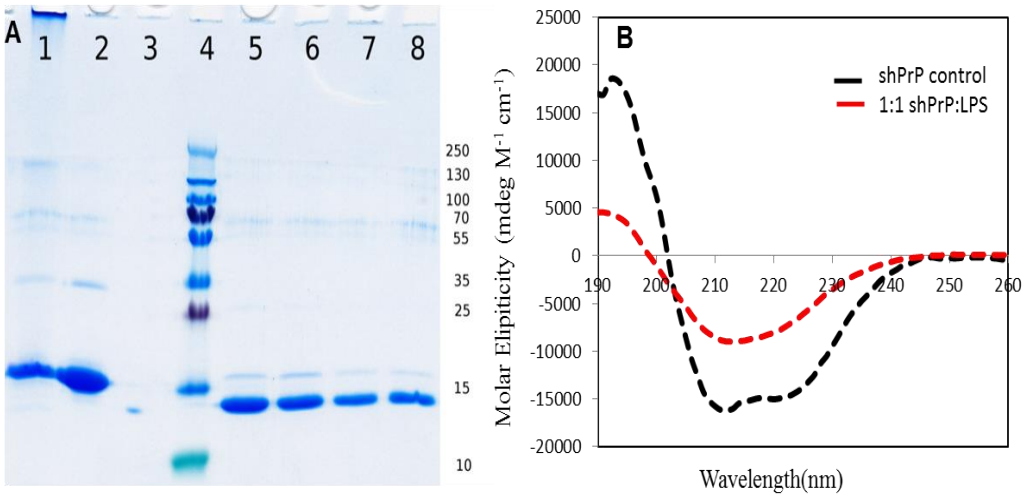

Figure 4.3. A) SDS-PAGE gel of proteinase-K treated shPrP isoform.
Lane **1**: LPS-generated $ShPrP^{\beta}$. Lane **2**: $ShPrP^{c}$(90-232). Lane **3**: $ShPrP^{C}$ digested with PK (PK:$ShPrP^{C}$ 1:1000). Lane **4**: Molecular weight ladder (molecular weights on the right). Lane **5**: PK:$ShPrP^{\beta}$ 1:1000. Lane **6**: PK:$ShPrP^{\beta}$ 1:750. Lane **7**: PK:$ShPrP^{\beta}$ 1:500. Lane **8**: PK:$ShPrP^{\beta}$ 1:250. **B)** CD spectra for the ShPrP(90-232) with 1:1 ratio of LPS at 0 hours.

These preliminary findings warranted a more in-depth characterization of the LPS mediated conversion process. An example of this conversion is shown in Figure 4.4A in which solutions with progressively lower $ShPrP^{C}$ to LPS ratios were

prepared and the conversion of the protein monitored over a period of several days. An apparent reduction in the rate of conversion was observed corresponding to the reduction in the amount of LPS in the solution. Molar ratios above 1:1 or milligram ratios above 1:0.5 (ShPrP:LPS) resulted in near instantaneous conversion of the prion to large oligomers. Meanwhile, solutions in which the LPS was below the critical micelle concentration (**CMC**) of 14 µg/mL did not show any conversion at all, even after 4 weeks of incubation (Figure 4.4).

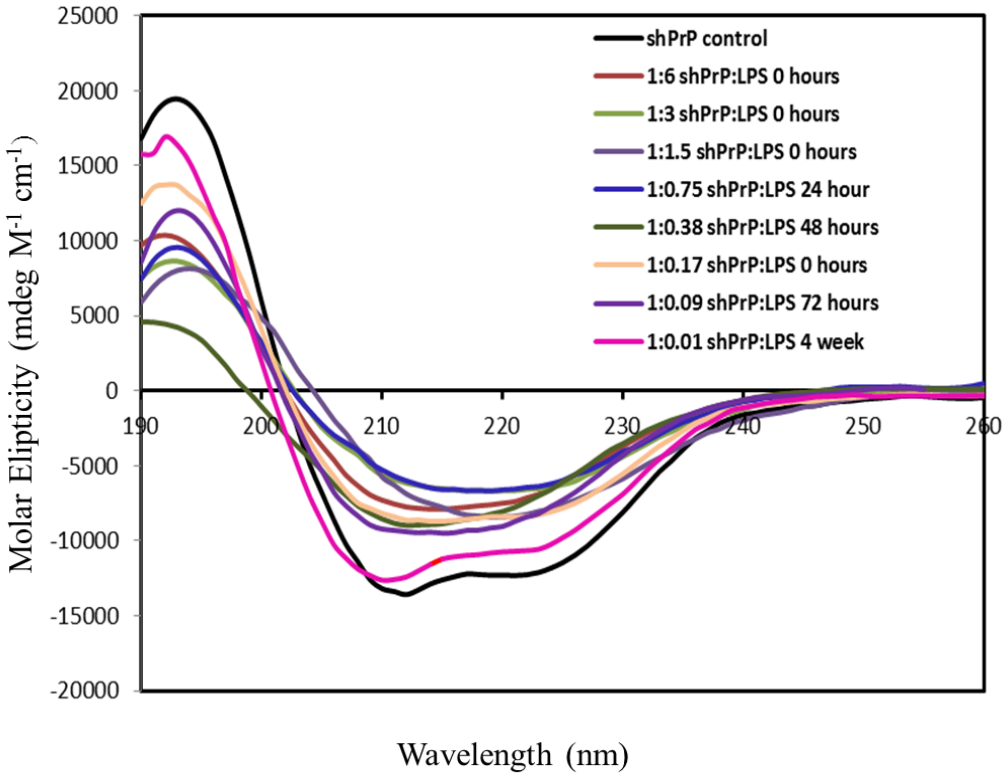

Figure 4.4 A) CD spectra for the shPrP(90-232) with various concentrations of LPS at selected time intervals.
The endpoints of conversion for each sub-molar ratio of $ShPrP^{c}$:LPS that remain above LPS's CMC are plotted in Fig. **B**) The secondary structure contents (% of α-helix and β-sheets) of each dilution were shown in Table 4.1.

However, we observed no conversion of the protein with this concentration of LPS. As no conversion occurred when the LPS concentration was below its CMC, even after 28 days, we conclude that a micelle form of LPS (as might be found in a live or lysed bacterial cell) is required for initiating conversion.

Table 4.1 Content of secondary structure of LPS mediated PrP conversion.

Sample	α-Helix (%)	β-Sheet (%)
$ShPrP^{C}$ control	42	9
$ShPrP^{C}$: LPS (1:6)	9	32
$ShPrP^{C}$: LPS (1:3)	10	31
$ShPrP^{C}$: LPS (1:1.5)	8	33
$ShPrP^{C}$: LPS (1:0.75)	12	31
$ShPrP^{C}$: LPS (1:0.0.38)	20	29
$ShPrP^{C}$: LPS (1:0.17)	26	24
$ShPrP^{C}$: LPS (1:0.09)	19	19
$ShPrP^{C}$: LPS (1:0.01)	41	10

4.2.2. Serial Propagation

The initial reaction mixtures described in the preceding text that contained LPS, uncoverted PrP^{C} and PrP^{β} (in various concentrations) was also used to assess the propagation properties of the prion protein. Mixing pure LPS in the presence of NaCl (150 mM) with recombinant $shPrP^{C}$ at ratios of 1:1.5 (LPS:PrP^{C}) resulted in near instantaneous conversion to PrP^{β} (as measured by the percentage of helical and beta-sheet structure determined by CD). After confirming the conversion, the LPS-containing solution (with PrP^{β}) was serially diluted by half, by adding equal

volumes of fresh PrP^C of the same concentration to the just-converted material. This serial dilution process generated solutions with $shPrP^C$ to LPS mg ratios (w/w) of 1:1.5, 1:0.75, 1:0.38, 1:0.17, 1:0.09 and 1:0.01. The solutions were then monitored by CD to monitor the conversion process over time. As seen in Figure 4.4 and Table 4.1, PrP^C to PrP^β conversion could be serially propagated over 5 dilutions as long as LPS was present in the solution. The conversion was essentially complete regardless of the dilution. However, once the LPS concentration dropped below the CMC ($ShPrP^C$ to LPS ratio of 1:0.01), no conversion was evident. From the data in Figure 4.4 it is also clear that the amount of LPS in the solution influenced the rate of conversion, with lower levels requiring more time. This serial dilution property appears to be unique to LPS-mediated conversion as every other conversion process where serial dilution was involved was largely arrested (see below).

LPS-mediated PrP^β conversion and propagation was compared with the conversion and propagation mediated by other chemical denaturants: namely SDS, POPG, DOPE and urea (Figure 4.5). While LPS-generated PrP^β demonstrates a sustained capacity to convert prions even as the concentration of LPS is reduced (down to its CMC), all other regents show a progressive dilution effect. In other words, as the concentration or urea, POPG and SDS is reduced, the extent of conversion is reduced. Interestingly SDS can only covert PrP^C to PrP^β at concentrations below its CMC of 8.2 mM (288.4 g/mol or 0.02% w/v). Urea, a chaotropic agent, on the other hand requires concentrations above the protein's denaturation mid-point to initiate the unfolding and conversion to a beta-

rich isoform. Concentrations below this do not result in conversion. POPG has been shown to facilitate the conversion of recombinant PrP into an infectious strain capable of propagating in mice (*290*). POPG contains two alkyl carbon chains attached to a dihydroxylated phosphate group. Like LPS, it requires concentrations above its CMC to convert PrP^{C} to PrP^{β}. However, unlike LPS, the extent of POPG conversion appears to be directly proportional to the concentration of POPG used (Figure 4.5D). Quite recently it was also reported that phosphatidylethanolamine (PE or DOPE) can act as a solitary cofactor in the propagation of recombinant PrP^{Sc} using brain homogenate and standard PMCA conditions (*297, 298*). To explore this further, we tested whether the same concentrations of DOPE described in the original publication (*297*) could facilitate the conversion of $shPrP^{C}$ (90-232) to a β-sheet conformation without brain homogenate and sonication. However, our results showed that no conversion to PrP^{β} occurred, even after seven days of incubation at 37 ^{o}C (Figure 4.5A). These findings suggest that other factors, such as temperature or additional brain homogenate cofactors are responsible for initiating the conversion process mediated by PE. While LPS, SDS, POPG and PE all share lipid moieties, only PE has a positive charge or a cationic group provided by a primary amine. Furthermore, while SDS and POPG both contain negatively charged polar heads only LPS contains a phosphate group along with a complex saccharide.

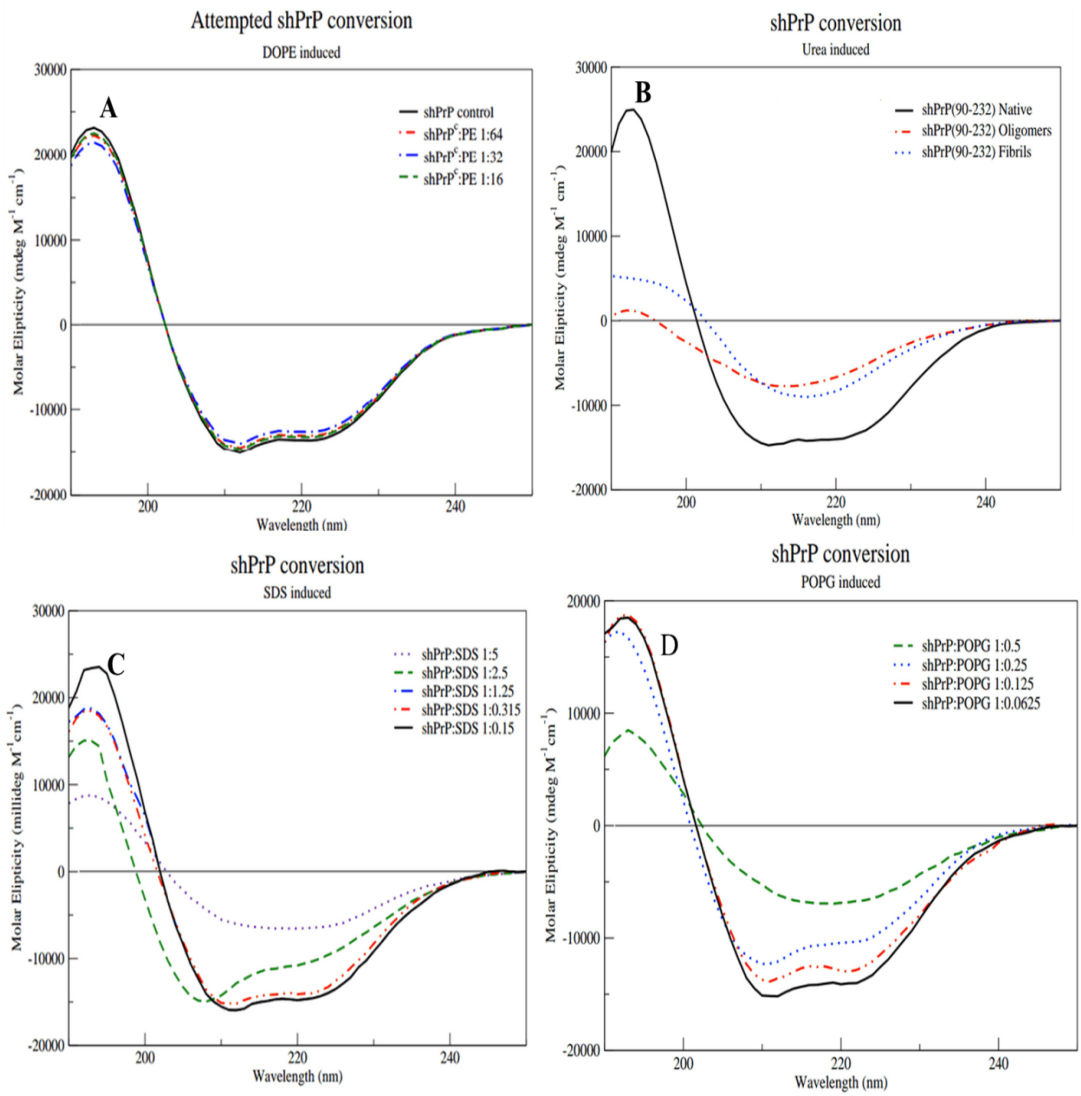

Figure 4.5 CD spectra for the shPrP(90-232) with various concentrations of DOPE, SDS, POPG and urea at selected time intervals.

A) CD spectra of the prion propagation studies using DOPE (diluting from 1:64 to 1:16 PrP^C:DOPE. **B)** Urea induced oligomers and fibrils (For comparison of secondary structure content). **C)** POPG (diluting from 1:0.5:1:0.065 of PrP^C:POPG). **D)** SDS (1:1 to 1:0.15 PrP^C:SDS). The secondary structure content (%α-helix and β-sheet) of each conversion is shown in Table 4.2.

Given that the previous *in-vivo* propagation studies of both DOPE and POPG were used in conjunction with other cellular components (cell extracts, RNA), it suggests that additional agents are required to mediate the conversion of PrP^C to a propagating strain. Our findings suggest that saccharide moieties may have the necessary requirements to facilitate propagation given the temporal effect observed at sub-molar ratios. The idea of propagation mediated by strain specificity is nothing novel and certainly one of great debate within the prion research community (*299*).

Table 4.2 Secondary structure content of urea, DOPE, POPG and SDS mediated conversion of prion protein.

DOPE induced conversion			***Urea induced conversion**		
Sample	α-Helix (%)	β-Sheet (%)	Sample	α-Helix (%)	β-Sheet (%)
$ShPrP^C$: DOPE (1:64)	41	10	ShPrP Native	43	11
$ShPrP^C$: DOPE (1:32)	40	12	Urea Induced shPrP Oligomers	14	23
$ShPrP^C$: DOPE (1:16)	40	13	Urea Induced shPrP Fibrils	10	27
SDS induced conversion			**POPG induced conversion**		
Sample	α-Helix (%)	β-Sheet (%)	Sample	α-Helix (%)	β-Sheet (%)
$ShPrP^C$: SDS (1:5)	13	31	$ShPrP^C$: POPG (1:0.5)	12	30
$ShPrP^C$: SDS (1:2.5)	27	18	$ShPrP^C$: POPG (1:0.25)	35	14
$ShPrP^C$: SDS (1:1.25)	38	13	$ShPrP^C$: POPG (1:0.125)	38	12
$ShPrP^C$: SDS (1:0.315)	40	10	$ShPrP^C$: POPG (1:0.0625)	42	8
$ShPrP^C$: SDS (1:0.15)	42	8			

Each diluted sample was also incubated for 19 days and collected CD spectra to find out any change in secondary structure.***Urea induced conversion:** secondary structure values calculated for urea/guanidine converted beta oligomers and fibrils used to compare with secondary structure values of controls (DOPE,SDS and POPG) and LPS converted shPrP.

4.2.3. Size Comparison of PrP^{β} Formed by Conversion and Fibril Propagation

To compare the size of PrP^{β} aggregates formed by the various prion conversion techniques we used a native gel technique called RENAGE (*295*). With RENAGE it has been previously shown that the PrP^{β} oligomers formed via urea/salt conversion consist of a distribution of heptamers to dodecamers (*295*). This size distribution of medium-sized oligomers is seen in Figure 4.6.

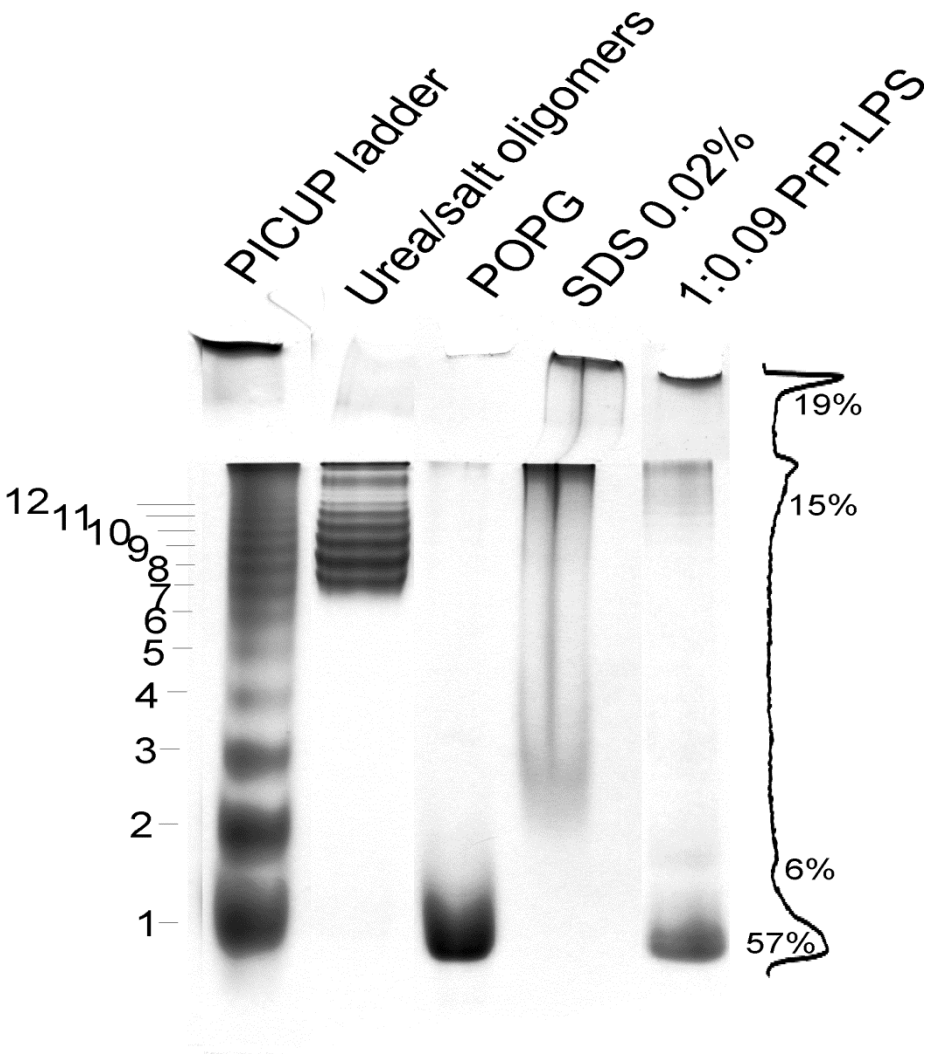

Figure 4.6 Resolution enhanced native acidic gel electrophoresis (RENAGE) showing the sizes of prion oligomers resulting from different conversion methods.

Lane 1: PrP ladder generated from moPrP$^{90\text{-}231}$ crosslinked non-specifically using PICUP (25). Lane 2: Urea/salt conversion shPrP$^{\beta}$. Lane 3: POPG converted shPrPβ (0.05:1 POPG to PrP incubated at 37 °C).). Lane 4: SDS converted shPrP$^{\beta}$ (0.02% SDS). Lane 5: LPS converted shPrP$^{\beta}$ (1:10 LPS to PrP, incubated at 37 °C.

In contrast, LPS-converted prions are characterized by very large aggregates that migrate just a few millimeters into the stacking gel. The large size of these oligomers may be due to the presence of tightly bound LPS. Quantifying the protein bands for the LPS-converted prions shows that 19% of PrP is found in the

large aggregate band, 15% is found in oligomers, 6% is in the dimer band and the rest is in the monomer band. The large monomer population (57%) in this LPS converted sample suggests that PrP^{β} aggregates are either not stable or that electrophoresis drives the release of monomeric PrP from the LPS-induced oligomers.

RENAGE was also used to compare oligomer sizes and structure induced by POPG and SDS. As seen in Figure 4.6, RENAGE of the POPG-converted prions shows only a small amount of aggregation. Like LPS-converted PrP^{C}, the POPG-converted oligomers appear to be unstable under native electrophoresis. Similarly, conversion of PrP with 0.02% SDS resulted in large aggregates that appear to dissociate as electrophoresis proceeds. While both the SDS and POPG conversion techniques produced beta-rich oligomers with about 30% beta sheet content (Figure 4.4), only the POPG formed oligomers could dissociate into a monomeric state, like the LPS formed PrP^{β}, while the SDS formed PrP^{β} remained in a loosely associated oligomeric state. Efforts to generate PrP^{β} oligomers or fibrils using DOPE were not successful and so they were not studied by RENAGE.

4.2.4. Nucleic Acid Control Experiments

Discrepancies exist in the literature regarding the necessary components required to induce conversion of the prion protein into a self-replicating form (*287, 288, 290, 300, 301*). While cofactors are not necessary for converting PrP^{C} to PrP^{Sc} in PMCA (*302*), cellular components like RNA and lipids are required to generate self-propagating prions from recombinant sources (*282, 303*). This fact needed to

be addressed given that the commercial sources of LPS are contaminated with various amounts of nucleic acids (RNA, DNA, short oligos, and free NTPs). To rule out the potential effects that certain bacterial cellular components from *E. coli* might have on our observed reactions we sought to control for these known LPS contaminants. While RNA is reported to interact with N-terminal residues of PrP (*301*, *304*), DNA has been shown to interact with the C-terminal residues of the prion protein (*300*). Given that our recombinant prion construct is devoid of any reported RNA binding site and that our lab does not control for RNase activity, the influence that RNA might have on the observed conversion was of less concern than that of DNA. Two sources of LPS were obtained from Sigma. One preparation (L3012) is purified by gel filtration and is reported to have in excess of 10% nucleic acid contamination, while the other (L3024) is further purified by ion-exchange chromatography and contains less than 1% of nucleic acid. The prion conversion reactions were repeated with the two different LPS preparations with no significant difference in the conversion rate observed (data not shown). Furthermore, the addition of DNAse and RNAse to the LPS stock solution (L3024) prior to initiating the reaction also yielded similar conversion rates.

However, given that residual nucleic acid fragments would still be present in the reaction, additional experiments with various forms of DNA (dNTP's, sheared plasmid, whole plasmid and genomic *E. coli* DNA) added to the conversion solution were also performed. These data are shown in Figure 4.7.

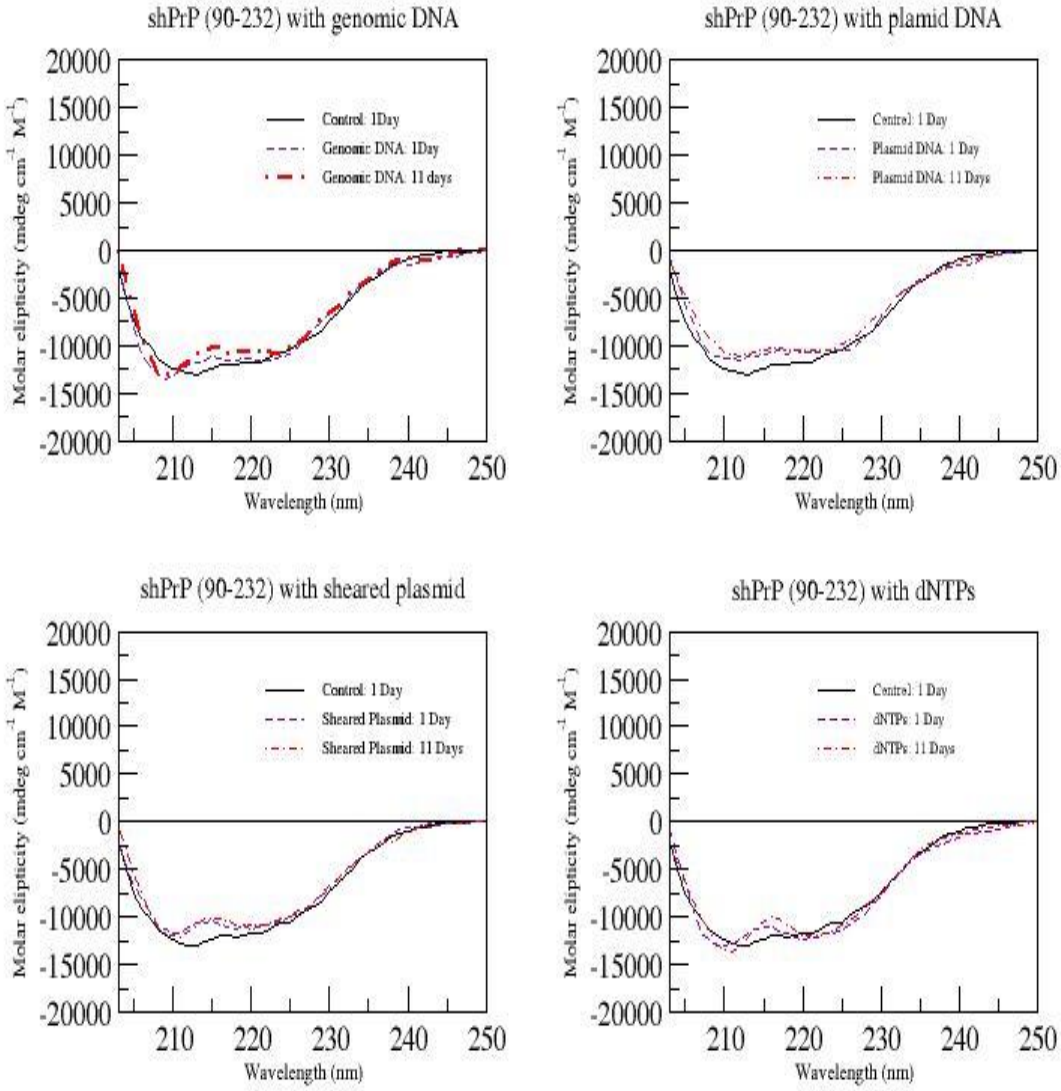

Figure 4.7 CD spectra for shPrPC mixed with either genomic DNA, plasmid DNA, sheared plasmid DNA or dNTP's.
The results for the first and last day of the experiment are shown.

These controls were followed for 4 days longer than normally required to convert the prion protein under the same conditions. Apart from the expected spectral changes due to the addition of nucleic acids, no significant change in secondary

structure of the protein was observed throughout the course of the experiment. Thus, we conclude that the observed changes in prion secondary structure arose from LPS alone and that LPS, alone, is responsible for initiating the PrP conversion reactions and those nucleic acids do not mediate the conversion or influence the LPS-directed conversion.

4.3 Discussion

In this study we have shown that LPS interacts with recombinant prion protein and that this interaction converts the α-helix-rich recombinant PrP^{C} into a beta-rich form (PrP^{β}) under physiological conditions. LPS induced PrP^{β} conversion does not require any brain-derived PrP^{β} seed, co-factors or denaturants, which are reported in other conversion and propagation protocols (*277, 279, 290, 305-307*). Furthermore, all of these conversion strategies rely on the continuous input of chemical denaturants (urea, guanidine hydrochloride), synthetic detergents (SDS), or extremes of pH or very high (denaturing) temperatures (*279, 303, 308-310*). However, LPS-mediated conversion is distinct from these methods in that a small amount can initiate conversion and propagation so long as the starting concentration remains above its CMC. Additionally, structural studies using RENAGE shows that the beta oligomers are not stable under standard electrophoresis conditions and can dissociate into a monomer, which parallels what has been observed with POPG converted PrP^{β}.

These findings may have significant consequences for laboratories using recombinant prion proteins in PMCA or *in-vitro* conversion assays and for

laboratories involved with animal prion transmission experiments. Any recombinant protein from a bacterial host will contain some amount of LPS and this LPS will remain with the protein unless special efforts are made to remove it during purification. Furthermore, most research laboratories, dissection rooms and animal housing facilities are heavily contaminated with LPS (*311-313*). Indeed, unless a facility is maintained under the strictest decontamination protocols LPS contamination is almost certain. Given that the initial conversion of the prion protein into PrP^{β} oligomers can be influenced by the presence of LPS, some previously published results on prion conversion may have been inadvertently affected by the presence of LPS. To guard against this, methods that maintain LPS concentrations below its CMC would be required. Finally, controls or assays to rule out bacterial or LPS contamination should also be routine for experiments evaluating prion conversion over extended time periods.While we have demonstrated the converting abilities of LPS *in-vitro,* these do not necessarily translate into propagating prions in animal models. As yet, we have not completed these ongoing animal studies that are investigating the disease potential of these recombinant beta oligomers. As discussed earlier, our findings indicate that a micelle form of LPS is required to initiate conversion. How and when such a form exists in nature and induces sporadic disease is certainly worth some further discussion. These findings partially support the hypothesis that prion-associated diseases may be the result of or augmented by the presence of bacteria.

LPS is present in the saliva, mammary glands, vagina and postpartum uterus, gastrointestinal tract and feces of most mammals, including sheep, elk, deer and

cattle. LPS is a key component of the normal Gram negative bacterial flora of all mammals. In the case of cattle, it has been documented that the levels of LPS in the gastrointestinal tract (i.e. the rumen) increases significantly when they are put on high grain diets compared to when they are left on pastures (*169, 314, 315*). One study (*316*) followed cattle fed on grain pellets comprised of 50% wheat and 50% barley. After four days on this diet, free ruminal LPS measured 12.8 $x10^4$ EU/mL or 12.8µg/mL, which is very close to LPS's CMC. Similar LPS values would likely be found in other ruminants (elk, deer, sheep) consuming similar high grain diets. It should also be noted that these values reflect free LPS, not bound material in living bacteria. In terms of bound LPS, it has been estimated that each *E. coli* bacterium contains between one and two million individual LPS molecules, which comprise over 70% of the its outer membrane. This corresponds to a LPS concentration of between 120 and 240 µg/mL. If normal prions were to come into contact with these high LPS concentrations in the gut (through consumption of meat or bone meal or eating prion-rich tissues), it is possible that the prions could convert to beta oligomeric forms. LPS is not restricted to the gut. It can also be found in blood and tissues of mammals too, especially those suffering bacterial infections such as septicemia or meningitis (*317*). Another possible route for prion-LPS association could be through contact with dead, dissected or slaughtered animals, which are decaying or awaiting rendering. Bacteria proliferate quite rapidly in such circumstances. Given that LPS is resistant to heat treatment (*318*), both chemical (1M NaOH) and thermal degradation is required for its complete removal. Interestingly, prior to the BSE

outbreak in the UK (circa 1987) and the ban on meat and bone meal in animal feed, carcasses were only wet rendered with only minimal heating (95 °C) (*319-321*). Consequently one could conclude that high levels of LPS must have been present in MBM in animal feed. However, despite these relatively high levels of LPS in everyday occurrence, we do not see high levels of sporadic prion disease, which indicates that while LPS may interact strongly with PrP^{C} and initiate its conversion, it is unlikely the sole mediator of propagation. Much like many of the denaturants reported before it, other cellular components and/or a breakdown of the body's natural housekeeping machinery is likely required for disease to present.

In conclusion, we have shown that LPS, a naturally occurring, ubiquitous agent found in almost all animals, is able to convert recombinant prions into PrP^{β} oligomers under normal, physiological conditions. This conversion can be temporal at low LPS:PrP^{C} levels providing the LPS concentration remains above its CMC. The beta-rich form of the prion that is produced by LPS is morphologically similar to that produced by another anionic lipid, POPG. However, the specific component of LPS (endotoxin, lipid A or polysaccharide) that might solely interact with the protein or initiate conversion remains to be determined. Studies to determine this and whether these synthetic prions are propagation-competent in animal models are ongoing.

Chapter 5

General Conclusions & Future Work

5.1 General Conclusions

My PhD thesis project was focused on addressing two major health challenges facing the Canadian cattle industry today: 1) Ruminal acidosis and acidosis-related metabolic disorders (laminitis, liver abscesses, bloat) in cattle and 2) Bovine spongiform encephalopathy (BSE), commonly known as mad cow disease. Specifically, to test the hypothesis that modern cattle feeding practices (i.e. grain rich diets) are, in part, responsible for these conditions. In particular, it was proposed that these feeding practices alter the chemical content of the ruminal fluid, thereby leading to elevated levels of LPS (endotoxin) which, in turn, lead to greater risk for developing these diseases. To test these hypotheses, modern metabolomics techniques to characterize the ruminal fluid of dairy cattle fed with different diets were used. From these experiments it was determined that a grain-rich diet leads to ruminal acidosis along with unusually high levels of ruminal and serum LPS. Based on the association of high-grain diets with various metabolic diseases, this suggests that acidic conditions in the rumen and the corresponding high serum levels of LPS are the "triggers" for these conditions. The inflammatory effects of LPS led me to inquire whether this molecule may also contribute to other bovine disesase. In particular, it was determined that LPS might play a role in the the induction of BSE (bovine spongiform encephalopathy) in cows. More specifically, LPS (in the test-tube) induces the conversion of helical native prion proteins into protease-resistant, beta-sheet rich proteins

similar to that of infectious prions. This suggests that elevated level of LPS in the rumen from grain-rich diets, may also play a role in the induction of BSE.

5.1.1 Unhealthy Alteration in Bovine Ruminal Metabolome with Feeding Grain-Rich Diets

As ruminants, cattle are specifically adapted to consume diets high in plant fiber. But today's modern, competitive and high throughput cattle industry, where grain is known to be a much more concentrated energy source than hay and other forages, grain-rich diets are now ubiquitous. Transitioning from a diet of grass and hay to one consisting primarily of grains significantly changes the rumen environment and its chemical composition. Because metabolomics is such a powerful approach for studying the chemical changes in biological systems, this approach was used to understand how this diet transition alters the rumen environment and potentially leads to certain metabolic disorders in dairy cattle.

By using improved metabolite detection techniques, including proton NMR spectroscopy, GC-MS and DFI-MS/MS, it was demonstrated that when cows were fed increasing amounts of cereal grain, corresponding increases were observed in the concentration of rumen putrescine, methylamines and other biogenic amines. Consumption of grain-rich diet also leads to high levels of glucose, alanine, maltose, ornithine, propionate, uracil, valerate, xanthine, and

phenylacetate as well as increased concentrations of *N*-nitrosodimethylamine (**NDMA**), urea, ethanolamine, maltose, and dimethylamine (**DMA**). My metabolomic studies also revealed a drop in ruminal pH and a decreased concentration of 3-phenylpropionate in cows fed greater amounts of cereal grain. It is well established that a decrease in rumen pH in dairy cows fed high-grain diets is associated with significant changes in microbiota composition. Many microbial species are not able to survive the stress of a low pH (*204*). In particular, high grain diets typically lead to a 10-14 fold increase in levels of rumen endotoxin or LPS. Therefore, the increased concentrations of xanthine, uracil, alanine, endotoxins (LPS) and certain amino acids in the ruminal fluid of cows fed high-grain diets appears to arise from widespread bacterial cell death. In addition to the release of harmful or proinflammatory compounds (LPS), urea, NH_3, ethanol, and biogenic amines) into the rumen, there is also increased production of volatile fatty acids or VFA (leading to ruminal acidosis). The ruminal acidosis may result in damage to intestinal epithelium that increases intestinal permeability to these compounds. Ruminal acidification due to high grain consumption also leads to further cell death, further microfloral changes, and the release of even more harmful compounds, thereby setting up a vicious cycle not unlike that seen in human gastrointestinal diseases or chronic inflammatory conditions such as ulcerative colitis and Crohn's disease. In Chapter 2, a variety of sophisticated multivariate and metabolic pathway analyses were used to confirm several additional rumen fluid compounds and rumen metabolic perturbations that might be involved in periparturient disease etiology (*169*). In

addition to these metabolic changes, it was also highlighted how some rumen-derived metabolites (particularly those associated with high-grain diets) have been previously associated with elevated risks or higher incidences of certain metabolic diseases such as SARA, acute rumen acidosis, urea toxicity, fatty liver disease, as well as inflammatory diseases such as mastitis, laminitis, milk fever, and other conditions. These data certainly underline the importance of gaining a better understanding of the biochemical function of rumen as a whole ecosystem. Improvements in our understanding of how diet influences rumen health, as well as improved methods for monitoring these changes should enable us to maintain the fine balance between high milk productivity and good herd health. The studies described in Chapters 2 also show how the use of modern metabolomic techniques could lead to the development and validation of new disease biomarkers for a variety of dairy cattle diseases.

Given the importance of the rumen in cattle health, it was decided that it would be essential to learn more about the ruminal fluid metabolome. In the second part of this thesis (Chapter 3), a combination of both commonly available metabolomics tools and literature-based approaches were used to identify and quantify the metabolites that can be detected in bovine ruminal fluid. Results revealed that this particular biofluid is metabolically diverse, with representative metabolites spanning 28 different compound categories. In particular data showed that ruminal fluid is mainly composed of endogenous metabolites from the cow

(phospholipids, inorganic ions, and gases) and metabolites derived from the rumen microbiota and diet (short chain fatty acids, volatile fatty acids, amino acids, dicarboxylic acids, and carbohydrates). This information has been deposited into the Bovine Rumen Metabolome Database (BRDB), which is freely available at http://www.rumendb.ca. Currently the BRDB contains information on 246 metabolites or metabolite species (corresponding to 334 unique structures), their concentrations, related literature reference and links to their known diet associations. The BRDB provide a convenient, centralized resource from which animal health scientist and veterinarians could potentially exploit to help in livestock disease detection and diagnosis. I believe it could be a valuable reference resource for livestock researchers wanting to learn more about the bovine rumen and its unique biochemical functions.

5.1.2 LPS (Endotoxins) May also Play a Role in the Induction of BSE and Other Prion Diseases

In Chapter 4 some of the information learned from these earlier metabolomic studies was used to explore whether some of the disease-inducing compounds generated from grain-rich diets may induce other diseases. In particular, an investigation was conducted as to whether LPS could potentially induce a prion disease known as bovine spongiform encephalopathy (BSE) or "mad cow" disease. Prions are known to be devoid of nucleic acids and exclusively composed of a modified isoform of PrP known as PrP^{Sc}. The ability of an infectious beta-rich prion isoform (PrP^{Sc}) to recruit and convert the cellular alpha helical prion isoform (PrP^{C}) into a self-propagating “like” strain is a central feature of prion

pathology (*322*). The process of conversion is still poorly understood, but several theories exist, including the involvement of "Factor X" or a cofactor that must be co-incubated with the prion to create a catalytically active entity (PrP^{Sc}), which is now widely supported by many lines of evidence. LPS is a component of the Gram-negative bacterial membrane, and is found in almost all animals, (in the study reported in Chapter 2 a 14 to 20 fold increase in the concentration of endotoxins in the cow's ruminal fluid following high-grain consumption was reported) is able to convert recombinant prions into beta-sheet rich isoform similar to that of PrP^{Sc} under normal, physiological conditions. This suggests that LPS might play a role as a "factor X" in the etiology and pathogenesis of prion diseases such as BSE.

Results described in Chapter 4 showed that LPS could convert recombinant hamster, mouse and bovine prions into similar beta-sheet rich isoforms that could also form beta-rich oligomers and fibrils. Three different techniques were used to evaluate the interaction of LPS with PrP^{C}: 1) Nuclear Magnetic Resonance (NMR) which indicated an interaction between the two molecules, 2) Electron Microscopy (EM) which showed binding of PrP^{C} to the LPS micelles, and 3) Circular Dichroism (CD) spectroscopy which demonstrated that LPS was able to initiate conversion of the alpha helical PrP^{C} into the beta-rich PrP^{Sc} like isoform. Interestingly, this conversion could be initiated at low micromolar concentrations. Furthermore, enzymatic (Proteinase K) digestion of the LPS-converted prions revealed a 12 kDa proteolytic resistant core, consistent with both oligomeric and

fibrillar isotypes of infectious or scrapie-like prions. The beta-rich isoform (PrP^{β}) produced by LPS is morphologically similar to that produced by another anionic lipid, POPG. Not only was it confirmed that LPS can initiate conversion of the prion protein, but it was also demonstrated that this converted beta-rich isoform could partially self-propagate by inducing conversion of additional unconverted protein – as long as the LPS concentration in the solution remained above the CMC. The specific component of LPS (i.e. Endotoxin, lipid A or polysaccharide) that might interact with the prion protein or initiate the conversion remains to be determined. Studies to determine whether these synthetic prions are propagation-competent in animal models are ongoing.

5.1.3 Potential Feed Ingredients to Replace Grains

My thesis research has clearly shown that high grain diets in cows lead to significant rumen dysbiosis which leads to a number of metabolic and other periparturient diseases. Given the potential harm that grain-rich diets have on dairy cows, the question is: Are there alternative feed ingredients to replace grains? Because of the high energy requirements of lactating dairy cows, barley grain is often used in feed due to its high energy and starch content. There are many different alternatives to grain and by-product feedstuffs are now available, often at a fairly low cost. These can be included in dairy cattle rations to provide supplemental nutrition without reducing lactation performance. If properly managed, pastures can also be used as a good source of non-grain nutrients for dairy cows. Though pasture handling is easier and there is far less manure

hauling, pasture-fed cows still need to be supplemented with forage or other high-energy feeds in balanced rations. Byproduct feeds such as corn gluten feed, beet pulp and soy hulls feeds from feed processing industries can be a cost-effective and feasible supplement to normal dairy rations. Byproduct feeds are not only a good source of nutrients but also used as an alternative to both forages and grain. These byproducts are much lower in starch as compared to grains but are readily degradable in the rumen and contain significant quantities of other NFC (nonfiber carbohydrates), including sugars, organic acids, fructans, glucans and pectins. Inclusion of byproduct feeds in early lactation diets of dairy cows allows the formulation of high neutral detergent fiber (NDF) with moderate nonfiber carbohydrates (NFC; primarily starch) and high energy density. When deciding on an alternative feeding program, careful consideration should be given to the handling, storage, variability, availability, and the nutrient content of alternative feeds and how the cows respond.

5.1.4 Future Work

For my future research work I intend to determine the plasma, milk and urinary metabolomes of dairy cattle under normal as well as under grain-induced stress. This will be done through computational and experimental methods. Specifically I will identify and quantify the detectable metabolites present in plasma, urine, and milk of dairy cows in different stages of lactation (during the dry period as well as during early-, mid- and late-lactation) using NMR, LC-MS, GC-MS, ICP-MS and other methods. This work will not only help us to understand how rumen acidosis

affects the metabolite composition of plasma, milk and urine but it will also help to establish a comprehensive metabolome database for dairy cattle. This database will serve to evaluate and compare the normal bovine metabolome with the metabolomic profiles of unhealthy cattle (i.e. those with general health, toxicity, infectious, or productivity problems). In addition to revealing important insights and diagnostic indicators into dairy cattle diseases, the characterization of the milk metabolome will also provide important insights into how dairy cattle diseases alter the nutritional content, utility and quality of milk. Milk contains proteins, complex carbohydrates, and small molecule metabolites that are vital to the growth and health of not only dairy calves but also to humans who regularly consume milk.

I believe the establishment of plasma, milk and urine metabolomes for different physiological groups of dairy cows will help the dairy industry in many ways including the: 1) establishment of a better understanding of the physiology of the dairy cow, 2) improvement of reproductive efficiency and longevity of dairy cows, 3) better understanding of the causes and mechanism(s) of metabolic and non-metabolic disorders in dairy cattle, 4) enhanced support for the health benefits of milk by more completely determining its composition, 5) design of healthy, productive, and efficient diets, 6) development of a novel method for checking problematic herds and diagnosing their problems, 7) diagnosing many common dairy cattle diseases at their earliest stages by identifying their key biomarkers.

References

1. Miller, D. (1999) Risk, science and policy: Definitional struggles, information management, the media and BSE, *Soc Sci Med 49*, 1239-1255.
2. Canadian Dairy Information Center. (2012) On-Line. Accessed at: http://www.dairyinfo.gc.ca/index_e.php?s1=cdi-ilc.
3. Report of the Standing Committee on Agriculture and Agri-Food (2004). Canadian livestock and beef pricing in the aftermath of the BSE crisis. House of Common, Canada.
4. Athwal, R. K. (2002) Integration of Canadian and U.S. cattle markets (agriculture and rural), *Working Paper No, 53*.
5. Nocek, J. E. (1997) Bovine acidosis: implications on laminitis, *J Dairy Sci 80*, 1005-1028.
6. Ametaj, B. N. (2005) A new understanding of the causes of fatty liver in dairy cows, *Adv Dairy Technol 17*, 97-112.
7. Emmanuel, D. G., Dunn, S. M., and Ametaj, B. N. (2008) Feeding high proportions of barley grain stimulates an inflammatory response in dairy cows, *J Dairy Sci 91*, 606-614.
8. Jenkins, T. C., and McGuire, M. A. (2006) Major advances in nutrition: impact on milk composition, *J Dairy Sci 89*, 1302-1310.
9. Zebeli, Q., and Ametaj, B. N. (2009) Relationships between rumen lipopolysaccharide and mediators of inflammatory response with milk fat production and efficiency in dairy cows, *J Dairy Sci 92*, 3800-3809.
10. Le Roy, D., and Klein, K. K. (2005) Mad cow chaos in Canada: was it just bad luck or did government policies play a role?, *Can Public Pol 31*, 381-399.
11. Prusiner, S. (1998) Prions, *Proc Natl Acad Sci USA 95*, 13363 - 13383.
12. Rasmussen, K. (1995) Trail blazers of canadian agriculture Ottawa: Agricultural institute of Cananda, Canadian cattlemen 1938b, *Public markets and Direct Shipments 1*, 115.
13. McCallum, J., (Ed.) (1980) *Unequal Beginnings: Agricultural and Economic Development in Quebec and Ontario Until 1870*, 2 ed., University of Toronto Press, Toronto.
14. Lutz, J. S. (1980) Interlude or Industry? Ranching in British Columbia, 1859-1885, *British Columbia Historical News 13*, 2-11.

15. Jameson, S. S., (Ed.) (1981) *"Era of the big ranches" in the best from Alberta history* Hugh Dempsey (Western Producer Prairie Books), Saskatoon:.
16. Laing, F. W. (1942).Some pioneers of the cattle industry" British Columbia historical quarterly, *6*, 257-275.
17. Fowke, V. C. (1946) Canadian agricultural policy, University of Toronto Press, Toronto.
18. Canada Beef Inc. Canadian Cattle Production System. Online Accessed at: http://www.canadabeef.ca/ca/en/rt/industry/CCPS/default.aspx.
19. (2004) Report of the Standing Committee on Agriculture and Agri-Food. Canadian livestock and beef pricing in the aftermath of the BSE crisis. House of Commons. Canada.
20. Wyatt, J., Pearson, G., and Gruffydd-Jones, T. (1993) Feline spongiform encephalopathy, *Feline Pract 21*, 7 - 9.
21. Bons, N., Mestre-Frances, N., Belli, P., Cathala, F., Gajdusek, D., and Brown, P. (1999) Natural and experimental oral infection of nonhuman primates by bovine spongiform encephalopathy agents, *Proc Natl Acad Sci USA 96*, 4046 - 4051.
22. Gajdusek, D., and Zigas, V. (1957) Degenerative disease of the central nervous system in New Guinea. The endemic occurrence of "kuru" in the native population, *New Engl J Med 257*, 974 - 978.
23. Zahn, R., Liu, A., Luhrs, T., Riek, R., von Schroetter, C., Lopez Garcia, F., Billeter, M., Calzolai, L., Wider, G., and Wuthrich, K. (2000) NMR solution structure of the human prion protein, *Proc Natl Acad Sci USA 97*, 145 - 150.
24. Galyean, M. L. (1999) Review: restricted and programmed feeding of beef cattle—definitions, application, and research results, *Profess Ani Scien 15*, 1-6.
25. Driedger, L. J., and Loerch, S. C. (1999) Limit-feeding corn as an alternative to hay reduces manure and nutrient output by Holstein cows, *J Anim Sci 77*, 967-972.
26. Loerch, S. C. (1990) Effects of feeding growing cattle high-concentrate diets at a restricted intake on feedlot performance, *J Anim Sci 68*, 3086-3095.
27. McDonald, P., Edwards, R. A. G., and Greennagh, J. F. D., (Eds.) (2002) *Animal Nutrition*, 6 ed., Pearson Prentice Hall, New York.
28. Van Soest, P. J., (Ed.) (1994) *Nutritional ecology of the ruminant*, 2nd ed., Cornell University press, Ithaca, New York.
29. Ametaj, B., Zebeli, Q., Saleem, F., Psychogios, N., Lewis, M., Dunn, S., Xia, J., and Wishart, D. (2010) Metabolomics reveals unhealthy alterations in rumen metabolism with increased proportion of cereal grain in the diet of dairy cows, *Metabolomics 6*, 583-594.
30. Klieve, A. V., Hennessy, D., Ouwerkerk, D., Forster, R. J., Mackie, R. I., and Attwood, G. T. (2003) Establishing populations of Megasphaera

elsdenii YE 34 and Butyrivibrio fibrisolvens YE 44 in the rumen of cattle fed high grain diets, *J Appl Microbiol 95*, 621-630.

31. Goad, D. W., Goad, C. L., and Nagaraja, T. G. (1998) Ruminal microbial and fermentative changes associated with experimentally induced subacute acidosis in steers, *J Ani Sci 76*, 234-241.
32. Schwartzkopf-Genswein, K. S., Beauchemin, K. A., Gibb, D. J., Crews, D. H., Hickman, D. D., Streeter, M., and McAllister, T. A. (2003) Effect of bunk management on feeding behavior, ruminal acidosis and performance of feedlot cattle: A review, *J Ani Sci 81*, E149-E158.
33. Bevans, D. W., Beauchemin, K. A., Schwartzkopf-Genswein, K. S., McKinnon, J. J., and McAllister, T. A. (2005) Effect of rapid or gradual grain adaptation on subacute acidosis and feed intake by feedlot cattle, *J Anim Sci 83*, 1116-1132.
34. Nagaraja, T., Bartley, E., Fina, L., and Anthony, H. (1978) Relationship of rumen Gram negative bacteria and free endotoxin to lactic acidosis in cattle, *J Anim Sci 47*, 1329 - 1336.
35. Ametaj, B. N., Zebeli, Q., and Iqbal, S. (2010) Nutrition, microbiota, and endotoxin-related diseases in dairy cows, *Rev Bra Zootecn 39*, 433-444.
36. Andersen, P., Hesselholt, M., and Jarlov, N. (1994) Endotoxin and arachidonic acid metabolites in portal, hepatic and arterial blood of cattle with acute ruminal acidosis, *Acta Vet Scand 35*, 223 - 234.
37. Nagaraja, T., Bartley, E., Fina, L., Anthony, H., and Bechtle, R. (1978) Evidence of endotoxins in the rumen bacteria of cattle fed hay or grain, *J Anim Sci 47*, 226 - 234.
38. Khafipour, E., Krause, D. O., and Plaizier, J. C. (2009) A grain-based subacute ruminal acidosis challenge causes translocation of lipopolysaccharide and triggers inflammation, *J Dairy Sci 92*, 1060-1070.
39. Tajima, K., Arai, S., Ogata, K., Nagamine, T., Matsui, H., Nakamura, M., Aminov, R. I., and Benno, Y. (2000) Rumen bacterial community transition during adaptation to high-grain diet, *Anaerobe 6*, 273-284.
40. Hardy, P. H., Jr., and Levin, J. (1983) Lack of endotoxin in *Borrelia hispanica* and *Treponema pallidum*, *Proc Soc Exp Biol Med 174*, 47-52.
41. Kawahara, K., Moll, H., Knirel, Y. A., Seydel, U., and Zahringer, U. (2000) Structural analysis of two glycosphingolipids from the lipopolysaccharide-lacking bacterium *Sphingomonas capsulata*, *Eur J Biochem 267*, 1837-1846.
42. Kawahara, K., Seydel, U., Matsuura, M., Danbara, H., Rietschel, E. T., and Zahringer, U. (1991) Chemical structure of glycosphingolipids isolated from *Sphingomonas paucimobilis*, *FEBS Lett 292*, 107-110.
43. Kawasaki, S., Moriguch, R., Sekiya, K., Nakai, T., Ono, E., Kume, K., and Kawahara, K. (1994) The cell envelope structure of the lipopolysaccharide-lacking Gram-negative bacterium *Sphingomonas paucimobilis*, *J Bacteriol 176*, 284–290.
44. Leone, S., Molinaro, A., Lindner, B., Romano, I., Nicolaus, B., Parrilli, M., Lanzetta, R., and Holst, O. (2006) The structures of glycolipids

isolated from the highly thermophilic bacterium Thermus thermophilus Samu-SA1, *Glycobiology 16*, 766-775.

45. Takayama, K., Rothenberg, R. J., and Barbour, A. G. (1987) Absence of lipopolysaccharide in the Lyme disease spirochete, Borrelia burgdorferi, *Infect Immun 55*, 2311-2313.
46. Yang, Y. L., Yang, F. L., Huang, Z. Y., Tsai, Y. H., Zou, W., and Wu, S. H. (2010) Structural variation of glycolipids from Meiothermus taiwanensis ATCC BAA-400 under different growth temperatures, *Org Biomol Chem 8*, 4252-4254.
47. Shear, M. J., and Turner, F. C. (1943) Isolation of the hemorrhageproducing fraction from *Serratia marcescens* (*Bacillus prodigiosus*) culture filtrate, *J Natl Cancer Res 4*, 81–97.
48. Nikaido, H. (2003) Molecular basis of bacterial outer membrane permeability revisited, *Microbiol Mol Biol Rev 67*, 593-656.
49. Burvenich, C., Bannerman, D. D., Lippolis, J. D., Peelman, L., Nonnecke, B. J., Kehrli, M. E., Jr., and Paape, M. J. (2007) Cumulative physiological events influence the inflammatory response of the bovine udder to Escherichia coli infections during the transition period, *J Dairy Sci 90*, E39-54.
50. Dal Nogare, A. R. (1991) Southwestern Internal Medicine Conference:septic shock, *Am. J. Med. Sci*, 0–65.
51. Raetz, C. R., Ulevitch, R. J., Wright, S. D., Sibley, C. H., Ding, A., and Nathan, C. F. (1991) Gram-negative endotoxin: an extraordinary lipid with profound effects on eukaryotic signal transduction, *FASEB J 5*, 2652-2660.
52. Rietschel, E., Schade, U., Jensen, M., Wollenweber, H., Luderitz, O., and Greisman, S., (Eds.) (1982) *Bacterial endotoxins: Chemical structure, biological activity and role in septicaemia*, Vol. 31, 2 ed.
53. Rietschel, E. T., and Wagner, H., (Eds.) (1996) *Bacterial Endotoxin. In Pathology of Septic Shock*, 2 ed., Springer-Verlag, Berlin,Germany.
54. Andersen, P. (2003) Bovine endotoxicosis - some aspects of relevance to production diseases, *Acta Vet Scand 44*, S141 - S155.
55. Nau, R., and Eiffert, H. (2002) Modulation of release of proinflammatory bacterial compounds by antibacterials: potential impact on course of inflammation and outcome in sepsis and meningitis, *Clin Microbiol Rev 15*, 95-110.
56. Drakley, J. K., and Dann, H. M. (2005) New concepts in nutritional management of dry cows, *Adv. Dairy Tech 15*, 11-23.
57. McAllister, T. A., Okine, E. K., Mathison, G. W., and Cheng, K. J. (1996) Dietary, environmental and microbiological aspects of methane production in ruminants, *Can J Anim Sci 76*, 231-243.
58. Owens, F. N., Secrist, D. S., Hill, W. J., and Gill, D. R. (1998) Acidosis in cattle: a review, *J Anim Sci 76*, 275-286.

59. Kleen, J. L., Hooijer, G. A., Rehage, J., and Noordhuizen, J. P. (2003) Subacute ruminal acidosis (SARA): a review, *J Vet Med A Physiol Pathol Clin Med 50*, 406-414.
60. Perry, T. W., and Cecava, M. J., (Eds.) (1980) *Beef Cattle Feeding and Nutrition*, 2 ed., Academic Press, San Francisco.
61. Diez-Gonzalez, F., Callaway, T. R., Kizoulis, M. G., and Russell, J. B. (1998) Grain feeding and the dissemination of acid-resistant *Escherichia coli* from cattle, *Science 281*, 1666-1668.
62. Plaizier, J. C., Khafipour, E., Li, S., Gozho, G. N., and Krause, D. O. (2012) Subacute ruminal acidosis (SARA), endotoxins and health consequences, *Anim Feed Sci Tech 172*, 9-21.
63. Khafipour, E., Li, S., Plaizier, J. C., and Krause, D. O. (2009) Rumen Microbiome Composition Determined Using Two Nutritional Models of Subacute Ruminal Acidosis, *Appl and Environ Microbiol 75*, 7115-7124.
64. Olson, J. D. (1997) The relationship between nutrition and management to lameness in dairy cattle *The Bovine Practitioner 31*, 65-68.
65. Bradley, R., and Wilesmith, J. W. (1993) Epidemiology and control of bovine spongiform encephalopathy (BSE), *Br Med Bull 49*, 932-959.
66. Smilie, R. H., Hoblet, K. H., Weiss, W. P., Eastridge, M. L., Rings, D. M., and Schnitkey, G. L. (1996) Prevalence of lesions associated with subclinical laminitis in first-lactation cows from herds with high milk production, *J Am Vet Med Assoc 208*, 1445-1451.
67. Vatandoost, M., Norouzian, M. A., and Nosrati, M. (2009) Estimation of milk Yield and economic Loss resulting to laminitis in holstein cow: case study, *J Anim Sci 8*, 880-882.
68. Nagaraja, T. G., and Lechtenberg, K. F. (2007) Liver abscesses in feedlot cattle, *Vet Clin North Am Food Anim Pract 23*, 351-369, .
69. Checkley, S. L., Janzen, E. D., Campbell, J. R., and McKinnon, J. J. (2005) Efficacy of vaccination against *Fusobacterium necrophorum* infection for control of liver abscesses and footrot in feedlot cattle in western Canada, *Can Vet J 46*, 1002-1007.
70. Nagaraja, T. G., and Chengappa, M. M. (1998) Liver abscesses in feedlot cattle: a review, *J Anim Sci 76*, 287-298.
71. Brink, D. R., Lowry, S. R., Stock, R. A., and Parrott, J. C. (1990) Severity of liver abscesses and efficiency of feed utilization of feedlot cattle, *J Anim Sci 68*, 1201-1207.
72. Smith, R. A. (1998) Impact of disease on feedlot performance: a review, *J Anim Sci 76*, 272-274.
73. Guo, A. C., Jewison, T., Wilson, M., Liu, Y., Knox, C., Djoumbou, Y., Lo, P., Mandal, R., Krishnamurthy, R., and Wishart, D. S. (2013) ECMDB: the E. coli Metabolome Database, *Nucleic Acids Res 41*, D625-630.
74. Hollywood, K., Brison, D. R., and Goodacre, R. (2006) Metabolomics: current technologies and future trends, *Proteomics 6*, 4716-4723.

75. Jewison, T., Knox, C., Neveu, V., Djoumbou, Y., Guo, A. C., Lee, J., Liu, P., Mandal, R., Krishnamurthy, R., Sinelnikov, I., Wilson, M., and Wishart, D. S. (2012) YMDB: the Yeast Metabolome Database, *Nucleic Acids Res 40*, D815-820.
76. Kaddurah-Daouk, R., Kristal, B. S., and Weinshilboum, R. M. (2008) Metabolomics: a global biochemical approach to drug response and disease, *Annu Rev Pharmacol Toxicol 48*, 653-683.
77. Wishart, D. S., Jewison, T., Guo, A. C., Wilson, M., Knox, C., Liu, Y., Djoumbou, Y., Mandal, R., Aziat, F., Dong, E., Bouatra, S., Sinelnikov, I., Arndt, D., Xia, J., Liu, P., Yallou, F., Bjorndahl, T., Perez-Pineiro, R., Eisner, R., Allen, F., Neveu, V., Greiner, R., and Scalbert, A. (2013) HMDB 3.0--The Human Metabolome Database in 2013, *Nucleic Acids Res 41*, D801-807.
78. Lindon, J. C., Holmes, E., Bollard, M. E., Stanley, E. G., and Nicholson, J. K. (2004) Metabonomics technologies and their applications in physiological monitoring, drug safety assessment and disease diagnosis, *Biomarkers 9*, 1-31.
79. Wishart, D. S., Tzur, D., Knox, C., Eisner, R., Guo, A. C., Young, N., Cheng, D., Jewell, K., Arndt, D., Sawhney, S., Fung, C., Nikolai, L., Lewis, M., Coutouly, M. A., Forsythe, I., Tang, P., Shrivastava, S., Jeroncic, K., Stothard, P., Amegbey, G., Block, D., Hau, D. D., Wagner, J., Miniaci, J., Clements, M., Gebremedhin, M., Guo, N., Zhang, Y., Duggan, G. E., Macinnis, G. D., Weljie, A. M., Dowlatabadi, R., Bamforth, F., Clive, D., Greiner, R., Li, L., Marrie, T., Sykes, B. D., Vogel, H. J., and Querengesser, L. (2007) HMDB: the Human Metabolome Database, *Nucleic Acids Res 35*, D521-526.
80. Holmes, E., Wilson, I. D., and Nicholson, J. K. (2008) Metabolic phenotyping in health and disease, *Cell 134*, 714-717.
81. Wishart, D. S. (2005) Metabolomics: the principles and potential applications to transplantation, *Am J Transplant 5*, 2814-2820.
82. Wishart, D. S. (2008) Applications of metabolomics in drug discovery and development, *Drugs R D 9*, 307-322.
83. Oliver, S. G., Winson, M. K., Kell, D. B., and Baganz, F. (1998) Systematic functional analysis of the yeast genome, *Trends Biotechnol 16*, 373-378.
84. Fiehn, O. (2002) Metabolomics--the link between genotypes and phenotypes, *Plant Mol Biol 48*, 155-171.
85. Kind, T., Scholz, M., and Fiehn, O. (2009) How large is the metabolome? A critical analysis of data exchange practices in chemistry, *PLoS One, 4*, e5440.
86. Psychogios, N., Hau, D. D., Peng, J., Guo, A. C., Mandal, R., Bouatra, S., Sinelnikov, I., Krishnamurthy, R., Eisner, R., Gautam, B., Young, N., Xia, J., Knox, C., Dong, E., Huang, P., Hollander, Z., Pedersen, T. L., Smith, S. R., Bamforth, F., Greiner, R., McManus, B., Newman, J. W., Goodfriend,

T., and Wishart, D. S. (2011) The human serum metabolome, *PLoS One 6*, e16957.
87. Wishart, D. S., Lewis, M. J., Morrissey, J. A., Flegel, M. D., Jeroncic, K., Xiong, Y., Cheng, D., Eisner, R., Gautam, B., Tzur, D., Sawhney, S., Bamforth, F., Greiner, R., and Li, L. (2008) The human cerebrospinal fluid metabolome, *J Chromatogr B Analyt Technol Biomed Life Sci 871*, 164-173.
88. Oliver, S. G. (2002) Functional genomics: lessons from yeast, *Philos Trans R Soc Lond B Biol Sci 357*, 17-23.
89. Slupsky, C. M., Rankin, K. N., Wagner, J., Fu, H., Chang, D., Weljie, A. M., Saude, E. J., Lix, B., Adamko, D. J., Shah, S., Greiner, R., Sykes, B. D., and Marrie, T. J. (2007) Investigations of the effects of gender, diurnal variation, and age in human urinary metabolomic profiles, *Anal Chem 79*, 6995-7004.
90. Dunn, W. B., and Ellis, D. I. (2005) Metabolomics: Current analytical platforms and methodologies, *Trend Anal Chem 24*, 285-294.
91. Bloch, F., Hansen, W. W., and Packard, M. (1946) The nuclear induction experiment, *Phys. Rev 70*, 474-485.
92. Purcell, E. M., Torrey, H. C., and Pound, R. V. (1946) Resonance absorption by nuclear magnetic moments in a solid, *Physl Rev 69*, 37-38.
93. Keun, H. C., Ebbels, T. M., Antti, H., Bollard, M. E., Beckonert, O., Schlotterbeck, G., Senn, H., Niederhauser, U., Holmes, E., Lindon, J. C., and Nicholson, J. K. (2002) Analytical reproducibility in (1)H NMR-based metabonomic urinalysis, *Chem Res Toxicol 15*, 1380-1386.
94. Nielsen, J., and Oliver, S. (2005) The next wave in metabolome analysis, *Trends Biotechnol 23*, 544-546.
95. (!!! INVALID CITATION !!!).
96. Wishart, D. S. (2008) Metabolomics: applications to food science and nutrition research, *Trends Food Sci Tech 19*, 482-493.
97. Bailey, S. R., Marr, C. M., and Elliott, J. (2003) Identification and quantification of amines in the equine caecum, *Research in Veterinary Science 74*, 113-118.
98. Le Roy, D., and Klein, K. K. (1995) Mad cow chaos in Canada: was it just bad luckor did government policies play a role?, *Can Public Pol 31*, 381-399.
99. Linden, R., Martins, V., Prado, M., Cammarota, M., Izquierdo, I., and Brentani, R. (2008) Physiology of the prion protein, *Physiol Rev 88*, 673 - 728.
100. Jones, T. (2004) "Mad cow" and prion diseases, *Tenn Med 97*, 413-414.
101. Millstone, E., and van Zwanenberg, P. (2001) Politics of expert advice: lesson from the early history of the BSE sage, *Sci Pub Pol 28*, 99-112.
102. Anderson, R. M., Donnelly, C. A., Ferguson, N. M., Woolhouse, M. E. J., Watt, C. J., Udy, H. J., MaWhinney, S., Dunstan, S. P., Southwood, T. R. E., Wilesmith, J. W., Ryan, J. B. M., Hoinville, L. J., Hillerton, J. E.,

Austin, A. R., and Wells, G. A. H. (1996) Transmission dynamics and epidemiology of BSE in British cattle, *Nature 382*, 779-788.

103. Donnelly, C. A., Ferguson, N. M., Ghani, A. C., and Anderson, R. M. (2002) Implications of BSE infection screening data for the scale of the British BSE epidemic and current European infection levels, *Proc Biol Sci 269*, 2179-2190.
104. Leiss, W., and Powell, D., (Eds.) (2004) *Mad cows and mother's milk.*, 2 ed., McGill-Queen's University Press., Montreal,Canda.
105. Poulin, D., and Boame, A. (2003) Mad cow disease and beef trade. Stats Canada Agriculture Division Ottawa, ON.
106. Kirkwood, J., Cunningham, A., Wells, G., Wilesmith, J., and Barnett, J. (1993) Spongiform encephalopathy in a herd of greater kudu (Tragelaphus strepsiceros): epidemiological observations, *Vet Rec 133*, 360 - 364.
107. Schneider, K., Fangerau, H., Michaelsen, B., and Raab, W. H. (2008) The early history of the transmissible spongiform encephalopathies exemplified by scrapie, *Brain Res Bull 77*, 343-355.
108. Schneider, K., Fangerau, H., and Raab, W. H. (2007) The early history of transmissible spongiform encephalopathies exemplified by scrapie, *Nervenarzt 78*, 156, 158-160, 162-155.
109. Gajdusek, D. C., and Zigas, V. (1957) Degenerative disease of the central nervous system in New Guinea; the endemic occurrence of kuru in the native population, *N Engl J Med 257*, 974-978.
110. Gibbs, C. J., Jr., Gajdusek, D. C., and Latarjet, R. (1978) Unusual resistance to ionizing radiation of the viruses of kuru, Creutzfeldt-Jakob disease, and scrapie, *Proc Natl Acad Sci USA 75*, 6268-6270.
111. Masters, C. L., Gajdusek, D. C., and Gibbs, C. J., Jr. (1981) The familial occurrence of Creutzfeldt-Jakob disease and Alzheimer's disease, *Brain 104*, 535-558.
112. Will, R. G., Ironside, J. W., Zeidler, M., Cousens, S. N., Estibeiro, K., Alperovitch, A., Poser, S., Pocchiari, M., Hofman, A., and Smith, P. G. (1996) A new variant of Creutzfeldt-Jakob disease in the UK, *Lancet 347*, 921-925.
113. Bruce, M. E., Will, R. G., Ironside, J. W., McConnell, I., Drummond, D., Suttie, A., McCardle, L., Chree, A., Hope, J., Birkett, C., Cousens, S., Fraser, H., and Bostock, C. J. (1997) Transmissions to mice indicate that `new variant' CJD is caused by the BSE agent, *Nature 389*, 498-501.
114. Hewitt, P. E., Llewelyn, C. A., Mackenzie, J., and Will, R. G. (2006) Creutzfeldt-Jakob disease and blood transfusion: results of the UK transfusion medicine epidemiological review study, *Vox Sang 91*, 221-230.
115. Alper, T., Cramp, W. A., Haig, D. A., and Clarke, M. (1967) Does the agent of scrapie replicate without nucleic acid?, *Nature 214*, 764-766.
116. Prusiner, S. B. (1982) Novel proteinaceous infectious particles cause scrapie, *Science 216*, 136-144.

117. Prusiner, S. B., Groth, D. F., Bildstein, C., Masiarz, F. R., McKinley, M. P., and Cochran, S. P. (1980) Electrophoretic properties of the scrapie agent in agarose gels, *Proc Natl Acad Sci USA 77*, 2984-2988.
118. Sparrer, H. E., Santoso, A., Szoka, F. C., and Weissman, J. S. (2000) Evidence for the prion hypothesis: Induction of the yeast [PSI+] factor by in vitro-converted Sup35 protein, *Science 289*, 595-599.
119. Telling, G. C., Scott, M., Mastrianni, J., Gabizon, R., Torchia, M., Cohen, F. E., DeArmond, S. J., and Prusiner, S. B. (1995) Prion propagation in mice expressing human and chimeric PrP transgenes implicates the interaction of cellular PrP with another protein, *Cell 83*, 79-90.
120. Ryou, C., and Mays, C. E. (2008) Prion propagation in vitro: are we there yet?, *Int J Med Sci 5*, 347-353.
121. Imran, M., and Mahmood, S. (2011) An overview of animal prion diseases, *Virol J 8*, 493.
122. Sigurdson, C. J., and Miller, M. W. (2003) Other animal prion diseases, *British Medical Bulletin 66*, 199-212.
123. Bolton, D. C., McKinley, M. P., and Prusiner, S. B. (1982) Identification of a protein that purifies with the scrapie prion, *Science 218*, 1309-1311.
124. Hosszu, L. L., Baxter, N. J., Jackson, G. S., Power, A., Clarke, A. R., Waltho, J. P., Craven, C. J., and Collinge, J. (1999) Structural mobility of the human prion protein probed by backbone hydrogen exchange, *Nat Struct Biol 6*, 740-743.
125. Jackson, G. S., Murray, I., Hosszu, L. L., Gibbs, N., Waltho, J. P., Clarke, A. R., and Collinge, J. (2001) Location and properties of metal-binding sites on the human prion protein, *Proc Natl Acad Sci USA 98*, 8531-8535.
126. Riek, R., Wider, G., Billeter, M., Hornemann, S., Glockshuber, R., and Wuthrich, K. (1998) Prion protein NMR structure and familial human spongiform encephalopathies, *Proc Natl Acad Sci USA 95*, 11667-11672.
127. Aguzzi, A., and Miele, G. (2004) Recent advances in prion biology, *Curr Opin Neurol 17*, 337-342.
128. Dodelet, V. C., and Cashman, N. R. (1998) Prion protein expression in human leukocyte differentiation, *Blood 91*, 1556-1561.
129. Wuthrich, K., and Riek, R. (2001) Three-dimensional structures of prion proteins, *Adv Protein Chem 57*, 55-82.
130. Riek, R., Hornemann, S., Wider, G., Billeter, M., Glockshuber, R., and Wuthrich, K. (1996) NMR structure of the mouse prion protein domain PrP(121-231), *Nature 382*, 180-182.
131. Eghiaian, F., Grosclaude, J., Lesceu, S., Debey, P., Doublet, B., Treguer, E., Rezaei, H., and Knossow, M. (2004) Insight into the PrPC-->PrPSc conversion from the structures of antibody-bound ovine prion scrapie-susceptibility variants, *Proc Natl Acad Sci USA 101*, 10254-10259.
132. Knaus, K. J., Morillas, M., Swietnicki, W., Malone, M., Surewicz, W. K., and Yee, V. C. (2001) Crystal structure of the human prion protein reveals a mechanism for oligomerization, *Nat Struct Biol 8*, 770-774.
133. Prusiner, S. B. (1998) Prions, *Proc Natl Acad Sci USA 95*, 13363-13383.

134. Cohen, F. E., Pan, K. M., Huang, Z., Baldwin, M., Fletterick, R. J., and Prusiner, S. B. (1994) Structural clues to prion replication, *Science 264*, 530-531.
135. Prusiner, S. B., Scott, M. R., DeArmond, S. J., and Cohen, F. E. (1998) Prion protein biology, *Cell 93*, 337-348.
136. Harper, J. D., and Lansbury, P. T., Jr. (1997) Models of amyloid seeding in Alzheimer's disease and scrapie: mechanistic truths and physiological consequences of the time-dependent solubility of amyloid proteins, *Annu Rev Biochem 66*, 385-407.
137. Bessen, R. A., Kocisko, D. A., Raymond, G. J., Nandan, S., Lansbury, P. T., and Caughey, B. (1995) Non-genetic propagation of strain-specific properties of scrapie prion protein, *Nature 375*, 698-700.
138. Bessen, R. A., Raymond, G. J., and Caughey, B. (1997) In situ formation of protease-resistant prion protein in transmissible spongiform encephalopathy-infected brain slices, *J Biol Chem 272*, 15227-15231.
139. Ironside, J. W. (1998) Prion diseases in man, *J Pathol 186*, 227-234.
140. Kocisko, D. A., Lansbury, P. T., Jr., and Caughey, B. (1996) Partial unfolding and refolding of scrapie-associated prion protein: evidence for a critical 16-kDa C-terminal domain, *Biochemistry 35*, 13434-13442.
141. Kocisko, D. A., Priola, S. A., Raymond, G. J., Chesebro, B., Lansbury, P. T., Jr., and Caughey, B. (1995) Species specificity in the cell-free conversion of prion protein to protease-resistant forms: a model for the scrapie species barrier, *Proc Natl Acad Sci USA 92*, 3923-3927.
142. Geoghegan, J. C., Miller, M. B., Kwak, A. H., Harris, B. T., and Supattapone, S. (2009) Trans-dominant inhibition of prion propagation in vitro is not mediated by an accessory cofactor, *PLoS Pathog 5*, e1000535.
143. Deleault, N. R., Geoghegan, J. C., Nishina, K., Kascsak, R., Williamson, R. A., and Supattapone, S. (2005) Protease-resistant prion protein amplification reconstituted with partially purified substrates and synthetic polyanions, *J Biol Chem 280*, 26873-26879.
144. Lloyd, S. E., Onwuazor, O. N., Beck, J. A., Mallinson, G., Farrall, M., Targonski, P., Collinge, J., and Fisher, E. M. (2001) Identification of multiple quantitative trait loci linked to prion disease incubation period in mice, *Proc Natl Acad Sci USA 98*, 6279-6283.
145. Manolakou, K., Beaton, J., McConnell, I., Farquar, C., Manson, J., Hastie, N. D., Bruce, M., and Jackson, I. J. (2001) Genetic and environmental factors modify bovine spongiform encephalopathy incubation period in mice, *Proc Natl Acad Sci USA 98*, 7402-7407.
146. Saborio, G. P., Soto, C., Kascsak, R. J., Levy, E., Kascsak, R., Harris, D. A., and Frangione, B. (1999) Cell-lysate conversion of prion protein into its protease-resistant isoform suggests the participation of a cellular chaperone, *Biochem Biophys Res Commun 258*, 470-475.
147. Stephenson, D. A., Chiotti, K., Ebeling, C., Groth, D., DeArmond, S. J., Prusiner, S. B., and Carlson, G. A. (2000) Quantitative trait loci affecting prion incubation time in mice, *Genomics 69*, 47-53.

148. Wang, F., Yang, F., Hu, Y., Wang, X., Jin, C., and Ma, J. (2007) Lipid interaction converts prion protein to a PrPSc-like proteinase K-resistant conformation under physiological conditions, *Biochemistry 46*, 7045-7053.
149. Wong, B. S., Chen, S. G., Colucci, M., Xie, Z., Pan, T., Liu, T., Li, R., Gambetti, P., Sy, M. S., and Brown, D. R. (2001) Aberrant metal binding by prion protein in human prion disease, *J Neurochem 78*, 1400-1408.
150. Wang, F., Wang, X., Yuan, C. G., and Ma, J. (2010) Generating a prion with bacterially expressed recombinant prion protein, *Science 327*, 1132-1135.
151. Bosque, P. J., and Prusiner, S. B. (2000) Cultured cell sublines highly susceptible to prion infection, *J Virol 74*, 4377-4386.
152. Enari, M., Flechsig, E., and Weissmann, C. (2001) Scrapie prion protein accumulation by scrapie-infected neuroblastoma cells abrogated by exposure to a prion protein antibody, *Proc Natl Acad Sci USA 98*, 9295-9299.
153. Raeber, A. J., Sailer, A., Hegyi, I., Klein, M. A., Rulicke, T., Fischer, M., Brandner, S., Aguzzi, A., and Weissmann, C. (1999) Ectopic expression of prion protein (PrP) in T lymphocytes or hepatocytes of PrP knockout mice is insufficient to sustain prion replication, *Proc Natl Acad Sci USA 96*, 3987-3992.
154. Klein, T. R., Kirsch, D., Kaufmann, R., and Riesner, D. (1998) Prion rods contain small amounts of two host sphingolipids as revealed by thin-layer chromatography and mass spectrometry, *Biol Chem 379*, 655-666.
155. Warner, R. G., Hundt, C., Weiss, S., and Turnbull, J. E. (2002) Identification of the heparan sulfate binding sites in the cellular prion protein, *J Biol Chem 277*, 18421-18430.
156. Gabizon, R., McKinley, M. P., Groth, D. F., Kenaga, L., and Prusiner, S. B. (1988) Properties of scrapie prion protein liposomes, *J Biol Chem 263*, 4950-4955.
157. Wilesmith, J., Wells, G., Cranwell, M., and Ryan, J. (1988) Bovine spongiform encephalopathy: epidemiological studies, *Vet Rec 123*, 638-644.
158. Smith, P. G., and Bradley, R. (2003) Bovine spongiform encephalopathy (BSE) and its epidemiology, *Br Med Bull 66*, 185-198.
159. Clauss, M., and Kienzle, E. (2002) Feeding practices in the German BSE epidemy: a preliminary survey of the first 65 Bavarian cases, Veterinaerstr. 13, 80539 Munich,Germany.
160. Argue, C. K., Ribble, C., Lees, V. W., McLane, J., and Balachandran, A. (2007) Epidemiology of an outbreak of chronic wasting disease on elk farms in Saskatchewan, *Can Vet J 48*, 1241-1248.
161. Williams, E. S., and Miller, M. W. (2002) Chronic wasting disease in deer and elk in North America, *Rev Sci Tech 21*, 305-316.

162. Wilesmith, J. W., Ryan, J. B., and Atkinson, M. J. (1991) Bovine spongiform encephalopathy: epidemiological studies on the origin, *Vet Rec 128*, 199-203.
163. Banks, W. A., and Erickson, M. A. (2010) The blood-brain barrier and immune function and dysfunction, *Neurobiol Dis 37*, 26-32.
164. Iqbal, S., Zebeli, Q., Mazzolari, A., Bertoni, G., Dunn, S. M., Yang, W. Z., and Ametaj, B. N. (2009) Feeding barley grain steeped in lactic acid modulates rumen fermentation patterns and increases milk fat content in dairy cows, *J Dairy Sci 92*, 6023-6032.
165. Zebeli, Q., Dijkstra, J., Tafaj, M., Steingass, H., Ametaj, B. N., and Drochner, W. (2008) Modeling the adequacy of dietary fiber in dairy cows based on the responses of ruminal pH and milk fat production to composition of the diet, *Journal of Dairy Science 91*, 2046-2066.
166. Ametaj, B. N., Zebeli, Q., and Iqbal, S. (2010) Nutrition, microbiota, and endotoxin-related diseases in dairy cows, *Revista Brasileira de Zootecnia 39*, 433-444.
167. Fernando, S. C., Purvis, H. T., 2nd, Najar, F. Z., Sukharnikov, L. O., Krehbiel, C. R., Nagaraja, T. G., Roe, B. A., and Desilva, U. (2010) Rumen microbial population dynamics during adaptation to a high-grain diet, *Appl Environ Microbiol 76*, 7482-7490.
168. Khafipour, E., Li, S. C., Plaizier, J. C., and Krause, D. O. (2009) Rumen Microbiome Composition Determined Using Two Nutritional Models of Subacute Ruminal Acidosis, *Applied and Environmental Microbiology 75*, 7115-7124.
169. Ametaj, B. N., Zebeli, Q., Saleem, F., Psychogios, N., Lewis, M. J., Dunn, S. M., Xia, J. G., and Wishart, D. S. (2010) Metabolomics reveals unhealthy alterations in rumen metabolism with increased proportion of cereal grain in the diet of dairy cows, *Metabolomics 6*, 583-594.
170. Stone, W. C. (2004) Nutritional Approaches to Minimize Subacute Ruminal Acidosis and Laminitis in Dairy Cattle, *Journal of Dairy Science 87, Supplement*, E13-E26.
171. Psychogios, N., Hau, D. D., Peng, J., Guo, A. C., Mandal, R., Bouatra, S., Sinelnikov, I., Krishnamurthy, R., Eisner, R., Gautam, B., Young, N., Xia, J. G., Knox, C., Dong, E., Huang, P., Hollander, Z., Pedersen, T. L., Smith, S. R., Bamforth, F., Greiner, R., McManus, B., Newman, J. W., Goodfriend, T., and Wishart, D. S. (2011) The Human Serum Metabolome, *Plos One 6*.
172. Statistics Canada. 2012c. Cattle and calves, farm and meat production. Table 003-0026, In *On-Line. Accessed at: http://www5.statcan.gc.ca/cansim/a26?lang=eng&retrLang=eng&id=0030026&tabMode=dataTable&srchLan=-1&p1=-1&p2=9*.
173. Emmanuel, D. G. V., Dunn, S. M., and Ametaj, B. N. (2008) Feeding high proportions of barley grain stimulates an inflammatory response in dairy cows, *Journal of Dairy Science 91*, 606-614.

174. Jiye, A., Trygg, J., Gullberg, J., Johansson, A. I., Jonsson, P., Antti, H., Marklund, S. L., and Moritz, T. (2005) Extraction and GC/MS analysis of the human blood plasma metabolome, *Analytical Chemistry 77*, 8086-8094.
175. A, J., Trygg, J., Gullberg, J., Johansson, A. I., Jonsson, P., Antti, H., Marklund, S. L., and Moritz, T. (2005) Extraction and GC/MS Analysis of the Human Blood Plasma Metabolome, *Analytical Chemistry 77*, 8086-8094.
176. Wishart, D. S. (2008) Metabolomics: applications to food science and nutrition research, *Trends in Food Science & Technology 19*, 482-493.
177. Broadhurst, D., and Kell, D. (2006) Statistical strategies for avoiding false discoveries in metabolomics and related experiments, *Metabolomics 2*, 171-196.
178. Xia, J. G., Psychogios, N., Young, N., and Wishart, D. S. (2009) MetaboAnalyst: a web server for metabolomic data analysis and interpretation, *Nucleic Acids Res 37*, W652-W660.
179. Dieterle, F., Ross, A., Schlotterbeck, G., and Senn, H. (2006) Probabilistic quotient normalization as robust method to account for dilution of complex biological mixtures. Application in H-1 NMR metabonomics, *Analytical Chemistry 78*, 4281-4290.
180. Szeto, S. S., Reinke, S. N., Sykes, B. D., and Lemire, B. D. (2010) Mutations in the Saccharomyces cerevisiae succinate dehydrogenase result in distinct metabolic phenotypes revealed through (1)H NMR-based metabolic footprinting, *J Proteome Res 9*, 6729-6739.
181. Seo, J. (2005) Information visualization design for multidimensional data: integrating the rank-by-feature framework with hierarchical clustering, University of Maryland, College Park.
182. Phuntsok, T., Froetschel, M. A., Amos, H. E., Zheng, M., and Huang, Y. W. (1998) Biogenic amines in silage, apparent post-ruminal passage, and the relationship between biogenic amines and digestive function and intake by steers, *Journal of Dairy Science 81*, 2193-2203.
183. Rice, S. L., and Koehler, P. E. (1976) Tyrosine and Histidine Decarboxylase Activities of Pediococcus-Cerevisiae and Lactobacillus Species and Production of Tyramine in Fermented Sausages, *J Milk Food Technol 39*, 166-169.
184. Hill, K. J., and Mangan, J. L. (1964) The formation and distribution of methylamine in the ruminant digestive tract, *Biochem J 93*, 39-45.
185. Bailey, S. R., Rycroft, A., and Elliott, J. (2002) Production of amines in equine cecal contents in an in vitro model of carbohydrate overload, *Journal of Animal Science 80*, 2656-2662.
186. Murooka, Y., Doi, N., and Harada, T. (1979) Distribution of membrane-bound monoamine oxidase in bacteria, *Appl Environ Microbiol 38*, 565-569.
187. Yamashita, Y., Bowen, W. H., Burne, R. A., and Kuramitsu, H. K. (1993) Role of the Streptococcus-Mutans-Gtf Genes in Caries Induction in the

Specific-Pathogen-Free Rat Model, *Infection and Immunity 61*, 3811-3817.

188. Matsui, I., and Pegg, A. E. (1980) Increase in Acetylation of Spermidine in Rat-Liver Extracts Brought About by Treatment with Carbon-Tetrachloride, *Biochemical and Biophysical Research Communications 92*, 1009-1015.
189. Blaschko, H., and Bonney, R. (1962) Spermine Oxidase and Benzylamine Oxidase - Distribution, Development and Substrate Specificity, *Proceedings of the Royal Society Series B-Biological Sciences 156*, 268-+.
190. Ronchi, B., Bernabucci, U., Lacetera, N., and Nardone, A. (2000) Oxidative and metabolic status of high yielding dairy cows in different nutritional conditions during the transition period, In *51st Annual Mtg. EAAP, Vienna, Austria. Wagningen Pers., Wageningen, the Netherlands.*, p 125.
191. Willard, F. L., and Kodras, R. (1967) Survey of chemical compounds tested in vitro against rumen protozoa for possible control of bloat, *Appl Microbiol 15*, 1014-1019.
192. Kawai, K., Fujita, M., and Nakao, M. (1974) Lipid components of two different regions of an intestinal epithelial cell membrane of mouse, *Biochim Biophys Acta 369*, 222-233.
193. Goodlad, R. A. (1981) Some Effects of Diet on the Mitotic Index and the Cell-Cycle of the Ruminal Epithelium of Sheep, *Quarterly Journal of Experimental Physiology and Cognate Medical Sciences 66*, 487-499.
194. Nagaraja, T. G., Bartley, E. E., Fina, L. R., and Anthony, H. D. (1978) Relationship of rumen gram-negative bacteria and free endotoxin to lactic acidosis in cattle, *J Anim Sci 47*, 1329-1337.
195. Bertin, Y., Girardeau, J. P., Chaucheyras-Durand, F., Lyan, B., Pujos-Guillot, E., Harel, J., and Martin, C. (2011) Enterohaemorrhagic Escherichia coli gains a competitive advantage by using ethanolamine as a nitrogen source in the bovine intestinal content, *Environmental Microbiology 13*, 365-377.
196. Thiennimitr, P., Winter, S. E., Winter, M. G., Xavier, M. N., Tolstikov, V., Huseby, D. L., Sterzenbach, T., Tsolis, R. M., Roth, J. R., and Baumler, A. J. Intestinal inflammation allows Salmonella to use ethanolamine to compete with the microbiota, *Proc Natl Acad Sci U S A 108*, 17480-17485.
197. Law, D. (2000) Virulence factors of Escherichia coli O157 and other Shiga toxin-producing E. coli, *J Appl Microbiol 88*, 729-745.
198. O'Brien, S. J., Adak, G. K., and Gilham, C. (2001) Contact with farming environment as a major risk factor for shiga toxin (Vero cytotoxin)-producing Escherichia coli O157 infection in humans, *Emerging Infectious Diseases 7*, 1049-1051.
199. Yatsuyanagi, J., Saito, S., and Ito, I. (2002) A case of hemolytic-uremic syndrome associated with shiga toxin 2-producing Escherichia coli O121

infection caused by drinking water contaminated with bovine feces, *Jpn J Infect Dis 55*, 174-176.
200. Jones, S. A., Jorgensen, M., Chowdhury, F. Z., Rodgers, R., Hartline, J., Leatham, M. P., Struve, C., Krogfelt, K. A., Cohen, P. S., and Conway, T. (2008) Glycogen and maltose utilization by Escherichia coli O157:H7 in the mouse intestine, *Infect Immun 76*, 2531-2540.
201. Hovde, C. J., Austin, P. R., Cloud, K. A., Williams, C. J., and Hunt, C. W. (1999) Effect of cattle diet on Escherichia coli O157:H7 acid resistance, *Appl Environ Microbiol 65*, 3233-3235.
202. McAllan, A. B., and Smith, R. H. (1973) Degradation of nucleic acids in the rumen, *Br J Nutr 29*, 331-345.
203. Trent, M. S., Stead, C. M., Tran, A. X., and Hankins, J. V. (2006) Diversity of endotoxin and its impact on pathogenesis, *J Endotoxin Res 12*, 205-223.
204. Slyter, L. L. (1976) Influence of Acidosis on Rumen Function, *Journal of Animal Science 43*, 910-929.
205. Broberg, G. (1958) Studies on the effect of over-feeding in sheep, pp 365–369, Proc. 8th Nordic VetCong. Pergamon Press, Oxford, UK
206. Golombeski, G. L., Kalscheur, K. F., Hippen, A. R., and Schingoethe, D. J. (2006) Slow-release urea and highly fermentable sugars in diets fed to lactating dairy cows, *J Dairy Sci 89*, 4395-4403.
207. Highstreet, A., Robinson, P. H., Robison, J., and Garrett, J. G. (2010) Response of Holstein cows to replacing urea with with a slowly rumen released urea in a diet high in soluble crude protein, *Livestock Science 129*, 179-185.
208. Blood, D. C., and Henderson, J. A., (Eds.) (1963) *Veterinary Medicine* 2ed., Baillière, Tyndall & Cassell, London, UK
209. Aschenbach, J. R., Penner, G. B., Stumpff, F., and Gabel, G. (2011) Ruminant Nutrition Symposium: Role of fermentation acid absorption in the regulation of ruminal pH, *J Anim Sci 89*, 1092-1107.
210. Crow, V. L., and Thomas, T. D. (1982) Arginine metabolism in lactic streptococci, *J Bacteriol 150*, 1024-1032.
211. Onodera, R., Yamaguchi, Y., and Morimoto, S. (1983) Metabolism of Arginine, Citrulline, Ornithine and Proline by Starved Rumen Ciliate Protozoa, *Agr Biol Chem Tokyo 47*, 821-828.
212. Onodera, R., and Kandatsu, M. (1968) Amino acid and protein metabolism of rumen ciliate protozoa. 1. Consumption of amino acids, *Jpn. J. Zootech. Sci*, 206–211.
213. McSweeney, C., and Mackie, R. (1997) Gastrointestinal detoxification and digestive disorders in ruminant animals, In *Gastrointestinal Microbiology* (Mackie, R., and White, B., Eds.), pp 583-634, Springer US.
214. Dawson, K. A., Rasmussen, M. A., and Allison, M. J., (Eds.) *Digestive disorders and nutritional toxicity*, The Rumen Microbial Ecosystem (2nd)Chapman & Hall,, London, UK.

215. Bugaut, M. (1987) Occurrence, absorption and metabolism of short chain fatty acids in the digestive tract of mammals, *Comp Biochem Physiol B 86*, 439-472.
216. Brossard, L., Martin, C., Chaucheyras-Durand, F., and Michalet-Doreau, B. (2004) Protozoa involved in butyric rather than lactic fermentative pattern during latent acidosis in sheep, *Reproduction Nutrition Development 44*, 195-206.
217. Orskov, E. R., and Oltjen, R. R. (1967) Influence of carbohydrate and nitrogen sources on the rumen volatile fatty acids and ethanol of cattle fed purified diets, *J Nutr 93*, 222-228.
218. Allison, M. J., Dougherty, R. W., Bucklin, J. A., and Snyder, E. E. (1964) Ethanol Accumulation in the Rumen after Overfeeding with Readily Fermentable Carbohydrate, *Science 144*, 54-55.
219. Kristensen, N. B., Storm, A., Raun, B. M., Rojen, B. A., and Harmon, D. L. (2007) Metabolism of silage alcohols in lactating dairy cows, *J Dairy Sci 90*, 1364-1377.
220. Purohit, V., Bode, J. C., Bode, C., Brenner, D. A., Choudhry, M. A., Hamilton, F., Kang, Y. J., Keshavarzian, A., Rao, R., Sartor, R. B., Swanson, C., and Turner, J. R. (2008) Alcohol, intestinal bacterial growth, intestinal permeability to endotoxin, and medical consequences: Summary of a symposium, *Alcohol 42*, 349-361.
221. Pike, R. L., and Brown, M. L., (Eds.) (1975) *Nutrition: An Integrated Approach*, 2 ed., ohn Wiley and Sons, New York, Ny.
222. Menke, K. H., Giesecke, D., and Henderickx, H. K., (Eds.) (1973) *Vitamin syntheses in the rumen:Biology and Biochemistry of Microbial Digestion*, 2 ed., BLV Verlagsgesellschaft,, Munich, Germany.
223. Hino, T., and Russell, J. B. (1985) Effect of reducing-equivalent disposal and NADH/NAD on deamination of amino acids by intact rumen microorganisms and their cell extracts, *Appl Environ Microbiol 50*, 1368-1374.
224. Pagella, J. H. (1998) Urinary benzylated compounds as potential markers of forage intake and metabolism of their precursors in ruminants, Aberdeen University,, Aberdeen. UK.
225. Chesson, A., Provan, G. J., Russell, W. R., Scobbie, L., Richardson, A. J., and Stewart, C. (1999) Hydroxycinnamic acids in the digestive tract of livestock and humans, *Journal of the Science of Food and Agriculture 79*, 373-378.
226. Burlingame, R., and Chapman, P. J. (1983) Catabolism of phenylpropionic acid and its 3-hydroxy derivative by Escherichia coli, *J Bacteriol 155*, 113-121.
227. Martin, A. K. (1982) The origin of urinary aromatic compounds excreted by ruminants. 3. The metabolism of phenolic compounds to simple phenols, *Br J Nutr 48*, 497-507.
228. Zeisel, S. H., and Holmes-McNary, M., (Eds.) (2001) *Handbook of Vitamins* 3ed., Marcel Dekker Inc, New York, NY.

229. Piepenbrink, M. S., and Overton, T. R. (2003) Liver metabolism and production of cows fed increasing amounts of rumen-protected choline during the periparturient period, *Journal of Dairy Science 86*, 1722-1733.
230. Neill, A. R., Grime, D. W., and Dawson, R. M. C. (1978) Conversion of Choline Methyl-Groups through Trimethylamine into Methane in Rumen, *Biochemical Journal 170*, 529-535.
231. Broad, T. E., and Dawson, R. M. (1976) Role of choline in the nutrition of the rumen protozoon Entodinium caudatum, *J Gen Microbiol 92*, 391-397.
232. Coleman, G. S. (1979) The role of rumen protozoa in the metabolism of ruminants given tropical feeds, *Trop. Anim. Prod. 4*, 199–213.
233. Goad, D. W., Goad, C. L., and Nagaraja, T. G. (1998) Ruminal microbial and fermentative changes associated with experimentally induced subacute acidosis in steers, *J Anim Sci 76*, 234-241.
234. Choat, W. T., Krehbiel, C. R., Brown, M. S., Duff, G. C., Walker, D. A., and Gill, D. R. (2002) Effects of restricted versus conventional dietary adaptation on feedlot performance, carcass characteristics, site and extent of digestion, digesta kinetics, and ruminal metabolism, *Journal of Animal Science 80*, 2726-2739.
235. Bevans, D. W., Beauchemin, K. A., Schwartzkopf-Genswein, K. S., McKinnon, J. J., and McAllister, T. A. (2005) Effect of rapid or gradual grain adaptation on subacute acidosis and feed intake by feedlot cattle, *Journal of Animal Science 83*, 1116-1132.
236. Craig, J. V., (Ed.) (1981) *Domestic animal behavior: causes and implications for animal care and management*, Prentice Hall PTR, Englewood Cliffs, NJ:.
237. Giuffra, E., Kijas, J. M., Amarger, V., Carlborg, O., Jeon, J. T., and Andersson, L. (2000) The origin of the domestic pig: independent domestication and subsequent introgression, *Genetics 154*, 1785-1791.
238. Bruford, M. W., Bradley, D. G., and Luikart, G. (2003) DNA markers reveal the complexity of livestock domestication, *Nat Rev Genet 4*, 900-910.
239. Hackmann, T. J., and Spain, J. N. (2010) Invited review: ruminant ecology and evolution: perspectives useful to ruminant livestock research and production, *J Dairy Sci 93*, 1320-1334.
240. McAllister, T. (2001) Learning more about rumen bugs: Genetic and environmental factors affecting rumen bugs, *Southern Alberta Beef Review 2*, 1.
241. Plaizier, J. C., Krause, D. O., Gozho, G. N., and McBride, B. W. (2008) Subacute ruminal acidosis in dairy cows: the physiological causes, incidence and consequences, *Vet J 176*, 21-31.
242. Drackley, J. K., and Dann, H. M. (2005) New concepts in nutritional management of dry cows, *Advances in Dairy Technology 17*, 11–23.
243. Ingvartsen, K. L. (2006) Feeding- and management-related diseases in the transition cow: Physiological adaptations around calving and strategies to

reduce feeding-related diseases, *Animal Feed Science and Technology 126*, 175-213.

244. Hess, M., Sczyrba, A., Egan, R., Kim, T.-W., Chokhawala, H., Schroth, G., Luo, S., Clark, D. S., Chen, F., Zhang, T., Mackie, R. I., Pennacchio, L. A., Tringe, S. G., Visel, A., Woyke, T., Wang, Z., and Rubin, E. M. (2011) Metagenomic discovery of biomass-degrading genes and genomes from cow rumen, *Science 331*, 463-467.
245. Bertram, H. C., Kristensen, N. B., Malmendal, A., Nielsen, N. C., Brod, R., and Andersen, H. J. (2005) A metabolomic investigation of splanchnic metabolism using 1H NMR spectroscopy of bovine blood plasma., *Analytica Chimica Acta, 536*, 1–6.
246. Attaelmannan, M. A., Dahl, A. A., and Reid, R. S. (1999) Analysis of volatile fatty acid in rumen fluid by proton NMR spectroscopy, *Canadian journal of animal science. 79*, 401-404.
247. Forano, E., Delort, A.-M., and Matulova, M. (2008) Carbohydrate metabolism in Fibrobacter succinogenes: What NMR tells us, *Microb Ecol Health Dis 20*, 94-102.
248. Saude, E., Slupsky, C., and Sykes, B. (2006) Optimization of NMR analysis of biological fluids for quantitative accuracy, *Metabolomics 2*, 113-123.
249. Weljie, A. M., Newton, J., Mercier, P., Carlson, E., and Slupsky, C. M. (2006) Targeted Profiling: Quantitative Analysis of 1H NMR Metabolomics Data, *Analytical Chemistry 78*, 4430-4442.
250. Wishart, D. S. (2008) Quantitative metabolomics using NMR, *TrAC Trends in Analytical Chemistry 27*, 228-237.
251. Fiehn, O., Wohlgemuth, G., and Scholz, M. (2005) Setup and Annotation of Metabolomic Experiments by Integrating Biological and Mass Spectrometric Metadata, In *Data Integration in the Life Sciences* (Ludäscher, B., and Raschid, L., Eds.), pp 224-239, Springer Berlin Heidelberg.
252. Cava-Montesinos, P., Cervera, M. L., Pastor, A., and de la Guardia, M. (2005) Room temperature acid sonication ICP-MS multielemental analysisof milk, *Analytica Chimica Acta 531*, 111–123.
253. Bailey, C. B. (1961) Saliva secretion and its relation to feeding in cattle. 3. The rate of secretion of mixed saliva in the cow during eating, with an estimate of the magnitude of the total daily secretion of mixed saliva, *Br J Nutr 15*, 443-451.
254. Hamilton, J. G., and Comai, K. (1984) Separation of neutral lipids and free fatty acids by high-performance liquid chromatography using low wavelength ultraviolet detection, *J Lipid Res 25*, 1142-1148.
255. Christie, W. W. (2003) Lipid analysis: Isolation, separation, identification and comparison of methods for quantitative metabolomicsof primary metabolism, *Analytical Chemistry 81*, 2135–2143.
256. Cheng, D., Knox, C., Young, N., Stothard, P., Damaraju, S., and Wishart, D. S. (2008) PolySearch: a web-based text mining system for extracting

relationships between human diseases, genes, mutations, drugs and metabolites, *Nucleic Acids Res 36*, W399-405.

257. Buscher, J. M., Czernik, D., Ewald, J. C., Sauer, U., and Zamboni, N. (2009) Cross-platform comparison of methods for quantitative metabolomics of primary metabolism, *Anal Chem 81*, 2135-2143.
258. Lewis, T. R., and Emery, R. S. (1962) Intermediate products in the catabolism of amino acids by rumen microorganisms, *Journal of Dairy Science 45*, 1363-1368.
259. Ivanova, P. T., Milne, S. B., Myers, D. S., and Brown, H. A. (2009) Lipidomics: a mass spectrometry based systems level analysis of cellular lipids, *Curr Opin Chem Biol 13*, 526-531.
260. Harfoot, C. G., Noble, R. C., and Moore, J. H. (1973) Factors influencing the extent of biohydrogenation of linoleic acid by rumen micro-organisms in vitro, *J Sci Food Agric 24*, 961-970.
261. Lock, A. L., Harvatine, K. J., Ipharraguerre, I., Amburgh, M., Drackley, J. K., and Bauman, D. E. (2006) Dynamics of ruminant fat digestion: Part 1. Fatty acid metabolism of ruminants., *Feedstuffs 78*, 6–17.
262. Abu-Ghazaleh, A. A., Schingoethe, D. J., Hippen, A. R., and Whitlock, L. A. (2002) Feeding fish meal and extruded soybeans enhances the conjugated linoleic acid (CLA) content of milk, *Journal of Dairy Science 85*, 624-631.
263. Jurgens, M. H., (Ed.) (1978) *Animal feeding and nutrition*, Kendall/Hunt Publishing Company, Dubuque, IA.
264. Zhang, Q., Wysocki, V. H., Scaraffia, P. Y., and Wells, M. A. (2005) Fragmentation pathway for glutamine identification: loss of 73 Da from dimethylformamidine glutamine isobutyl ester, *J Am Soc Mass Spectrom 16*, 1192-1203.
265. Pan, K. M., Baldwin, M., Nguyen, J., Gasset, M., Serban, A., Groth, D., Mehlhorn, I., Huang, Z. W., Fletterick, R. J., Cohen, F. E., and Prusiner, S. B. (1993) Conversion of alpha-helices into beta-sheets features in the formation of the scrapie prion proteins, *Proc. Natl. Acad. Sci. U.S.A. 90*, 10962-10966.
266. Kretzschmar, H. A., Prusiner, S. B., Stowring, L. E., and Dearmond, S. J. (1986) Scrapie prion proteins are synthesized in neurons, *Am. J. Pathol. 122*, 1-5.
267. Moser, M., Colello, R. J., Pott, U., and Oesch, B. (1995) Developmental expression of the prion protein gene in glial-cells, *Neuron 14*, 509-517.
268. Riek, R., Hornemann, S., Wider, G., Glockshuber, R., and Wuthrich, K. (1997) NMR characterization of the full-length recombinant murine prion protein, mPrP(23-231), *Febs Lett 413*, 282-288.
269. Brown, D. R., Qin, K. F., Herms, J. W., Madlung, A., Manson, J., Strome, R., Fraser, P. E., Kruck, T., vonBohlen, A., SchulzSchaeffer, W., Giese, A., Westaway, D., and Kretzschmar, H. (1997) The cellular prion protein binds copper in vivo, *Nature 390*, 684-687.

270. Walter, E. D., Stevens, D. J., Visconte, M. P., and Millhauser, G. L. (2007) The prion protein is a combined zinc and copper binding protein: Zn2+ alters the distribution of Cu2+ coordination modes, *J. Am. Chem. Soc. 129*, 15440-15441.
271. Rudd, P. M., Endo, T., Colominas, C., Groth, D., Wheeler, S. F., Harvey, D. J., Wormald, M. R., Serban, H., Prusiner, S. B., Kobata, A., and Dwek, R. A. (1999) Glycosylation differences between the normal and pathogenic prion protein isoforms, *Proc. Natl. Acad. Sci. U.S.A. 96*, 13044-13049.
272. Stimson, E., Hope, J., Chong, A., and Burlingame, A. L. (1999) Site-specific characterization of the N-linked glycans of murine prion protein by high-performance liquid chromatography electrospray mass spectrometry and exoglycosidase digestions, *Biochemistry. 38*, 4885-4895.
273. Caughey, B. W., Dong, A., Bhat, K. S., Ernst, D., Hayes, S. F., and Caughey, W. S. (1991) Secondary structure-analysis of the scrapie-associated Protein Prp 27-30 in Water byinfrared-spectroscopy, *Biochemistry. 30*, 7672-7680.
274. Safar, J., Roller, P. P., Gajdusek, D. C., and Gibbs, C. J. (1993) Conformational transitions, dissociation, and unfolding of scrapie amyloid (prion) protein, *J Biol Chem 268*, 20276-20284.
275. Yutani, K., Takayama, G., Goda, S., Yamagata, Y., Maki, S., Namba, K., Tsunasawa, S., and Ogasahara, K. (2000) The process of amyloid-like fibril formation by methionine aminopeptidase from a hyperthermophile, Pyrococcus furiosus, *Biochemistry. 39*, 2769-2777.
276. Nielsen, L., Khurana, R., Coats, A., Frokjaer, S., Brange, J., Vyas, S., Uversky, V. N., and Fink, A. L. (2001) Effect of environmental factors on the kinetics of insulin fibril formation: elucidation of the molecular mechanism, *Biochemistry. 40*, 6036-6046.
277. Stohr, J., Weinmann, N., Wille, H., Kaimann, T., Nagel-Steger, L., Birkmann, E., Panza, G., Prusiner, S. B., Eigen, M., and Riesner, D. (2008) Mechanisms of prion protein assembly into amyloid, *Proc. Natl. Acad. Sci. U.S.A. 105*, 2409-2414.
278. Konno, T., Murata, K., and Nagayama, K. (1999) Amyloid-like aggregates of a plant protein: a case of a sweet-tasting protein, monellin, *Febs Lett 454*, 122-126.
279. Bjorndahl, T. C., Zhou, G. P., Liu, X. H., Perez-Pineiro, R., Semenchenko, V., Saleem, F., Acharya, S., Bujold, A., Sobsey, C. A., and Wishart, D. S. (2011) Detailed biophysical characterization of the acid-Induced PrP^c to PrP beta conversion process, *Biochemistry. 50*, 1162-1173.
280. Aiken, J. M., Williamson, J. L., Borchardt, L. M., and Marsh, R. F. (1990) Presence of Mitochondrial D-Loop DNA in Scrapie-Infected Brain Preparations Enriched for the Prion Protein, *J Virol 64*, 3265-3268.
281. Cordeiro, Y., Machado, F., Juliano, L., Juliano, M. A., Brentani, R. R., Foguel, D., and Silva, J. L. (2001) DNA converts cellular prion protein

into the beta-sheet conformation and inhibits prion peptide aggregation, *J Biol Chem 276*, 49400-49409.

282. Deleault, N. R., Lucassen, R. W., and Supattapone, S. (2003) RNA molecules stimulate prion protein conversion, *Nature 425*, 717-720.
283. Andrievskaia, O., Potetinova, Z., Balachandran, A., and Nielsen, K. (2007) Binding of bovine prion protein to heparin: a fluorescence polarization study, *Arch Biochem Biophys 460*, 10-16.
284. Deleault, N. R., Geoghegan, J. C., Nishina, K., Kascsak, R., Williamson, R. A., and Supattapone, S. (2005) Protease-resistant prion protein amplification reconstituted with partially purified substrates and synthetic polyanions, *J Biol Chem 280*, 26873-26879.
285. Luhrs, T. T., Zahn, R., and Wuthrich, K. (2006) Amyloid formation by recombinant full-length prion proteins in phospholipid bicelle solutions, *J. Mol. Biol. 357*, 833-841.
286. Sanghera, N., and Pinheiro, T. J. T. (2002) Binding of prion protein to lipid membranes and implications for prion conversion, *J Mol Biol 315*, 1241-1256.
287. Wang, F., Yang, F., Hu, Y. F., Wang, X., Wang, X. H., Jin, C. W., and Ma, J. Y. (2007) Lipid interaction converts prion protein to a PrP^{Sc}-like proteinase K-Resistant conformation under physiological conditions, *Biochemistry. 46*, 7045-7053.
288. Wong, C., Xiong, L. W., Horiuchi, M., Raymond, L., Wehrly, K., Chesebro, B., and Caughey, B. (2001) Sulfated glycans and elevated temperature stimulate PrP^{Sc}-dependent cell-free formation of protease-resistant prion protein, *Embo J 20*, 377-386.
289. Singh, N., Das, D., Singh, A., and Mohan, M. L. (2010) Prion protein and metal interaction: physiological andpathological Implications, *Curr. Issues. Mol. Biol. 12*, 99-107.
290. Wang, F., Wang, X. H., Yuan, C. G., and Ma, J. Y. (2010) Generating a prion with bacterially expressed recombinant prion protein, *Science 327*, 1132-1135.
291. Pasupuleti, M., Roupe, M., Rydengard, V., Surewicz, K., Surewicz, W. K., Chalupka, A., Malmsten, M., Sorensen, O. E., and Schmidtchen, A. (2009) Antimicrobial activity of human prion protein Is mediated by Its N-terminal region, *Plos One 4*, e7358.
292. Johnson, W. C. (1999) Analyzing protein circular dichroism spectra for accurate secondary structures, *Proteins 35*, 307-312.
293. Sreerama, N., and Woody, R. W. (2004) On the analysis of membrane protein circular dichroism spectra, *Protein. Sci. 13*, 100-112.
294. Bessen, R. A., and Marsh, R. F. (1994) Distinct Prp properties sggest the molecular-basis of strain variation in transmissible mink nncephalopathy, *J. Virol. 68*, 7859-7868.
295. Ladner, C. L., and Wishart, D. S. (2012) Resolution-enhanced native acidic gel electrophoresis: A method for resolving, sizing, and quantifying prion protein oligomers, *Anal. Biochem. 426*, 54-62.

296. Neuhoff, V., Stamm, R., and Eibl, H. (1985) Clear background and highly sensitive protein staining with coomassie bluedyes in polyacrylamide gels - a systematic analysis, *Electrophoresis 6*, 427-448.
297. Deleault, N. R., Piro, J. R., Walsh, D. J., Wang, F., Ma, J. Y., Geoghegan, J. C., and Supattapone, S. (2012) Isolation of phosphatidylethanolamine as a solitary cofactor for prion formation in the absence of nucleic acids, *Proc. Natl. Acad. Sci. U.S.A. 109*, 8546-8551.
298. Deleault, N. R., Walsh, D. J., Piro, J. R., Wang, F., Wang, X., Ma, J., Rees, J. R., and Supattapone, S. (2012) Cofactor molecules maintain infectious conformation and restrict strain properties in purified prions, *Proc. Natl. Acad. Sci. U.S.A. 109*, 8546-8551.
299. Lawson, V. A., Collins, S. J., Masters, C. L., and Hill, A. F. (2005) Prion protein glycosylation, *J. Neurochem 93*, 793-801.
300. Nandi, P. K., Leclerc, E., Nicole, J. C., and Takahashi, M. (2002) DNA-induced partial unfolding of prion protein Leads to itspolymerisation to amyloid, *J. Mol. Biol. 322*, 153-161.
301. Weiss, S., Proske, D., Neumann, M., Groschup, M. H., Kretzschmar, H. A., Famulok, M., and Winnacker, E. L. (1997) RNA aptamers specifically interact with the prion protein PrP, *J. Virol. 71*, 8790-8797.
302. Kim, J. I., Cali, I., Surewicz, K., Kong, Q. Z., Raymond, G. J., Atarashi, R., Race, B., Qing, L. T., Gambetti, P., Caughey, B., and Surewicz, W. K. (2010) Mammalian prions generated from bacterially expressed prion protein in the absence of any mammalian cofactors, *J Biol Chem 285*, 14083-14087.
303. Eghiaian, F., Daubenfeld, T., Quenet, Y., van Audenhaege, M., Bouin, A. P., van der Rest, G., Grosclaude, J., and Rezaei, H. (2007) Diversity in prion protein oligomerization pathways results from domain expansion as revealed by hydrogen/deuterium exchange and disulfide linkage, *Proc. Natl. Acad. Sci. U.S.A. 104*, 7414-7419.
304. Gomes, M. P. B., Millen, T. A., Ferreira, P. S., Silva, N. L. C. E., Vieira, T. C. R. G., Almeida, M. S., Silva, J. L., and Cordeiro, Y. (2008) Prion protein complexed to N2a cellular RNAs through its N-terminal domain forms aggregates and is toxic to murine neuroblastoma cells, *J Biol Chem 283*, 19616-19625.
305. Atarashi, R., Moore, R. A., Sim, V. L., Hughson, A. G., Dorward, D. W., Onwubiko, H. A., Priola, S. A., and Caughey, B. (2007) Ultrasensitive detection of scrapie prion protein using seeded conversion of recombinant prion protein, *Nat. Methods. 4*, 645-650.
306. Jain, S., and Udgaonkar, J. B. (2010) Salt-Induced modulation of the pathway of amyloid fibril formation by the mouse prion protein, *Biochemistry-Us 49*, 7615-7624.
307. Saborio, G. P., Permanne, B., and Soto, C. (2001) Sensitive detection of pathological prion protein by cyclic amplification of protein misfolding, *Nature 411*, 810-813.

308. Caughey, B., Kocisko, D. A., Raymond, G. J., and Lansbury, P. T. (1995) Aggregates of scrapie-associated prion protein induce the cell-free conversion of protease-sensitive prion protein to the protease-resistant state, *Chem. Biol. 2*, 807-817.
309. Chabry, J., Caughey, B., and Chesebro, B. (1998) Specific inhibition of in vitro formation of protease-resistant prion protein by synthetic peptides, *J Biol Chem 273*, 13203-13207.
310. Mehlhorn, I., Groth, D., Stockel, J., Moffat, B., Reilly, D., Yansura, D., Willett, W. S., Baldwin, M., Fletterick, R., Cohen, F. E., Vandlen, R., Henner, D., and Prusiner, S. B. (1996) High-level expression and characterization of a purified 142-residue polypeptide of the prion protein, *Biochemistry-Us 35*, 5528-5537.
311. Gorbet, M. B., and Sefton, M. V. (2005) Endotoxin: The uninvited guest, *Biomaterials 26*, 6811-6817.
312. Haslett, C., Guthrie, L. A., Kopaniak, M. M., Johnston, R. B., and Henson, P. M. (1985) Modulation of multiple neutrophil functions by preparative methods or trace concentrations of bacterial lipopolysaccharide, *Am. J. Pathol. 119*, 101-110.
313. Hirayama, C., and Sakata, M. (2002) Chromatographic removal of endotoxin from protein solutions by polymer particles, *J. Chromatogr. B. 781*, 419-432.
314. Emmanuel, D. G. V., Dunn, S. M., and Ametaj, B. N. (2008) Feeding high proportions of barley grain stimulates an inflammatory response in dairy cows, *J. Dairy. Sci. 91*, 606-614.
315. Gozho, G. N., Krause, D. O., and Plaizier, J. C. (2006) Rumen lipopolysaccharide and inflammation during grain adaptation and subacute ruminal acidosis in steers, *J. Dairy Sci. 89*, 4404-4413.
316. Gozho, G. N., Krause, D. O., and Plaizier, J. C. (2007) Ruminal lipopolysaccharide concentration and inflammatory response during grain-induced subacute ruminal acidosis in dairy cows, *J. Dairy Sci. 90*, 856-866.
317. Banks, W. A., and Robinson, S. M. (2010) Minimal penetration of lipopolysaccharide across the murine blood-brain barrier, *Brain. Behav. Immun. 24*, 102-109.
318. Magalhaes, P. O., Lopes, A. M., Mazzola, P. G., Rangel-Yagui, C., Penna, T. C. V., and Pessoa, A. (2007) Methods of endotoxin removal from biological preparations: a review, *J. Pharm. Pharm. Sci. 10*, 388-404.
319. Smith, P. G., and Bradley, R. (2003) Bovine spongiform encephalopathy (BSE) and its epidemiology, *Brit. Med. Bull. 66*, 185-198.
320. Taylor, D. M. (2000) Inactivation of transmissible degenerative encephalopathy agents: A review, *Vet. J. 159*, 10-17.
321. Taylor, D. M., and Woodgate, S. L. (2003) Rendering practices and inactivation of transmissible spongiform encephalopathy agents, *Rev. Sci. Tech. Oie. 22*, 297-310.

322. Prusiner, S. B. (1998) Prions, *Proc. Natl. Acad. Sci. U.S.A. 95*, 13363-13383.